Aus dem Institut für Virologie
des medizinischen Zentrums für Hygiene und Mikrobiologie
mit Medizinal-Untersuchungsamt
der Philipps-Universität Marburg

Direktor: Prof. Dr. S. Becker

Structural Analyses of Borna Disease Virus Nucleoprotein- Phosphoprotein and Nucleoprotein- RNA Interactions

Dissertation
Zur Erlangung des Doktorgrades der Naturwissenschaften
(Dr. rer. nat.)

dem Fachbereich Biologie
der Philipps-Universität Marburg
vorgelegt von

Miriam Hock

aus Gernsbach

Marburg an der Lahn
November 2009

Die Untersuchungen zur vorliegenden Arbeit wurden von November 2005 bis Dezember 2006 am europäischen Molekularbiologielabor (EMBL), Direktor: Dr. S. Cusack; und von Januar 2007 bis Mai 2009 an der Unit of Virus Host Cell Interactions (UVHCI), Direktoren Dr. Stephen Cusack und Prof. Dr. Rob Ruigrok in Grenoble, Frankreich unter der Leitung von Prof. Dr. Wolfgang Garten und Prof. Dr. Winfried Weissenhorn durchgeführt.

Vom Fachbereich Biologie der Philipps-Universität Marburg als
Dissertation angenommen am

Erstgutachter: Prof. Dr. Klaus Lingelbach
Zweitgutachter: Prof. Dr. Wolfgang Garten

Weitere Mitglieder der Prüfungskommission:
Prof. Dr. Erhard Bremer
Prof. Dr. Wolfgang Buckel

Tag der mündlichen Prüfung am

ZUSAMMENFASSUNG

Borna Disease Virus (BDV) ist ein Vertreter der *Bornaviridae* in der Ordnung *Mononegavirales* (MNV). Unter denjenigen Viren dieser Ordnung, die Tiere infizieren, ist es bezüglich seiner Replikation und Transkription im Nukleus, einzigartig. BDV ist nicht zytolytisch, strikt neurotrop und verursacht Erkrankungen des zentralen Nervensystems (ZNS) bei einer großen Anzahl von Vertebraten, insbesondere beim Pferd.

Der aktive BDV Polymerase Komplex besteht wie bei allen MNVs, aus dem Nukleoprotein N, dem Phosphoprotein P und der Polymerase L. Bei BDV ist daran außerdem noch das Protein X beteiligt.

BVD N bildet Homotetramere und assoziiert nicht, wie im Gegensatz zu Nukleoproteinen anderer MNVs, mit zellulärer RNA. Jedes N Protomer besteht aus zwei helikalen Domänen und kurzen N- und C—terminalen Fortsätzen, mit deren Hilfe das N Tetramer stabilisiert wird.

Es war jedoch nicht klar, wie BDV N mit der viralen RNA interagiert, obwohl die starke strukturelle Ähnlichkeit mit den Nukleoproteinen der Rhabdoviren auf vergleichbare RNA Interaktions-Modi hinwiesen.

BDV-P spielt durch Interaktionen mit X, N, L und sich selbst eine essentielle Rolle beim Aufbau und der Regulierung des Polymerase-Komplexes, wobei die Oligomerisierung ähnlich wie bei anderen MNVs, für die Bildung eines aktiven Polymerase-Komplexes notwendig ist.

P benötigt einen intakten C-terminus zur Interaktion mit dem Nukleoprotein N und kontaktiert möglicherweise zwei unterschiedliche Stellen auf N. Phosphoproteine von Rhabdoviren und Sendai Virus enthalten jeweils zwei unterschiedliche Bindestellen für N. Über die eine wird die Bindung des Nukleoproteins an unspezifische RNA verhindert, über die andere binden die Phosphoproteine an N-RNA Komplexe und vermitteln so die Ausbildung eines aktiven Polymerase Komplexes. Interessanterweise benötigt das Nukleoprotein von BDV das Phosphoprotein nicht, um die Interaktion mit unspezifischer RNA zu verhindern, da das Nukleoprotein spontan Tetramere ausbildet, ohne dabei RNA zu komplexieren, was eine Ausnahme unter den *Mononegavirales* darstellt.

Das Ziel meiner Untersuchungen war es, die Wechselwirkungen zwischen dem Nukleo- und dem Phosphoprotein, und dem Nukleoprotein und der viralen RNA mithilfe von biochemischen, biophysikalischen und strukturaufklärenden Methoden aufzuklären.
Obwohl es nicht gelang, röntgenkristallographische Daten, weder von N-P, noch N-RNA Komplexen zu erhalten, konnte gezeigt werden dass P‘, eine N-terminal verkürzte und in BDV infizierten Zellen vorkommende Isoform des Phosphoproteins, zu Tetrameren oligomerisiert. Es interagiert mit N und formt mit diesem Heterooktamere, wobei die letzten 5 C-terminalen Aminosäurereste zur stabilen Komplexbildung benötigt werden. Das tetramerische Nukleoprotein wird in Anwesenheit von BDV genomischer 5’ RNA destabilisiert, was zu N-RNA Polymeren führt. Solche N-RNA Polymere, werden auch in Anwesenheit von P‘ gebildet. Elektronenmikroskopische Analysen der N-RNA und N-P‘-RNA Komplexe zeigen große “offene” Ring- und Stäbchenartige Strukturen. Die RNA innerhalb dieser Strukturen bleibt dabei ungeschützt und zugänglich für RNase. Beim enzymatischen Abbau der RNA bleiben die N oder N-P‘ Polymere jedoch intakt, was die Vermutung zulässt, dass die Polymere nicht alleine durch die RNA stabilisiert werden. Interaktionen zwischen N und der viralen RNA werden durch Erkennung basischer Aminosäurereste im Inneren einer Spalte im Nukleoprotein vermittelt.

SUMMARY

Borna disease virus (BDV) is the only representative of the *Bornaviridae* in the order *Mononegavirales*. It is unique among the animal viruses of this order with respect to its transcription and replication in the nucleus, which provides access to the splicing machinery. BDV is noncytolytic, highly neurotropic and causes diseases of the central nervous system (CNS) in a wide range of vertebrates. As in other *Mononegavirales,* the BDV polymerase complex or ribonucleoprotein complex, consists of the nucleoprotein N, the phosphoprotein P, the polymerase L and viral genomic RNA. In the case of BDV another protein is involved, termed protein X.

BVD N forms a homotetramer and does not spontaneously interact with cellular RNA. Each protomer consists of two helical domains and N- and C-terminal extensions, involved in domain exchange and tetramer stabilization.

An open question remained how BVD N interacts with RNA, although overall structural similarities with nucleoproteins from rhabdoviruses and vesiculoviruses suggested similar modes of RNA interaction.

Protein P plays an essential role in assembly and regulation of the polymerase complex via interactions with X, N, L and itself. Oligomerization of P is required for the formation of an active polymerase complex, similar to other negative strand RNA polymerase complexes.

P requires an intact C-terminus for N interaction and may contact two different sites on N. Phosphoproteins from *Rhabdoviruses* and Sendai virus contain two different binding sites for N, one to keep N soluble and free from unspecific RNA and the other to bind to N-RNA complexes forming the polymerase complex together with the polymerase L. However, BVD N does not require P binding to prevent non-specific RNA interaction, since BDV N oligomerizes spontaneously into tetramers that do not complex RNA, thus the precise role of N-P interaction in the absence of RNA is not known.

The aim of our study was to understand the interaction between the BDV nucleo- and the phosphoprotein as well as the nucleoprotein and the viral RNA. Even though, no conclusive data were obtained upon crystallographic approaches, concerning N in complex with different truncated P-constructs and BDV genomic RNA, we present data about N-P and N-RNA interactions.

I show that P', an N-terminally truncated isoform of the phosphoprotein, present in BDV infected cells, oligomerizes into tetramers. The tetrameric P' interacts with BDV-N, thus forming hetero-octamers. The P'-N interaction requires five C-terminal amino acids of P' to form a stable complex with a k_D of 1.66 µM.

Tetrameric N is destabilized in the presence of 5' genomic BDV RNA, which leads to the formation of N-RNA polymers. Similar N-RNA polymers are formed in the presence of P', leading to P'-N-RNA polymers. Electron microscopy analyses of N-RNA and N-P'-RNA complexes revealed large "open" ring-like and string-like assemblies with the RNA exposed and accessible for degradation. The N or N-P polymers remain intact after RNA degradation indicating that polymerization is not mainly stabilized by RNA interaction. The N-RNA interaction is mediated via recognition of basic residues within the cleft of the N-and C-terminal domains similar to the observed nucleoprotein-RNA recognition of other negative strand-RNA viruses.

In conclusion, these data provide insight on the molecular interactions between the viral RNA and the nucleo- and phosphoprotein of the BDV ribonucleoprotein complex.

1 INTRODUCTION

1.1 GENERAL INTRODUCTION

1.1.1 NEGATIVE-SENSE RNA VIRUSES

Negative-sense RNA viruses are enveloped viruses with a single-strand RNA genome in negative orientation. Their genomic RNA is either segmented or monopartite. Those representatives with a monopartite RNA genome are summarized within the order *Mononegavirales* (MNV) and are sub-divided into four families: *Rhabdoviridae, Paramyxoviridae, Filoviridae and Bornaviridae.* Their genes are arranged in a similar order on the genome and flanked by untranslated regions (UTRs) at the 5' and 3' termini, termed trailer and leader sequences, respectively. These regions contain promoter sequences within inverted terminal repeats (ITRs).

MNVs are different in size and morphology (Figure 1) and infect a large spectrum of hosts, like plants, invertebrates and mammals.

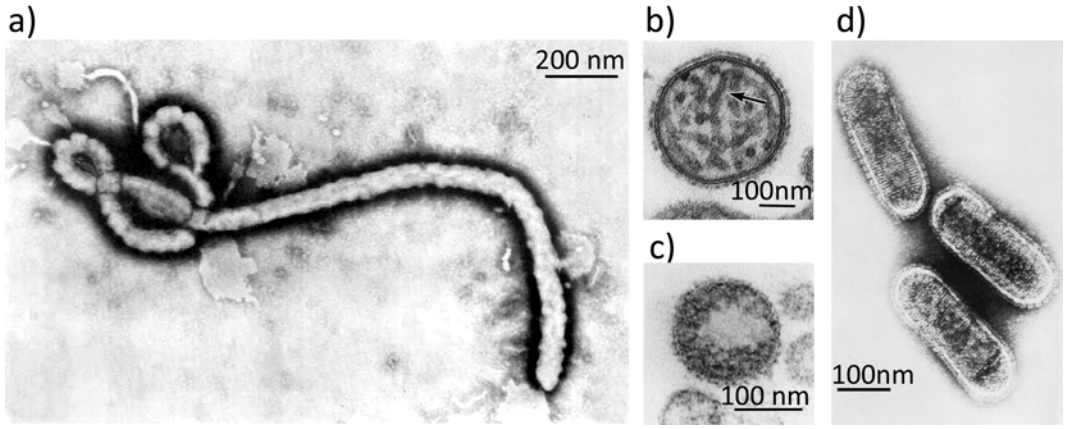

Figure 1: Electronmicroscopy images of *Mononegavirales* virus particles
a) Ebola virus, *Filoviridae* (ICTVdB - Picture Gallery)
b) Hemagglutinating virus of Japan, *Paramyxoviridae* (Kohno *et al.*, 1999)
c) Borna disease virus, *Bornaviridae* (Kohno *et al.*, 1999)
d) Vesiular stomatitis virus, *Rhabdoviridae* (ICTVdB - Picture Gallery)

In non-segmented negative-sense RNA viruses, the active transcription and replication complex, called ribonucleoprotein (RNP) complex (Szilágyi & Uryvayev, 1973; Murphy & Lazzarini, 1974) is composed of the viral RNA, the nucleoprotein N, the phosphoprotein P and the viral polymerase L (Emerson & Wagner, 1972; Emerson & Yu, 1975; Pattnaik *et al.*, 1992). The major RNP component is N, which encapsidates the viral genome, thus forming N-RNA complexes to serve as a template for L (Emerson & Wagner, 1972).

Because L cannot bind directly to N-RNA complexes, it is dependent on P, the polymerase cofactor (Portner & Murti, 1986; Horikami & Moyer, 1995). P tethers the polymerase towards the N-RNA complexes, stabilizes the RNP complex and serves as a scaffold for L (Mellon & Emerson, 1978; Emerson & Schubert, 1987; Curran, 1998).

1.1.2 BORNA DISEASE HISTORY

Borna disease obtained its name from the Saxon city of Borna, where in1885 a large number of horses from a cavalry regiment died from a fatal neurological disease. The disease has been described as *Hitzige Kopfkrankheit* or *Enzootische Gehirn-Rückenmarksentzündung der Pferde*. Due to the major outbreaks around Borna and the tremendous losses of horses in this region, the disease was finally termed *Bornasche Krankheit* (Borna disease, BD).

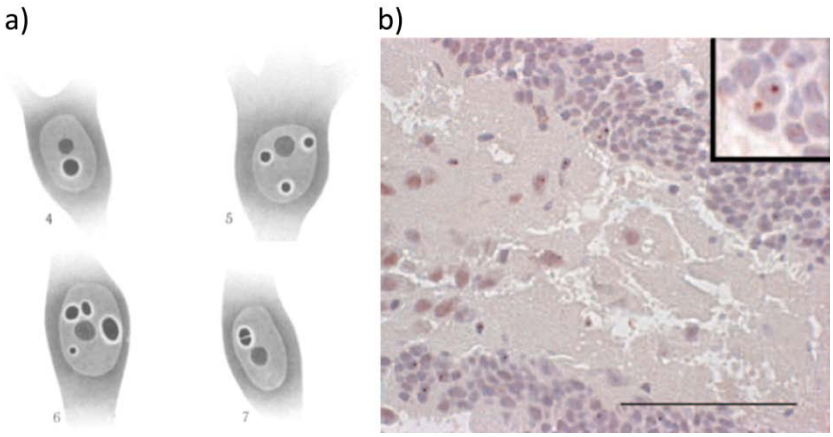

Figure 2: BDV-protein accumulation: Joest- Degen bodies
a) Drawings of Joest-Degen bodies as seen by Ernst Joest in ganglion cells of horses with Borna disease (Joest, 1911). **b)** Inset: Joest Degen bodies (red) in multiple neurons of a BDV infected shrew. The scale bar indicates 100nm, (Hilbe *et al.*, 2006).

In 1909 Joest and Degen discovered the acidophilic inclusion bodies in the nuclei of infected horse ganglion cells, characteristic for Borna disease (Figure 2) (Joest & Degen, 1909; Joest, 1911). The causative agent of Borna disease was later attributed to a virus (Borna disease virus, BDV) by Wilhelm Zwick, since ultrafiltrated brain homogenates from infected horses caused BD in laboratory animals (Zwick & Seifried, 1925; Zwick *et al.*, 1926).

In 1994 the complete genome sequence of BDV has been discovered and the virus was finally classified as the prototype member of the family *Bornaviridae* in the order *Mononegavirales* (Cubitt *et al.*, 1994).

1.2 BORNA DISEASE VIRUS

BDV is noncytolytic, highly neurotropic and leads to persistent infections in cell culture. It causes diseases (mostly meningoencephalitis and encephalomyelitis) of the central nervous system (CNS) mainly in horses and sheep. Also other animals such as cats, dogs, cattle and donkeys are susceptible to natural infection with BDV (Rott & Becht, 1995; Ludwig & Bode, 2000; Staeheli *et al.*, 2000; Richt & Rott, 2001).

Recently, two new BDV strains have been discovered in psittacine birds with proventricular dilatation disease, a fatal inflammatory central, autonomic, and peripheral nervous system disease (Honkavuori *et al.*, 2008). Experimental BDV infections were successful in rodents, non-human primates and chickens (Narayan *et al.*, 1983, Hallensleben, 1998 #5, Krey, 1979 #232; Lipkin & Briese, 2007). It has also been proposed that BDV may infect humans and causes a variety of neuropsychiatric disorders, but this idea is still discussed controversially (Richt & Rott, 2001; Dürrwald *et al.*, 2007).

The reservoir host is unknown so far, although the bicolored white-toothed shrew, *Crocidura leucodon*, has been considered as a potential virus reservoir due to BD cases in an area in Switzerland (Hilbe *et al.*, 2006).

BD occurs usually sporadically in horse populations and only limited to certain areas in middle- and southern- Germany, as well as Switzerland and Austria. Less than 100 BD cases occur per year. However, antibodies against BDV can be found in horses all over Europe, North America, Asia and Africa, assuming a wide spread of BDV or related viruses.

The incubation time ranges from two weeks to several months and the symptoms of naturally occurring BDV infections are variable. Some of the infected animals are devoid of any symptoms. In other cases, unspecific symptoms as fever, asitia, nervous or lethargic behaviour and constipation may appear. With further progression of acute infection, classical Borna disease is manifesting. This is a result of the destruction of the

CNS through the T-cell mediated immune response of the host. This is manifested by significant drawback of motor function coordination and behavioural disorders, such as depression, excitement and somnolence. The course of disease lasts 3 to 20 days and ends usually fatal (Richt *et al.*, 2006). The animals die from exhaustion, aspiratory pneumonia and by decubitus-caused sepsis. Surviving horses often show sensory and motor damage (Becht & Richt, 1996). Efficient therapy or vaccines are currently not available.

1.2.1 BDV MORPHOLOGY

BDV particles are spherical, enveloped, and between 50 and 190nm in diameter; however, it is assumed that particles smaller than 80 nm are defective or immature particles, since infective particles did not pass through a filter with less than 80nm pore size (Danner & Mayr, 1979; Zimmermann *et al.*, 1994; Kohno *et al.*, 1999).

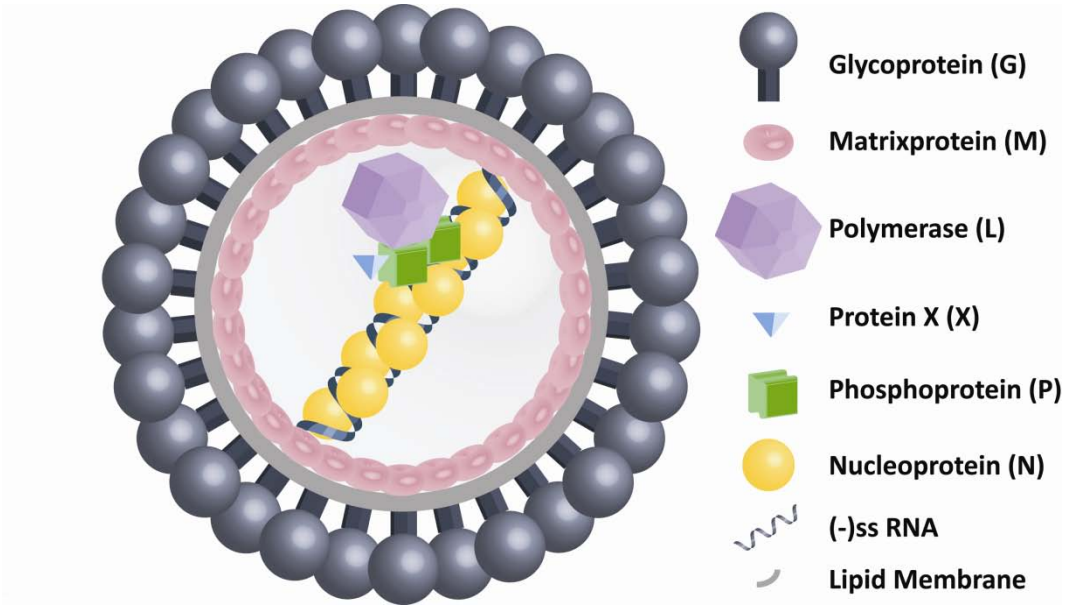

Figure 3: Schematic drawing of BDV particle

The envelope contains spikes of ~7 nm in length. A crescent-shaped inner structure is visible in EM images of negatively stained ultrathin sections of BDV infected MDCK cells (Figure 1c), embedded in epoxy-resin. This structure had a diameter of ~4nm and was supposed to constitute the nucleocapsid. Structures, slightly larger in mean size have

also been observed, assuming that other BDV proteins like the phosphoprotein and the polymerase were attached (Kohno *et al.*, 1999). Figure 3 shows a schematic drawing of the BDV particle.

1.2.2 PATHOGENESIS

Studies on experimentally infected animals strongly contributed to the understanding of the pathogenesis. This is best studied in rats, since the pathology found after intracerebral infection of Lewis rats is comparable to the immunopathology found in naturally infected horses and sheep (Richt *et al.*, 2006).

Infection in adult rats is achieved by any route that allows virus-access to nerve terminals (by olfactory, ophthalmic, or intraperitoneal inoculation), which ultimately results in CNS infection and classic disease. Transmission may occur via direct contact with body fluids, such as saliva, nasal mucous, tears and urine or by exposure to contaminated objects (Kishi *et al.*, 2002; Richt *et al.*, 2006).

After entering the nervous system, BDV migrates along the axons of the olfactory system to the brain. There, it replicates in neurons and glial cells, primarily in the limbic system and spreads over time throughout the CNS and further to the peripheral nervous system. Axonal transport shields BDV from the humoral immune response, explaining the lack of neutralizing antibodies until late in infection. Nevertheless, they seem to control virus tropism and are able to prevent the spread of virus from peripheral infection sites to the CNS (Furrer *et al.*, 2001; Stitz *et al.*, 2002).

BDV infected adult rats develop an encephalomyelitis in which infiltrating lesions can be found mainly in the cortex and in the hippocampus in areas where the virus is present. The symptoms are not a result of viral replication, but of a T-cell mediated immunopathologic reaction (Richt *et al.*, 1992; Stitz *et al.*, 1993). Thereby CD8+ T cells significantly contribute to the destruction of virus-infected brain cells *in vivo* by triggering their lysis, which leads to behavioural disorder and usually ends fatal (Stitz *et al.*, 2002).

1.2.3 THE BDV LIFE CYCLE

VIRUS ENTRY. BDV G (GP-N and GP-C), the surface glycoprotein, plays a pivotal role in receptor recognition and cell entry (Gonzalez-Dunia *et al.*, 1997) (Figure 4). BDV enters the cells via receptor-mediated endocytosis with the aid of an unknown cellular receptor (Gonzalez-Dunia *et al.*, 1998; Perez *et al.*, 2001). After intracranial inoculation BDV replicates primarily in neurons, implying that this receptor has a restricted expression pattern *in vivo*.

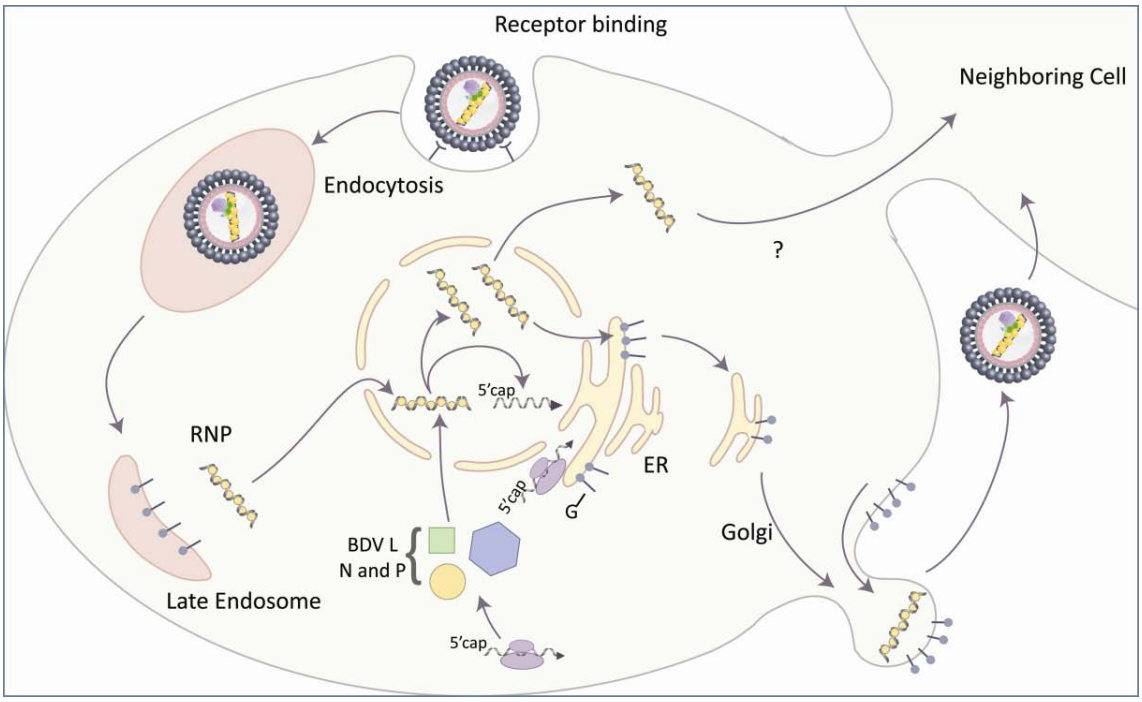

Figure 4: Replication cycle of BDV adapted and modified from (de la Torre, 2006)

While BDV GP-N was found to be competent for receptor recognition and virus entry, GP-C seems to be responsible for the pH-dependent fusion event in the endosome, required to release the viral ribonucleoprotein (RNP) into the cytoplasm of infected cells (Gonzalez-Dunia *et al.*, 1998). No data are available yet, concerning intracellular trafficking of the nucleocapsid after membrane fusion.

REPLICATION AND TRANSCRIPTION. BDV RNA replication and gene transcription occurs in the nucleus, which requires active nucleocytoplasmic transport of viral RNA and proteins. Based on the nuclear localization sites (NLS) and nuclear export signals (NES), located on N, P, and X, several hypotheses have been brought up regarding nucleocytoplasmic

shuttling of BDV nucleocapsid components, but no conclusive data are available (Kobayashi *et al.*, 2001; Yanai *et al.*, 2006).

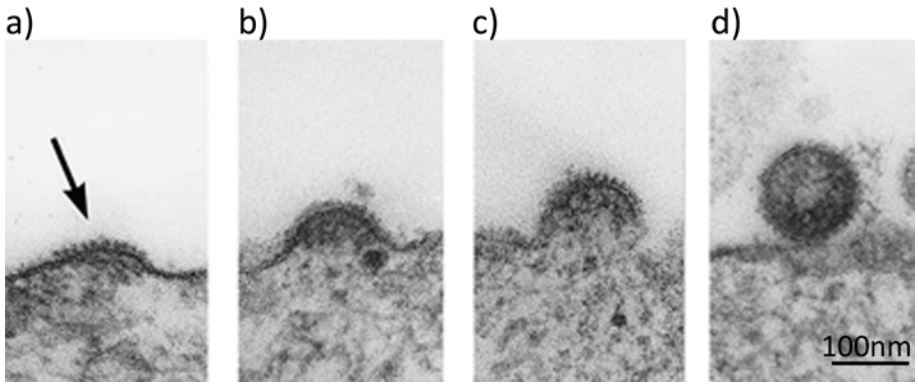

Figure 5: Sequential electron microscope images of the budding process in induced MDCK/BDV cells. The spiked membrane area (arrow in panel **a**) becomes an extracellular particle (**d)**. (**b** and **c**)are intermediate stages of the budding. Scale bar, 100 nm. Images were taken from (Kohno *et al.*, 1999)

PACKAGING AND EGRESS. Assembly of mature viral particles requires nuclear export of newly synthesized viral RNPs and their association with viral surface glycoproteins. The subcellular location and mechanisms underlying BDV particle formation have not been determined and no packaging signals are defined yet. There is evidence that cell-to-cell propagation of BDV might proceed in absence of the formation of mature viral particles. This process may be mediated by the BDV RNP complex (de la Torre, 2006). Budding of virion structures was observed from spike-containing membrane regions in n-butyrate treated, persistently infected cultured cells (Pauli & Ludwig, 1985; Kohno *et al.*, 1999) (Figure 5). Late in infection, BDV is detected in many tissues and organs as a consequence of its centrifugal spread through the axoplasm of peripheral nerve tissues. However, the underlying mechanisms remain unknown so far.

1.2.4 GENOME ORGANIZATION

The BDV genome has a size of 8.9 kB and is hence the smallest among the genomes of NNS viruses. It shows the typical organization of the *Mononegavirales*; six major partially overlapping open reading frames (ORFs) are contained within the sequence (Cubitt *et al.*, 1994; Briese *et al.*, 1995; Schneemann *et al.*, 1995; Wehner *et al.*, 1997; de la Torre, 2002) (Figure 6). Due to the biochemical properties and functions of the encoded

proteins, they were assigned as the counterparts of N, P, M, G and L proteins of the other NNS viruses (Perez *et al.*, 2003; Schneider *et al.*, 2003; Perez & de la Torre, 2005; Schneider, 2005). Another typical feature is the existence of short untranslated regions (UTR) at the 3'- and 5'-ends of the genome which possess promoter elements for transcription and replication. However, the BDV UTRs appear to be heterogeneous (Briese *et al.*, 1994; Cubitt & de la Torre, 1994; Pleschka *et al.*, 2001; Rosario *et al.*, 2005), which is in contrast to the UTRs of the other NNS viruses, where these sequences of up to 20 nucleotides are perfectly complementary to each other.

The genome is divided into three transcription units (I-III) with three different transcription initiation sites (S1-S3, Figure 7) and four polyadenylation signals/termination sites (T1-T4) (Schneemann *et al.*, 1994), which can be partially read through by the polymerase L, leading to the synthesis of a wider variety of transcripts and the generation of a template RNA (+RNA or antigenome) for genome replication.

Figure 6: Open reading frames of BDV
ORFs from 3' to 5': Nucleoprotein (N), protein X (X), partially overlapping with the ORF of the phosphoprotein (P), matrixprotein (M), polymerase (L) and the glycoprotein (G) ORF, which partially overlaps with the ORFs of M and L

1.2.5 TRANSCRIPTION AND REPLICATION

As mentioned above, Borna disease virus is the only known animal NNS virus with a nuclear phase (Briese *et al.*, 1992). The genomic RNA, encapsidated by the nucleoprotein N, serves as a template for the associated polymerase complex components L and P like in other negative-strand RNA viruses. Recombinant minigenome systems verified that N, P, and L proteins are essential and sufficient for BDV transcription and replication (Perez & de la Torre, 2005), although there is recent evidence that the BDV protein X is required too for efficient replication of BDV (Poenisch *et al.*, 2008).

Transcription of the genome is presumably starting at position +44 of the genomic 3' end (Figure 7) resulting in a transcription gradient, which however, is less pronounced than in most other *Mononegavirales* (Schneider, 2005). All mRNAs are polyadenylated

and contain a 5'-cap structure. The nucleoprotein (N) is the only protein translated from a monocistronic mRNA, emerging from transcription unit I. Read-through of the polymerase from S1 leads to a 1.9 kB RNA, including the ORFs of N, P and X. Unlike previously assumed, it is a fully functional mRNA, serving as an additional template for the three proteins and is suggested to serve a regulatory function in viral gene expression (Schneemann *et al.*, 1994; Poenisch *et al.*, 2008).

A bicistronic mRNA is produced from transcription unit II, starting at S2 and terminated at T2, encoding accessory protein X and the phosphoprotein P (Figure 7), (Schneider, 2005). The ORFs of these two proteins partially overlap in a different frame (de la Torre, 2006). Polymerase read-through at T2 occurs rarely till T3, the synthesized transcript is suggested to serve as an additional template for X and P translation No evidence exists of splicing to eliminate the first AUG codon initiating translation of X. Thus, it is likely that P is expressed through a leaky scanning mechanism.

Splicing occurs exclusively in transcripts from transcription unit III (Cubitt *et al.*, 1994; Schneider *et al.*, 1994; Tomonaga *et al.*, 2000). All primary transcripts of transcription unit III (S3) contain the overlapping ORFs of M and G. Introns are within the coding regions of M (Intron 1) and G (Intron 2). M is translated from all transcripts containing Intron 1, whereas splicing of this intron is necessary for efficient translation of G. Splicing of Intron 2 from the primary transcript terminated at T4 creates a large ORF encoding L (p190), which is only translated efficiently if Intron 1 is removed. Variable splicing of these introns thus enables BDV to regulate the expression of M, G and L. It is suggested that the viral polymerase complex influences splicing events because splicing is unlike in cDNA derived BDV mRNAs rather inefficient in BDV infected cells (Jehle *et al.*, 2000). BDV persistence requires a stringent regulation of viral replication, but little is known so far about the respective mechanisms. The 5' and 3' UTRs of NNS viruses contain promoter sequences which constitute inverted terminal repeats (ITR) with a high degree of sequence complementarity, which has the potential to form a panhandle structure with matching 5' and 3' termini. Such panhandle structures were found to be important regulatory elements of replication for members of the *Orthomyxoviridae* and *Bunyaviridae* families.

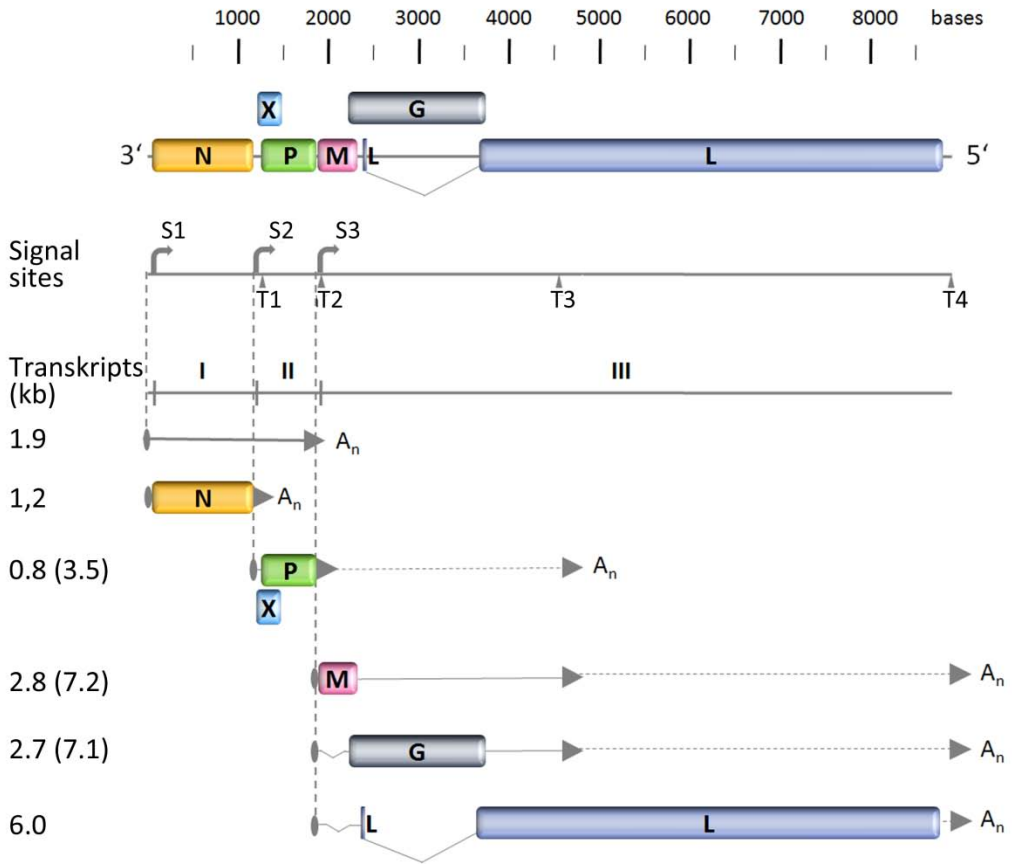

Figure 7: Genomic organization and transcription map of BDV.
N, nucleoprotein p38/p40N; X, protein X; P, phosphoprotein p24/p16; M, matrix protein; G, envelope glycoprotein; L, polymerase protein; S1-S3, transcription initiation sites; T1-T4 polyadenylation/termination sites. Positions of the introns are indicated by 1 and 2.

In the case of MNVs, it is unclear whether a panhandle structure is formed during viral replication, or whether the terminal complementarity of the genome simply reflects similar sequence requirements of the genomic and antigenomic promoters (Schneider, 2005). Analysis of genomic termini in acute and persistent BDV infection indicated the accumulation of genomes with truncated 3' and 5' termini in persistent cultures (Rosario *et al.*, 2005). Rescue of infectious recombinant BDV constructs demonstrated that trimming of the genomic 5'-terminus is an intrinsic feature of the BDV polymerase complex (Schneider *et al.*, 2005). In this system, genomic trimming generated termini with a recessed 5' end, leads to a strongly attenuated replication phenotype. The transcriptional activity, however, was not affected by the noncomplementary termini. This is compatible with high levels of antigen expression accompanied by extremely low levels of infectious virus, characteristic for persistent BDV infection.

1.2.6 BDV PROTEINS

The BDV genome encodes six proteins: nucleoprotein (N), phosphoprotein (P), matrix protein (M), glycoprotein (G), polymerase (L) and accessory protein X. The virus is made up of two major structural components: a ribonucleoprotein (RNP) core (Figure 8) and a surrounding envelope. In the RNP, genomic RNA is encased by the nucleoprotein. Furthermore, two other viral proteins, P and L, are associated and form the RNP complex. The glycoprotein and the host-cell derived membrane it is embedded in, constitute the viral envelope. The M protein is associated with both the envelope and the RNP and forms the inner lining of the virus (see 1.2.1 and figure 3). Protein X is abundantly present in infected cells and is supposed to serve an essential role in the formation of an active polymerase complex.

Figure 8: Schematic drawing of the BDV ribonucleoprotein complex
The viral RNA is encapsidated by the nucleoprotein (yellow). The phosphoprotein (green) serves as a mediator between the polymerase L (blue) and the N-RNA. The singular components are indicated in the picture.

X PROTEIN

Similar to the C-protein of VSV, BDV X is encoded from a shared ORF with BDV P (see Figure 6 and 7). It is with 87 amino acid residues (10 kDa) the smallest BDV protein (Wehner *et al.*, 1997). Protein X exhibits various functions in the BDV replication cycle; recently, it has been shown to play an essential role during the viral multiplication cycle by stimulating the assembly of an active polymerase complex. (Poenisch *et al.*, 2004; Poenisch *et al.*, 2007; Poenisch *et al.*, 2008). Furthermore it is suggested that regulation of X expression contributes to viral fitness (Poenisch *et al.*, 2009).However, very low levels of X have been detected (X:P ratio was 1:300) in purified BDV stocks and X has thus been proposed as a non- structural BDV protein (Schwardt *et al.*, 2005).

Protein X occurs in both nuclear and cytoplasmic compartments. Nuclear localization of X may be achieved via its interaction with P. On the other hand, the P interaction site is

located at the N-terminus (S_3DLRLTLLELVRRL_{16}) which partially overlaps with an unusual importin-binding motif (R_6LTLLELVRRNGN$_{19}$) for nuclear transport (Malik *et al.*, 2000; Wolff *et al.*, 2000; Wolff *et al.*, 2002).

The abundance of NLS and NES of BDV proteins makes it however difficult to attribute these sites to particular events during viral multiplication.

THE VIRAL ENVELOPE

GLYCOPROTEIN

BDV cell entry follows a receptor-mediated endocytosis pathway which is initiated by the recognition of an as-yet-unidentified receptor on the cell surface by the viral glycoprotein G (Figure 3 and 4).

The primary translation product of BDV G is a 56 kDa polypeptide, but posttranslational modification by N-glycosylation with high-mannose oligosaccharides of the complex type, results in a 94 kDa protein (gp94) (Schneider *et al.*, 1997; Richt *et al.*, 1998; Kiermayer *et al.*, 2002). Therefore G might play a critical role in virus persistence by protection of antigenic epitopes via decoration with host identical N-glycans (Eickmann *et al.*, 2005).

Only the cleaved form of G is incorporated into the virus particles (Eickmann *et al.*, 2005). This is achieved by the cellular protease furin which cleaves BDV G into an N- (GP-N, 51 kDa) and a C-terminal fragment (GP-C, 43 kDa) (Richt *et al.*, 1998; Kiermayer *et al.*, 2002). While GP-N is sufficient for receptor recognition and virus entry, GP-C may be involved in fusion events after internalization of the virus by endocytosis (Gonzalez-Dunia *et al.*, 1998; Perez *et al.*, 2001).

MATRIXPROTEIN (M)

The matrix protein M of Borna disease virus (BDV) is a constituent of the viral envelope covering the inner leaflet of the lipid bilayer. It has a size of ~16 kDa (142aa) and is therefore the smallest among the NNS virus matrixproteins. BDV M oligomerizes *in vivo* and *in vitro*, whereas the most stable structural unit is a tetramer (Figure 9). The tetramers in turn can form 2D lattice-like structures, supporting the view that M

constitutes the major driving force for the formation of viral particles (Stoyloff *et al.*, 1997; Kraus *et al.*, 2005).

The recently determined crystal structure of recombinant BDV M (Figure 9a-c) revealed a mainly basic surface charge on one face of the structure, indicating membrane interaction properties (Figure 9a) (Neumann *et al.*, 2009).

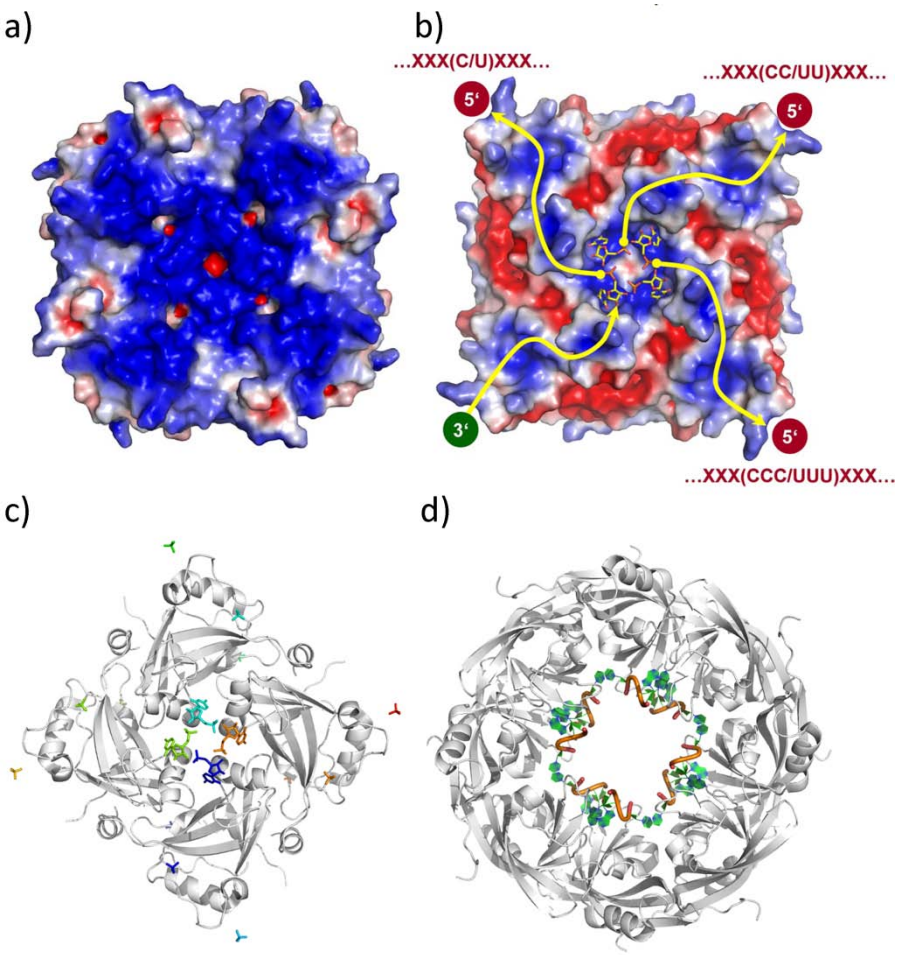

Figure 9: Membrane- and RNA-binding properties of BDV M
a) and **b)**: Surface properties of the putative membrane-binding face of the BDV-M tetramer. a) The electrostatic surface potential reveals this face to be highly basic (areas colored in white, red, and blue denote neutral, negative and positive potentials, respectively). b) Bottom view of a) rotated 180° around the y-axis. Schematic depiction of the possible binding mode of ssRNA according to (Neumann *et al.*, 2009). A distinctive basic patch along the tetramer diagonals could accommodate the polyphosphate backbone (yellow arrows), such that an incoming chain (3'-end bottom left) ends with the observed bound nucleotide (center). Assuming a specificity for cytidine/uridine, there are 3 possible exit routes for the 5'-end: (*i*) at the top left, with 1 pyrimidine base bound near the tetramer axis; (*ii*) at the top right, with 2 nt; and (*iii*) at the bottom right, with 3 central bases contributing to specificity. It is not possible to distinguish between them because of the 4-fold crystallographic symmetry. Figures from a) and b) were taken from (Neumann *et al.*, 2009). **c)** Ribbon diagram of the BDV M tetramer, bound to RNA. PDB ID: 3F1J **d)** Ribbon diagram of the Ebola virus VP40 N-terminus octamer bound to RNA. PDB ID: 1H2C. Proteins are depicted in white, RNA in color; ribbon diagrams were generated with Pymol 0.99.

The opposite face however, was shown to be associated with RNA, as demonstrated for the N-terminus of Ebola virus VP40 (Figure 9d) and the M protein of respiratory syncytial virus(Gomis-Rüth *et al.*, 2003; Rodríguez *et al.*, 2004). Two S-shaped basic patches, running diagonally over the surface (Figure 9b), may accommodate the phosphate backbone of the RNA (Figure 9b, c). The only similarity between known structures of MNV M proteins is exhibited by the BDV M monomer and the N- and C-terminal domains of VP 40 of Ebola virus. The RNA binding properties of M suggest that it could play a role in ribonucleoprotein (RNP) complex formation or nucleocapsid condensation as shown for VSV M (Newcomb & Brown, 1981; Neumann *et al.*, 2009). Besides, BDV M co-localizes with N, P and X in the nuclei and cytoplasms of persistently infected cells and binds to P *in vitro*. This implies that M is an integral component of the viral RNP (Chase *et al.*, 2007).

PROTEINS OF THE RIBONUCLEOPROTEIN COMPLEX

PHOSPHOPROTEIN (P)

The BDV phosphoprotein (24 kDa, 201 aa) plays a pivotal role in the BDV life cycle. It influences the cellular immune response and signaling pathways through interaction with cellular factors. Moreover, P acts as a mediator for the assembly and regulation of the polymerase complex via interactions with X, N, L and itself (Schwemmle *et al.*, 1998; Walker *et al.*, 2000; Schneider *et al.*, 2004). Due to replication and transcription of BDV in the nucleus, components of the polymerase complex are shuttling between nucleus and cytoplasm. Therefore, P contains two NLS and one NES (Figure 10). Although it is not clear to which extent P contributes to nuclear and cytoplasmic trafficking of BDV components, since N and X exhibit such properties as well (Shoya *et al.*, 1998; Schwemmle *et al.*, 1999; Yanai *et al.*, 2006).

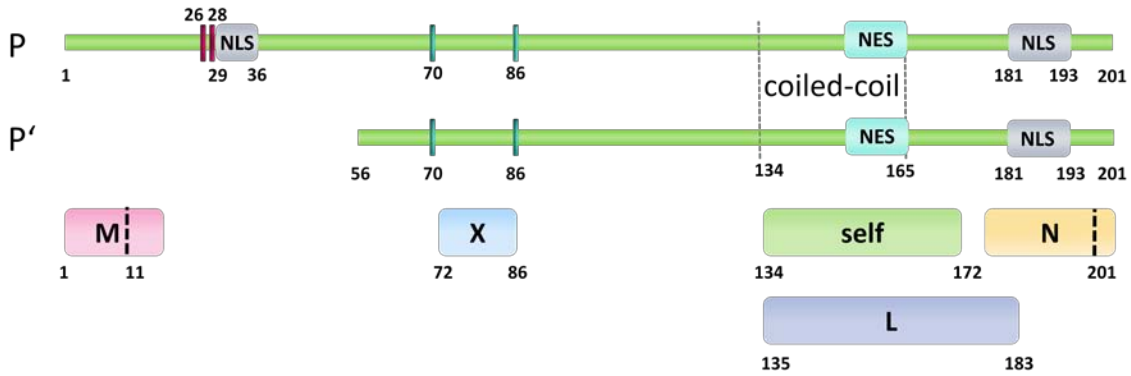

Figure 10: Schematic representation of the BDV-P protein.
The long (P) and the short (P') isoform of the BDV phosphoprotein are represented by green bars. The two independent nuclear localization signals (NLS) are indicated by grey boxes and nuclear export signals (NES) in turquoise. The self, N, L, M and X boxes indicate the domains responsible for the interaction of P with the respective BDV protein. Phosphorylation sites are indicated by red (PKCε sites) and blue (CKII sites) sticks). Positions of amino acids defining the boundaries of the NLS, the coiled coil motif (vertical dashed line) and the various interaction domains are indicated.

P activity as a co-factor of L is negatively regulated by phosphorylation at Serines (Figure 10) (Schwemmle *et al.*, 1997; Schmid *et al.*, 2007). Phosphorylation is predominantly attained by protein kinase Cε (PKCε) (not present in all strains) and- to a lesser extent- by Casein kinase II (CKII) (Schwemmle *et al.*, 1997). Mutational analysis of the phosphorylation sites revealed that aspartate substitutions (to mimic phosphorylation) at CKII sites inhibited the polymerase supporting activity of P. Aspartate substitutions at PKC_{ε} sites however, showed no inhibition (Schmid *et al.*, 2007).

BDV P oligomerization is required for the formation of an active polymerase complex, similar to other negative-strand RNA polymerase complexes (Curran, 1998; Choudhary *et al.*, 2002; Schneider *et al.*, 2004; Möller *et al.*, 2005; Albertini *et al.*, 2008). It is likely achieved via a predicted coiled coil motif that partially overlaps with the interaction site of L (Schneider *et al.*, 2004; Schneider, 2005).

Two isoforms of BDV-P have been detected in infected cells, resulting from alternative usage of in-frame AUG-initiation codons. The short isoform P' (16 kDa, aa 56-201; Figure 10) lacks the N-terminal 55 aa of full-length P, and one of two independent NLS (Figure 10). Due to its nuclear localization and the ability to interact with N, L, X and itself (P' and P) *in vivo*, it was proposed to play an important role during replication and transcription in BDV infected cells (Kobayashi *et al.*, 2000). However, it does not seem to

support reporter-gene expression in a viral minireplicon system (Kobayashi *et al.*, 2000; Schneider *et al.*, 2004).

NUCLEOPROTEIN (N)

Viral nucleoproteins are the major components of the RNP; they encapsidate the viral genome, thus forming N-RNA complexes to serve as a template for the viral polymerase L (Horikami *et al.*, 1992). However, direct BDV nucleoprotein-RNA interaction has previously not been demonstrated. BVD N consists of 371 aa and forms a planar homotetramer in the crystal structure and in solution (Figure 11). As it is able to interact with P but not with L, it exhibits the typical characteristics of NNS virus nucleoproteins, which are dependent on P mediation for the formation of an active polymerase complex as a prerequisite for successful viral replication and transcription (Horikami *et al.*, 1992; Schneider *et al.*, 2004).

Furthermore, the protein exhibits nucleo-cytoplasmic shuttling activity via a nuclear localization signal (NLS; $_{3}$PKRRLVDDA$_{11}$) and a nuclear export signal (NES; $_{128}$LTELEISSIFSHCC$_{141}$), which is consistent with the requirement of RNA transport into and out of the nucleus for replication and transcription (Figure 11c) (Kobayashi *et al.*, 1998; Kobayashi *et al.*, 2001). In contrast to other MNVs, BDV N-P interaction is supposed to be achieved by two motifs located at the N-terminus of N (K_{56}- Y_{100} and L_{131}-$I_{158,}$ Figure 11c) (Berg *et al.*, 1998). The first motif is solvent exposed in the N tetramer structure, whereas the second motif however is entirely inaccessible to solvent and deeply buried within the hydrophobic core of the N-terminal domain, ruling out any possible involvement in P binding (Rudolph *et al.*, 2003).

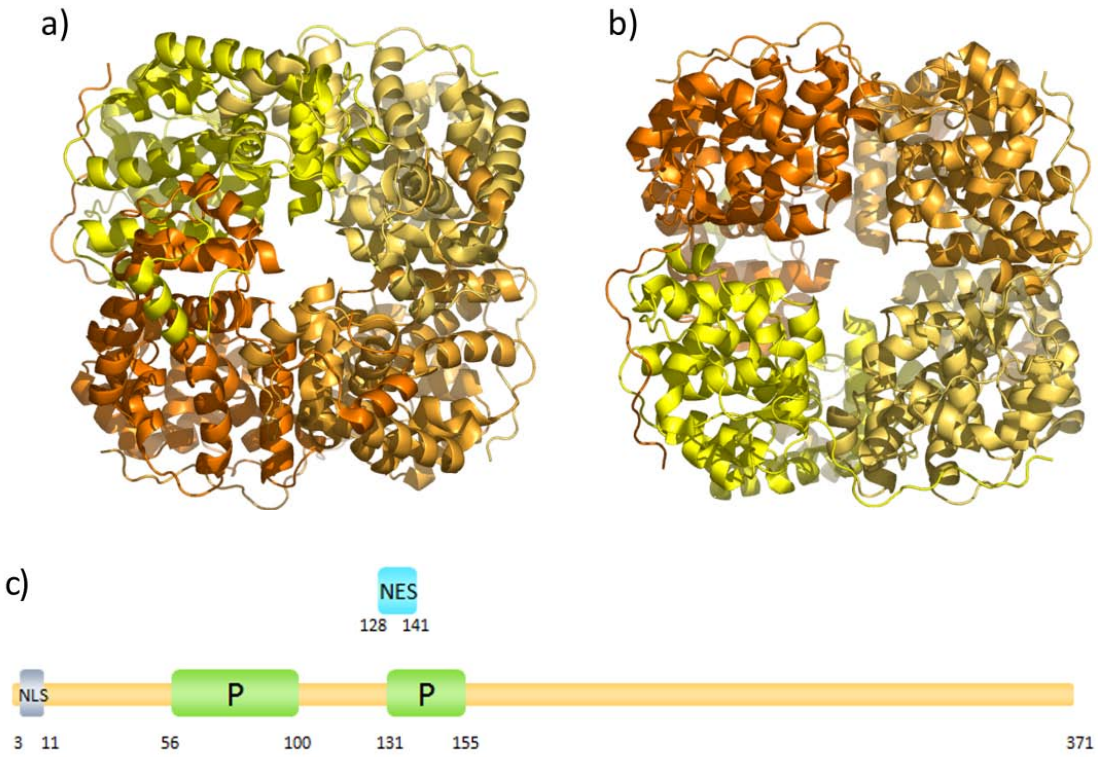

Figure 11: The BDV Nucleoprotein
a) Ribbon diagram of the nucleoprotein tetramer, top-view (on the N-terminaldomain). **b)** Bottom view (on the C-terminal domain) of a), rotated 180° around the X-axis. Each N-protomer is depicted in a different colour. Ribbon diagrams were generated with Pymol 0.99. Protein Data Bank ID: 1PP1, by (Rudolph *et al.*, 2003). **c)** Schematic representation of BDV N. Putative interaction sites with BDV P, NLS and NES are depicted in green, grey and blue respectively.

RNA-DEPENDENT RNA POLYMERASE (L)

The 1711 aa (190 kDa) BDV L protein is translated from a continuous ORF, fused after splicing of a short (6 nucleotides) to a large (5118 nucleotides) exon (Briese *et al.*, 1994; Schneemann *et al.*, 1994; Schneider *et al.*, 1994). It interacts with the BDV phosphoprotein and is phosphorylated by cellular kinases (Walker *et al.*, 2000; Schneider *et al.*, 2003). Nuclear localization of L is accomplished either by an NLS motif (R_{844}VVKLRIAP_{852}) or by interaction with P (Walker *et al.*, 2000; Walker & Lipkin, 2002; Schneider *et al.*, 2003). The interaction-site with P has not been mapped yet; despite sequence similarities among MNV L proteins, there is no consensus for P interaction (Chenik *et al.*, 1998; Holmes & Moyer, 2002).

As mentioned above, BDV L harbours conserved domains and motives and is thus the only BDV protein, showing sequence similarities with other NNS viruses (Poch *et al.*, 1990; Tordo *et al.*, 1992; de la Torre, 1994; Schneemann *et al.*, 1995). The presence of

three RGD motifs in the C-terminal region and the exchange of a lysine residue against a serine in domain III of motif A -a highly conserved motif among ATP- or GTP-binding proteins, which interacts with one of the phosphate groups of nucleotides- makes BDV L unique. It is yet unknown if these features are directly linked to L functions or if they are matter of evolutionary signatures (de la Torre, 2006).

NUCLEOPROTEIN-RNA INTERACTION

Nucleoproteins of negative strand RNA viruses condense the viral RNA into helical structures (Figure 12a-c) and thus serve, together with the encapsidated RNA, as a template for the viral polymerase.

However, the mode of RNA interaction and condensation differs from virus to virus.

Nucleoproteins of many MNVs, such as Rhabdoviruses, Sendai and Marburg virus, interact spontaneously with RNA, albeit its origin is cellular or viral. To prevent N-association with unspecific RNA, P acts as a chaperone by interaction with N (Fooks *et al.*, 1993; Iseni *et al.*, 1998; Yang *et al.*, 1998; Schoehn *et al.*, 2001; Mavrakis *et al.*, 2002; Green & Luo, 2006; Albertini *et al.*, 2007). Yet, BDV N does not spontaneously interact with cellular RNA, but forms homooligomers in the crystal structure as well as in solution, as demonstrated for influenza virus nucleoproteins (Rudolph *et al.*, 2003; Ye *et al.*, 2006).

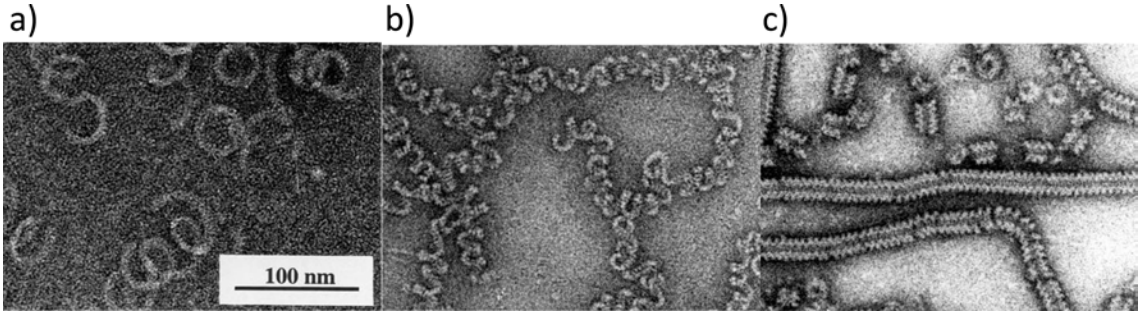

Figure 12: Electron micrographs of negatively stained nucleoprotein–RNA complexes of nonsegmented negative-strand RNA viruses.
a) Marburg virus N-RNA, recombinant from insect cells. **b)** Rabies virus N-RNA, virus isolate. **c)** Sendai virus N-RNA, virus isolate. The scale bar indicates 100nm for all three images. Images were taken and modified from (Mavrakis *et al.*, 2002).

AIMS

BDV holds a special position among animal Mononegavirales, regarding its replication and transcription in the nucleus of the infected cell. Furthermore its nucleoprotein N is, amongst others responsible for encapsidation of the viral genome and does not spontaneously interact with cellular RNA. Therefore, the encapsidation of RNA is not dependent on the phosphoprotein P, which acts as a "chaperone" regarding RNA packaging, as shown for the other members of this order. On the other hand, the BDV nucleoprotein shows overall structural similarities with N proteins of rabies and vesicular stomatitis virus.

Those special features make BDV an interesting item to study, elaborating differences and similarities with other MNVs, concerning RNP complexes and their various roles within the viral replication cycle, in particular.

The main goal of this work was to contribute to a better understanding of the structure and function of components of the BDV RNP complex, in particular the regulation of viral transcription and replication.

Therefore, we used biochemical, biophysical and structural approaches to characterize different complexes, which are part of the BDV ribonucleoprotein complex:

- Nucleoprotein- phosphoprotein
- Nucleoprotein- RNA
- Nucleoprotein-Phosphoprotein-RNA.

Due to difficulties with the full-length phosphoprotein, the N-terminally truncated and isoform P' has been used during almost all experiments.

The following specific aims have been proposed at different stages during the work, in order to answer the subsequent questions:

Part 1

Characterization and structural analysis of the BDV N-P interaction and oligomerization properties of N-P' and P'. Does BDV N undergo significant conformational changes upon interaction with P/P', possibly in order to render the RNA accessible for the viral polymerase L? Which is the stoichiometry of an N-P/P' complex. How do N and P' interact with each other, concerning interaction sites and affinity?

Part 2

Characterization and structural analysis of N-RNA and N-P'-RNA complexes and specificity of N-RNA complex-formation. Which are the similarities and differences between BDV N-RNA complexes and those of other MNVs? How does N recognize viral specific RNA and is the RNA protected upon interaction with N? Which amino acid residues are involved in N-RNA interaction? Does P interfere with the formation of N-RNA complexes or does it loosen a possibly tight N-RNA association to facilitate replication and transcription?

2 MATERIALS AND METHODS

2.1 MATERIALS

2.1.1 CHEMICALS AND REAGENTS

2-Mercaptoethanol	Sigma, Lyon, F
Acetic acid	Euromedex, Mundolsheim, F
Acryl amide 30% Rotiphorese	Roth, Karlsruhe, D
AccuGel 19:1 Acrylamide 40%	National Diagnostics, Atlanta, USA
Agar-agar	Merck, Darmstadt, D
Agarose	Biorad, Marnes-la-Coquette, F
Ampicilline	Euromedex, Mundolsheim, F
Anhydrotetracycline	IBA, Göttingen, D
APS (*Ammonium persulfate*)	Euromedex, Mundolsheim, F
ATP (*Adenosine-triphosphate*)	Fluka, Seelze, D
Boric Acid	Sigma, Lyon, F
Bromophenol blue	Biorad, Marnes-la-Coquette, F
BSA (*Bovine serum albumine*)	Roche, Meylan, F
Calcium Chloride ($CaCl_2$)	Fluka, Seelze, D
Carbenicilline	Euromedex, Mundolsheim, F
Complete® EDTA free protease inhibor	Roche, Meylan, F
Coomassie brilliant blue G-250	Serva, Heidelberg, D
CTP (*Cytosine-triphosphate*)	Euromedex, Mundolsheim, F
D-Desthiobiotine	Jena Bioscience, Jena, D
DMSO	Sigma, Lyon, F
DTT (*Dithiotreitol*)	Sigma, Lyon, F
EDTA (*ethylene diamine tetraacetic acid*)	Euromedex, Mundolsheim, F
EGS (*ethylene glycol bis succinimidyl-succinate*)	Euromedex, Mundolsheim, F
Ethanol	Pierce, Brebières, F
Ethidium bromide	Fisher Scientific, Pittsburgh, USA
Formaldehyde 37%	Euromedex, Mundolsheim, F
Glutaraldehyde	Sigma, Lyon, F
Glutathione	Sigma, Lyon, F
Glycerol	Euromedex, Mundolsheim, F
Glycine	Euromedex, Mundolsheim, F
GTP (*Guanosine-triphosphate*)	Euromedex, Mundolsheim, F
HABA (*2-(4-Hydroxyphenylazo)benzoeacid*)	Jena Bioscience, Jena, D
HEPES (*4-(2-hydroxyethyl)-1-piperazineethanesulfonic acid*)	Sigma, Lyon, F
Hydrochloric acid (*HCl*)	Euromedex, Mundolsheim, F
IPTG (*Isopropyl-ß-D-thiogalactopyranoside*)	Carlo Erba Reactifs, Val de Reuil, F
Isopropanol	Euromedex, Mundolsheim, F
	Fisher Scientific, Pittsburgh,

	USA
Potassium chloride (*KCl*)	Sigma, Lyon, F
Luria Bertani Medium	AthenaES, Baltimore, UK
Magnesium Chloride ($MgCl_2$)	Sigma, Lyon, F
Methylene blue	Roth, Karlsruhe, D
PEG	Fluka, Seelze, D
Phenol-Chloroform-Isoamyalcohol (25 :24 :1)	MP Biomedicals, Illkirch,F
SDS (*Sodiumdodecylsulphate*)	Serva, Heidelberg, D
Sodium acetate (CH_3COONa)	Fluka, Seelze, D
Sodium Chloride (*NaCl*)	Euromedex, Mundolsheim, F
Sodium Hydroxide (*NaOH*)	Carlo Erba Reactifs, Val de Reuil, F
Spermidine	Roth, Karlsruhe
Streptomycine	Euromedex, Mundolsheim, F
TEMED	Roth, Karlsruhe, D
Tris Base	Euromedex, Mundolsheim, F
Triton X	Roth, Karlsruhe, D
Tween 20	Roth, Karlsruhe, D
Urea ($(NH_2)_2CO$)	Euromedex, Mundolsheim, F
UTP (*Uracyl-triphosphate*)	Fluka, Seelze, D
Xylene Cyanol blue	Roth, Karlsruhe, D

2.1.2 EQUIPMENT

Aektaprime plus	GE Healthcare Europe, Saclay, F
Aekta Purifier	GE Healthcare Europe, Saclay, F
Biophotometer	Eppendorf, Hamburg, D
Hoefer SemiPhor Transfer Unit	Hoefer Inc., San Francisco, USA
Centrifuge 5424	Eppendorf, Hamburg, D
Centrifuge 5804R	Eppendorf, Hamburg, D
Concentrator Vivaspin 4 (10k MWO)	Sartorius, Göttingen, D
Concentrator Vivaspin 15 (10k MWO)	Sartorius, Göttingen, D
Slide-a-Lyzer Dialysis Cassette (3-12 MWO)	Pierce (Perbio Science), Brebières, F
GeBAflex Dialysis Maxi kit (6-8 MWO)	GEBA, Kfar Hanagid, IL
Dialysis bag	Spectrum, DG Breda, NL
Minispin plus	Eppendorf, Hamburg, D
Filters (45 and 22µm)	Dominique Dutscher, Brumath, F
PCR Thermo Cycler	Biometra, Göttingen, D
Electric Power supply	Biorad, Marnes-la-Coquette, F
Protane Mini gel System	Biorad, Marnes-la-Coquette, F
pH-meter Docu pH	Sartorius
Research® Pipette (0.1-2.5µl)	Eppendorf, Hamburg, D
Research® Pipette (0.5-10µl)	Eppendorf, Hamburg, D
Research® Pipette (10-100µl)	Eppendorf, Hamburg, D
Research® Pipette (20-200µl)	Eppendorf, Hamburg, D
Research® Pipette (100-1000µl)	Eppendorf, Hamburg, D

Syringe (1,2,5,10,20 and 50ml)	Terumo Europe, Leuven, B
Thermoblock	Falc, Treviglio, I

2.1.3 KITS

BugBuster	Novagen, Darmstadt, D
DIG Northern starter kit	Roche, Meylan, F
EndoFree Plasmid Mega Kit	Qiagen, Courtaboeuf, F
HiSpeed Plasmid Maxi Kit	Qiagen, Courtaboeuf, F
QIAquick gel extraction Kit	Qiagen, Courtaboeuf, F
QIAquick PCR purification Kit	Qiagen, Courtaboeuf, F
Wizard® plus Minipreps DNA purification Systems	Promega, Charbonnieres, F
Wizard® plus Midipreps DNA purification Systems	Promega, Charbonnieres, F
Wizard® plus Megapreps DNA purification Systems	Promega, Charbonnieres, F
SV Total RNA Isolation System	Promega, Charbonnieres, F
Z-competent E.coli transformation buffer set	ZymoResearch,

2.1.4 COLUMNS AND RESINS

Chelating Sepharose Fast Flow
Glutathion Sepharose Fast Flow
HighLoad 16/60 Superdex 75
HighLoad 16/60 Superdex 200
HighTrap DEAE Fast Flow
MonoQ® HR 5/5
PD-10 desalting columns
Streptactin MacroPrep
Superdex 75 10/300 GL
Superdex 200 10/300 GL
Superose 6 10/300 GL
All columns and resins were from GE Healthcare, except Streptactin MacroPrep, which was purchased from IBA (Göttingen, G)

2.1.5 Miscellaneous

BioBond plus nylon membrane	Sigma, Lyon, F
epT.I.P.S. Pipette tips (0.1-10µl)	Eppendorf, Hamburg, D
epT.I.P.S.Pipette tips (10-200µl)	Eppendorf, Hamburg, D
epT.I.P.S.Pipette tips (100-1000µl)	Eppendorf, Hamburg, D
ep Dualfilter T.I.P.S. Pipette tips (0.1-10µl)	Eppendorf, Hamburg, D
ep Dualfilter T.I.P.S. Pipette filtre tips (20-300µl)	Eppendorf, Hamburg, D
ep Dualfilter T.I.P.S. Pipette filtre tips (100-1000µl)	Eppendorf, Hamburg, D
PCR tubes	Eppendorf, Hamburg, D
Tubes (50 and 15ml)	BD Biosciences, San Jose CA, USA
Tubes (1.5 and 2ml)	Eppendorf, Hamburg, D

Tubes (1.5 and 2ml, without lid)	TreffLab
Tubes (5ml)	BD Biosciences, San Jose CA, USA
Petridishes	BD Biosciences, San Jose CA, USA
Pipettes sterile plastic (5,10 and 25ml)	BD Biosciences, San Jose CA, USA
Whatman paper	Whatman, GE Healthcare Europe, Saclay, F

2.1.6 ENZYMES

AflII	NEB, Ozyme, Saint-Quentin-en-Yvelines, F
BamHI	NEB, Ozyme, Saint-Quentin-en-Yvelines, F
Benzonase	Novagen, Darmstadt, D
BsaI	NEB, Ozyme, Saint-Quentin-en-Yvelines, F
DNaseI (*Deoxyribonuclease I*)	Roche, Meylan, F
DpnI	NEB, Ozyme, Saint-Quentin-en-Yvelines, F
Egg-white Lysozyme	Sigma
HindIII	NEB, Ozyme, Saint-Quentin-en-Yvelines, F
NcoI	NEB, Ozyme, Saint-Quentin-en-Yvelines, F
NdeI	NEB, Ozyme, Saint-Quentin-en-Yvelines, F
NsiI	NEB, Ozyme, Saint-Quentin-en-Yvelines, F
Pfu Polymerase	EMBL Heidelberg, D
RNaseA (*Ribonuclease A*)	Roche, Meylan, F
T7 Polymerase	EMBL Heidelberg, D
TEV protease	EMBL Heidelberg, D
Turbo Pfu	Stratagene
XbaI	NEB, Ozyme, Saint-Quentin-en-Yvelines, F
XhoI	NEB, Ozyme, Saint-Quentin-en-Yvelines, F

2.1.7 BUFFERS, SOLUTIONS AND MEDIA

LB Medium (*Luria-Bertani Medium*) (from QBiogene, Illkirch, F)	20 capsules Ad 1L H_2Od autoclaved
10x Electro-blotting Buffer for Nylon membranes	0.1M Tris-acetate, pH 7.8 50mM Na-Acetate

50x TAE buffer (*Tris-Acetate-EDTA*)	2M Tris base 57.1% (v/v) Acetic acid 0.05M EDTA pH8.0
10x TBE buffer (*Tris-borate-EDTA*)	0.89M Tris base 0.89M Boric acid 0.02M EDTA pH 8.0
TE buffer pH 7.4(*Tris-EDTA*)	10mM Tris HCL, pH 7.4 1mM EDTA, pH 8.0
2x denaturing RNA loading buffer	8M Urea 1mM EDTA pH 8.0 0.02% Bromophenolblue 0.02% Xylene cyanol blue
4x SDS protein sample buffer	200mM Tris HCl pH 6.8 20% (v/v) 2-Mercaptoethanol 8% (w/v) SDS 0.1% (w/v) bromophenol blue 40% (v/v) glycerol
10x SDS running buffer (tris-glycine)	0.25M Tris base 2.5M Glycine 1% (w/v) SDS
4x native protein loading buffer	0.25M Tris HCL, pH 6.8 40% (v/v) Glycerol 0.1% bromophenolblue
10x native running buffer	30g Tris base 144g Glycine ad H2O 1L

4x denaturing protein sample buffer for Tris-Tricine gels	0.2M Tris HCL, pH 6.8 60% (w/v) Glycerol 16% (w/v) SDS 0.2M DTT 0.02% (w/v)Coomassie brilliant blue G-250
10x upper cathode running buffer for Tris-Tricine gels	1M Tris HCl pH 8.25 1% (w/v) SDS 1M Tricine
10x lower anode running buffer for Tris-Tricine gels	2M Tris HCl, pH 8.9
6x DNA loading buffer	10mM Tris HCl, pH 7.6 0.03% (w/v) bromophenolblue 60% (v/v) Glycerol 60mM EDTA, pH 8.0
Coomassie brilliant blue stain	45% (v/v) Ethanol (v/v) Acetic Acid 0.25% (w/v) Coomassie brilliant blue G-250 powder ad H2O Filter through Whatman paper
Methylene Blue stain	2% (w/v) Methylene Blue

2.1.8 BUFFERS FOR PROTEIN PURIFICATION

AFFINITY CHROMATOGRAPHY

Proteins with His-Tag
20mM Hepes pH 7.8, 100mM NaCl, 20mM Imidazole (lysis buffer, **Buffer1**)
20mM Hepes pH 7.8, 100mM NaCl, 50mM Imidazole (washing buffer)
20mM Hepes pH 7.8, 1M NaCl, 1M KCl (removal of nucleic acids)
20mM Hepes pH 7.8, 100mM NaCl, 500mM Imidazole (elution buffer)

Proteins with Strep-TagII
20mM Hepes pH 7.8, 100mM NaCl (lysis/washing buffer)
20mM Hepes pH 7.8, 1M NaCl, 1M KCl (removal of nucleic acids)
20mM Hepes pH 7.8, 100mM NaCl, 10mM ATP, 10mM KCl (removal of chaperones)
20mM Hepes pH 7.8, 100mM NaCl, D-Desthiobiotin (elution buffer)

Proteins with MBP-Tag

20mM Hepes pH 7.8, 100mM NaCl (lysis/washing buffer)
20mM Hepes pH 7.8, 1M NaCl, 1M KCl (removal of nucleic acids)
20mM Hepes pH 7.8, 100mM NaCl, 10mM Maltose (elution buffer)

Proteins with GST-Tag
20mM Hepes pH 7.8, 100mM NaCl (lysis/washing buffer)
20mM Hepes pH 7.8, 1M NaCl, 1M KCl (removal of nucleic acids)
20mM Hepes pH 7.8, 100mM NaCl, 10mM Glutathion adjusted to pH7.8 with NaOH

ANION EXCHANGE

20mM Hepes pH 7.8, 100mM NaCl
20mM Hepes pH 7.8, 1M NaCl (Elution buffer)

GELFILTRATION

20mM Hepes pH 7.8, 100mM NaCl **Buffer 1**
20mM Hepes pH 7.8, 20mM NaCl **Buffer 2**

BUFFERS FOR RNA PURIFICATION

3M Na-Acetate, pH 5.3
0.1M Na- Acetate, pH 5.3
Both buffers were filtered through a 0.2µM filter.

2.1.9 BACTERIA STRAINS

XL10 gold Stratagene, La Jolla, CA, USA

Genotype : TetrD(*mcrA*)*183* D(*mcrCB-hsdSMR-mrr*)*173 endA1 supE44 thi-1 recA1 gyrA96 relA1 lac* Hte [F´ *proAB lacI*qZD*M15* Tn*10* (Tetr) Amy Camr].

DH5α subcloning efficiency Invitrogen, Cergy pontoise, F

Genotype : *F- φ80lacZΔM15 Δ(lacZYA-argF)U169 recA1 endA1 hsdR17(rk -, mk +) phoA supE44 thi-1 gyrA96 relA1 λ-*

BL21(DE3) Novagen, Darmstadt, D

Genotype: F– *ompT hsdS*B(rB– mB –) *gal dcm* (DE3)

2.1.10 SOFTWARE

PyMol	(DeLano)	
	http://www.pymol.org/	
mFold 3.2 and 2.3	(Walter *et al.*, 1994; Zuker, 2003)	
	http://mfold.bioinfo.rpi.edu/cgi-bin/rna-form1.cgi and	
	http://mfold.bioinfo.rpi.edu/cgi-bin/rna-form1-2.3.cgi	

BLAST blastn blastp	(Gertz) http://blast.ncbi.nlm.nih.gov
Consensus secondary structure prediction	(Deléage *et al.*, 1997) http://npsa-pbil.ibcp.fr

2.1.11 PLATFORMS

Mass spectrometry	Institut Biologie Structurale (IBS, Grenoble)
Electron microscopy	Unit of Virus Host Cell Interactions (UVHCI, Grenoble)
High Throughput Crystallization	European Molecular Biology Laboratory (EMBL, Grenoble)
Proteomics core facility	European Molecular Biology Laboratory (EMBL Heidelberg)

2.1.12 OLIGONUCLEOTIDES

N FL expression constructs	
BamHI_Tev_N	CGCGGATCCTGAGAATCTTTATTTTCAGGGCATGCCACCCAAGAGACGCCTGGTTGATGAC
BamHI-N-AfI-re	CCG CTT AAG CTA GTT TAG ACC AGT CAC C
P deletion expression constructs for crystallization	
NcoICT30pepP	CATGCCATGGGGACCTCTGCACCCATGTTG
CT30pepPBamHI	CGCGGATCCTTATGGTATGATGTCCCACTCATCCGC
pCDFp14fo	ATGGTGCAGCTATCGAATGATGAGC
pCDFp14re	ATGTATATCTCCTTCTTATACTTAACTAATATACTAAGATGGGGA
X FL expression constructs for crystallization	
NotIXre	ATAAGAATGCGGCCGCTCATTCGATAGCTGCTCCCTTCCG
NcoIXfo	CATGCCATGGACATGAGTTCCGACCTCCGGC
BamHIXPfo	CGCGGATCCCGAGAATCTTTATTTTCAGGGC
HindIIIXPre	CCCAAGCTTTCATTCGATAGCTGCTCCCTTCCG
N point mutation and deletion expression constructs	
BDV-Nk164D /R165Afo	GCAGGAGCCGAGCAGATCAAGGACGCCTTTAAAACTATGATGGCAGCCTTAAACCGG
BDV-Nk164D /165Rre	CCGGTTTAAGGCTGCCATCATAGTTTTAAAGGCGTCCTTGATCTGCTCGGCTCCTGC
BDV-NK242Afo	GCGCAGATGACTACGTACACTACTATAGCGGAGTACCTCGCAGAATGTATGGATGC
BDV-NK242Are	GCATCCATACATTCTGCGAGGTACTCCGCTATAGTAGTGTACGTAGTCATCTGCGC
BDV-NR297Dfo	ACGCTATCAAGCTTGCGCCAGACAGCTTTCCCAATCTGGCTTCTGC
BDV-NR297Dre	GCAGAAGCCAGATTGGGAAAGCTGTCTGGCGCAAGCTTGATAGCGT
BDV-N_delNfo	GACCCGCATCCGGGTATAGGG
NshortRe	GCC CTG AAA ATA AAG ATT CTC AGG ATC CTG GC
BDV-N_delCfo	TAGCTTAAGTCGAACAGAAAGTAATCGTATTGTACAC
BDV-N_delCre	[Phos]CGAGATATCTCGCGGCGCCTATAC
BDVNQ161Sfo	AGCATCAAGAAAAGGTTTAAAACTATGATGGCAGCCTT
BDVNQ161Sre	[Phos]CTCGGCTCCTGCTTTAATCT
BDVNR287Dfo	GATCACCCCGACGCTATCAAGCTTGC
BDVNR287Dre	[Phos]AATAGCCCCCAGGAACGGAAACAG
P FL and deletion expression constructs	
pASKreCdelp	CATGCCATGGTTATATGATGTCCCACTCATCCGCTG
pASKNcoIrep	CATGCCATGGTTATGGTATGATGTCCCACTCATCCG
pASKBamHITevp	CGCGGATCCCGAGAATCTTTATTTTCAGGGCATGATCTCAGACCCAGACCAGC
pASKPCdel5new	CATGCCATGGTTACTCATCCGCTGTCGGAGCACTT

BDV 5‘-RNA constructs	
SfiIT7rev	TTTGGCCAAGTCGGCCTCTAA
XbaBam40fo	TCTAGAGGATCCGTGTAGTGCTTGGGCTTGGT
XbaBam35fo	TCTAGAGGATCCGTGCTTGGGCTTGGTTGTTGC
XbaBam30fo	TCTAGAGGATCCTGGGCTTGGTTGTTGCTTTGT
XbaBam25fo	TCTAGAGGATCCTTGGTTGTTGCTTTGTTGTAGCGC
pGem9zfXbarev	[Phos]TCTAGAGCAAAGCTTACTAGTGATGCATATTCTATAGTG

2.1.13 PLASMIDS

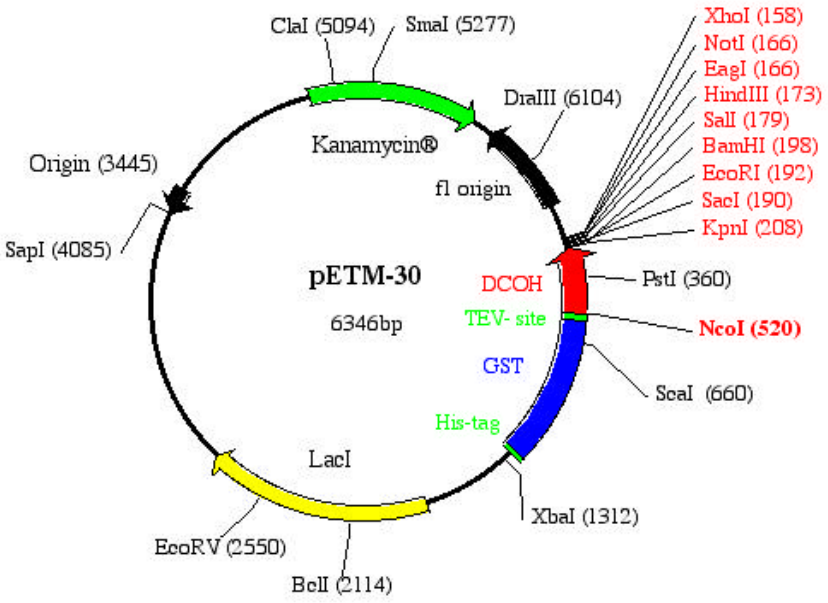

Figure 17: pETM-30 E. coli Expression Vector
Plasmid provided by EMBL Heidelberg Protein Expression and Purification core Facility.
The multiple cloning site is depicted in red. The plasmid provides a TEV-cleavable N-terminal His-GST (6x Histidine-Glutathion-S-Transferase)-Tag. Plasmid-containing bacteria are selected by acquired Kanamycin-resistance.

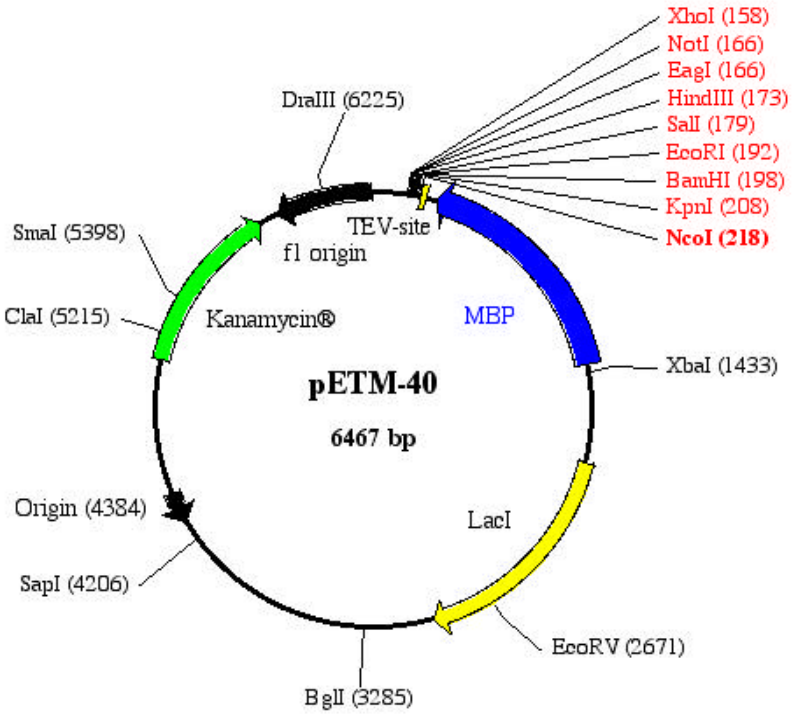

Figure 18: pETM-40 E. coli Expression Vector
Plasmid provided by EMBL Heidelberg Protein Expression and Purification core Facility.
The multiple cloning site is depicted in red. The plasmid provides a TEV-cleavable N-terminal MBP (maltose-binding protein)-Tag. Plasmid-containing bacteria are selected by acquired Kanamycin-resistance.

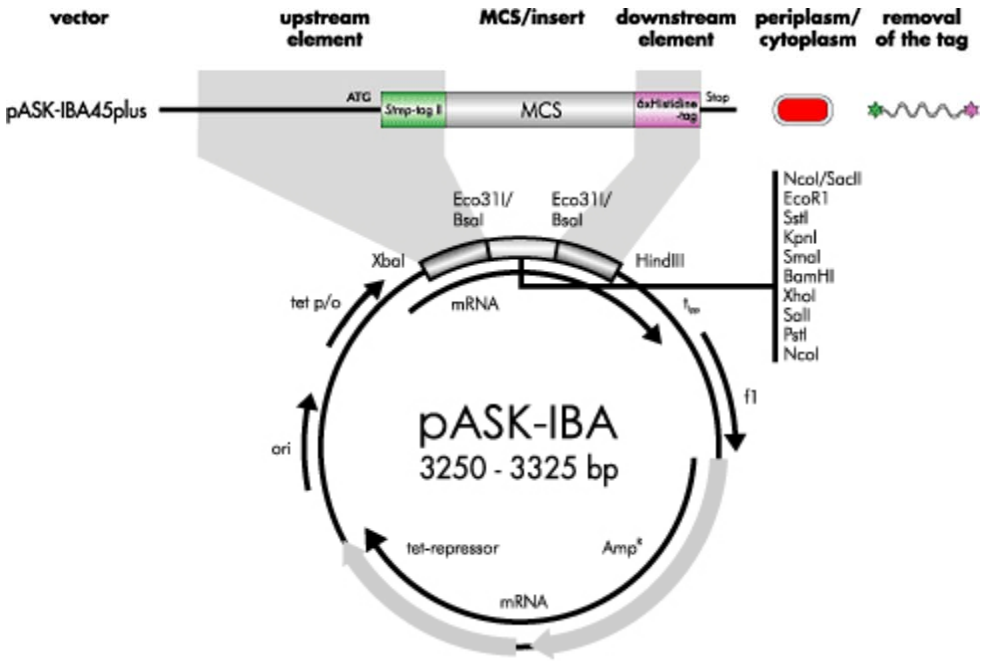

Figure 19: pASK-IBA45 plus vector
The multiple cloning site is depicted on the right. The plasmid provides an N-terminal StrepTagII and a C-terminal His-Tag. The insert is under the control of a tet-promoter. Plasmid-containing bacteria are selected by aquired Ampicillin-resistance.

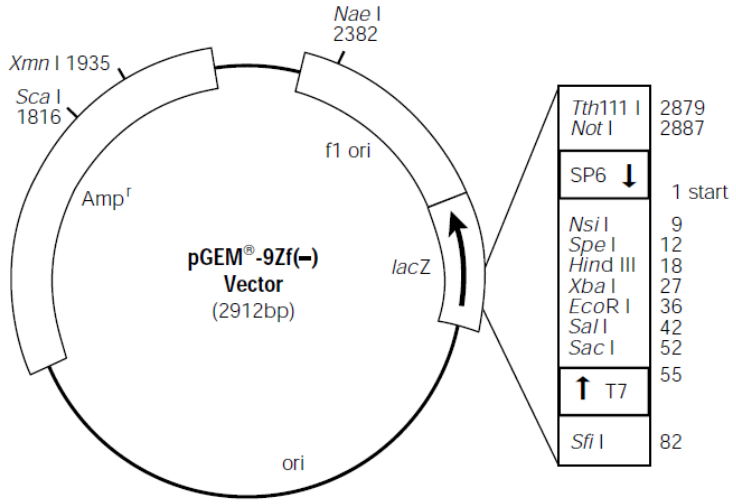

Figure 20: pGEM-9Zf(-) in-vitro transcription Vector
Plasmid provided by Novagen.
The multiple cloning site is depicted in a box together with the SP6 and T7 promoters. Plasmid-containing bacteria are selected by acquired Ampicillin-resistance.

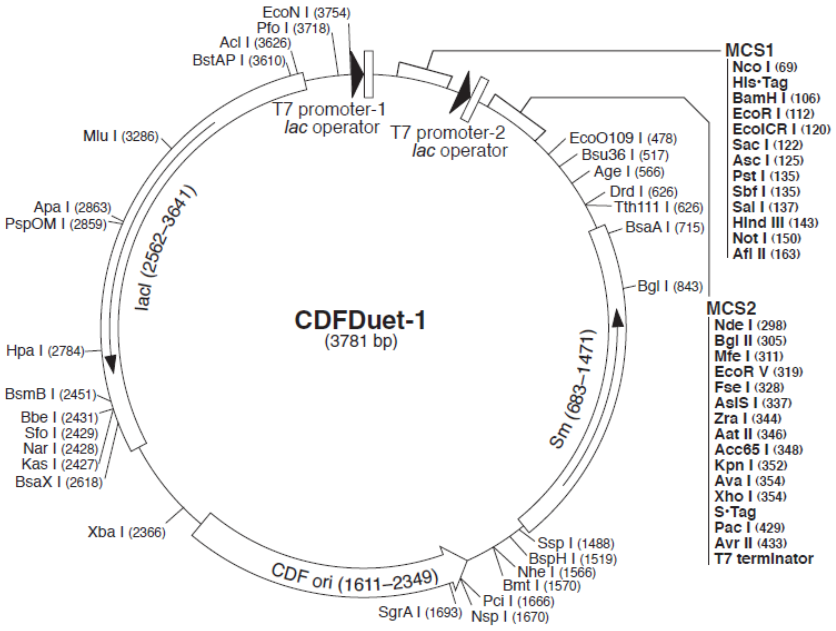

Figure 21: pCDF-Duet *E. coli* Expression Vector
Plasmid provided by Novagen.
It contains two multiple cloning sites (MCS1 and 2). And each insert is under the control of a T7-Promoter. The plasmid provides an N-terminal His-Tag in the first expression cassette and a C-terminal S-tag in the second. Plasmid-containing bacteria are selected by acquired Streptomycin-resistance.

2.2 METHODS

2.2.1 CLONING OF EXPRESSION- AND *IN-VITRO* TRANSCRIPTION-CONSTRUCTS

Cloning was carried out, according to standard cloning protocols, with the aid of the appropriate kits. The protocol for the generation of constructs with deletions and point-mutations however is described more detailed in the next paragraph.

DELETION AND SITE-DIRECTED MUTAGENESIS

For deletion, oligonucleotide primers were designed in inverted tail-to-tail directions to amplify the cloning vector together with the target sequence. The deletion was generated by amplification with primers that have a gap between their 5' ends (Figure 22, left). Point mutations were generated with a similar strategy, with primers with affiliating or overlapping 5'ends, one of which or both respectively, carried the desired mutation (Figure 22, right).

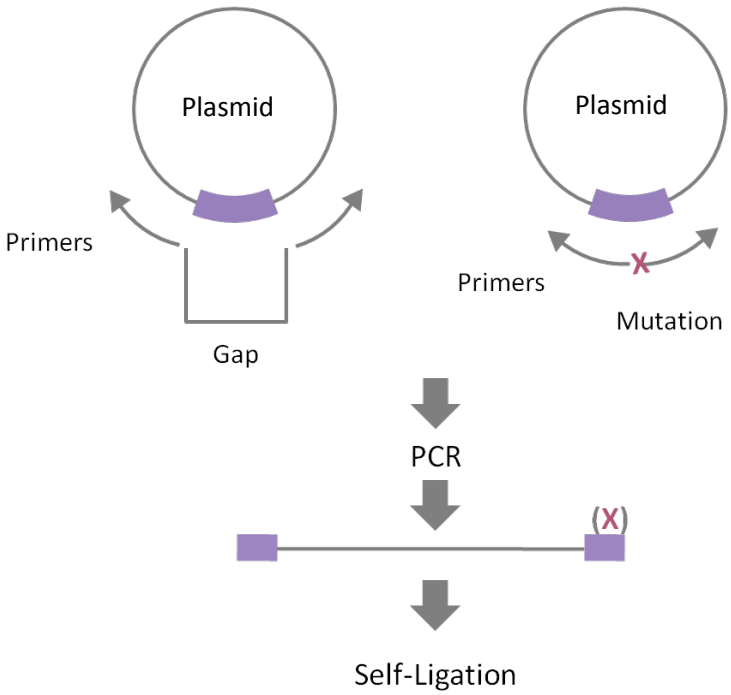

Figure 22: Strategy for generating a deletion or point-mutation in a sequence cloned into a plasmid. Lines, blue boxes, small arrows and red x, indicate plasmid DNAs, target sequences, PCR primers and point mutations, respectively. PCR in inverted directions is done with primers that have a gap between their 5' ends or carry a mutation and affiliate/overlap, and the resulting DNA is self-ligated to transform *E. coli*.

One of two affiliating primers is phosphorylated at the 5' end. After the PCR, amplified linear DNA was digested O/N with DpnI at 37°C to remove methylated template DNA, self-ligated and used to transform DH5α or XL10gold competent *E. coli* cells. The protocol was adapted and modified from (Imai *et al.*, 1991).

Components	Volume
Template DNA	50ng
forward primer (10pM)	1µl
reverse primer (10pM)	1µl
Turbo-Pfu DNA Polymerase	0.5µl
dNTPs (10mM)	1µl
10x Pfu buffer	5µl
H_2O dd	ad 50 µl

Table 2: PCR composition

Steps	Temperature	Duration	Number of Cycles
Initialization	95ºC	2min	1
Denaturation	95ºC	1min	
Annealing	55-66ºC	1min	18
Elongation	72ºC	1min/kb	
Final elongation	72ºC	10min	1

Table 3: PCR cycles

The annealing temperature was dependent on the Tm of the respective primers.

2.2.2 EXPRESSION AND PURIFICATION OF RECOMBINANT PROTEINS

BDV-N (370 aa) and the BDV-N mutant N-CΔ24 were cloned into the pCDFDuet-1 vector (Novagen), containing an N-terminal His-Tag. N-CΔ24 comprises aa 43-370 of BDV N. Single and double aa substitution mutants N-K164D/R165D, N-K242A and N-R297D were cloned via site directed mutagenesis according to (Imai *et al.*, 1991) with pCDFDuet-1 containing full-length N as a template. K164D/R165D corresponds to Lys 164 and Arg

165 exchanged against an Asp each. K242A corresponds to Lys 242 changed to Ala, R297D contains an Asp instead of Arg at position 297. Gln 161 is substituted by Ser in Q161S. Proteins were expressed in *E. coli* BL21 (DE3)- Gold cells. Cells were harvested by centrifugation, resuspended in buffer 1 (20mM Hepes pH 7.8; 100mM NaCl) and lysed by sonication in presence of protease inhibitors (Complete EDTA-free protease inhibitors, Roche). The cleared supernatant was loaded onto a Ni2+- charged Chelating Sepharose (GE Healthcare) column. The column was washed in buffer 1 plus 1 M NaCl and 1 M KCl followed by extensive washes with buffer 1 plus 50mM Imidazole, pH 7.8. Proteins were eluted with Buffer 1 plus 500mM imidazole, pH 7.8. The His-tag was cleaved off overnight at 4ºC with TEV protease (1:100 w/w) in presence of 1mM DTT and 1mM EDTA, pH 8.0. The tag was removed by a second Ni2+-Chelating Sepharose column after dialysis into buffer 1. Further purification was carried out via a MonoQ anion exchange column (GE Healthcare). Proteins were eluted by performing a salt gradient with buffer 1 plus 1M NaCl.

A Superdex 200 size-exclusion column (GE Healthcare) was used as a final purification step in buffer 1. Protein concentration was determined by absorbance at 280 nm under denaturing conditions (6M guanidinium hydrochloride). BDV-N-P' was co-expressed from pCDFDuet-1, but P' remained untagged in order to co-elute with His-tagged N. Expression and purification was performed as described for BDV-N. BDV-P' (146 aa, from aa 56-201) and C-terminal deletion P' mutants P'-CΔ1 and P'-CΔ5 were cloned into pASK45-plus vector (IBA), containing an N-terminal StrepTagII. P'-CΔ1 comprises aa 56-200 and P'-CΔ5 corresponds to aa 56-196. Proteins were expressed in *E. coli* BL21 (DE3)-Gold cells. Production of cleared lysates was identical with that of BDV-N. Lysates were passed over a Streptactin sepharose column (IBA) and washed with Buffer 1, followed by buffer 1 plus 1 M NaCl and 1 M KCl and buffer 1 plus 10mM ATP, 10mM MgCl2. Elution was performed with buffer 1 plus 10mM Desthiobiotin. Further purification steps were performed as described for BDV-N. BDV-N, N-P', P' and P' mutants were cloned by standard PCR methods, N mutants were cloned according to (Imai *et al.*, 1991). All constructs were sequenced.

BDV-X was expressed as an MBP-fusion protein in *E. coli* BL21(DE3) from pETM-40. Lysis was performed as for the other proteins and cleared lysates were purified via an Amylose resin (GE Healthcare). After washing with buffer 1 and buffer 1 plus 1M NaCl

and 1M KCl, the protein was eluted with buffer 1 plus 10mM Maltose. For the assembly of a BDV N-P-X triple complex *E. coli* pellets containing MBP-X and Strep-TagII-P' were mixed and lysed together. The proteins were purified by using an Amylose resin, prior to mixing with purified and buffer1-dialysed His-N. This was done, since in a large scale purification, MBP-X did not bind to StrepTagII-P' anymore, when P' was already bound to His-N (unfortunately, this could not be confirmed with a small-scale pulldown assay). The proteins were incubated 10min, RT prior to purification by Ni^{2+}-charged chelating Sepharose (GE Healthcare). The last affinity purification step was by Streptactin resin (IBA), where after washing with buffer 1, the proteins were eluted with buffer 1 plus 1mM Desthiobiotin. Since further purification by anion exchange was never successful, the proteins were directly purified by gel filtration with a Superose 6 column (GE Healthcare) in buffer 1.

2.2.3 IN-VITRO TRANSCRIPTION AND PURIFICATION OF BDV-RNA

BDV-3'-Leader and 5'-Trailer RNA (BDV He/80/FR strain genome, GenBank AJ311522; nucleotides 1-125 and 8784-8909 respectively) were cloned into pGem-9zf (Novagen) and in-vitro transcribed after cleavage of the plasmid with NsiI (3'-RNA) and XbaI (5'-RNA). The genome sequence entry in the NCBI nucleotide database for BDV He/80/FR corresponds to the trimmed genome as described (Pleschka *et al.*, 2001) lacking 2 nucleotides at the 5' trailer for entire complementarity with the 3' leader and ends with nucleotide 8909. Transcription reaction was carried out for 3-4 h at 37°C, modified from (Price *et al.*, 1995).

IN-VITRO TRANSCRIPTION (LARGE SCALE)

Components	
Linearized Template DNA	1-2mg
Tris, pH8.0	100mM
DTT	5mM
NTPs	4mM each
Triton X	0.01% (v/v)
Spermidine	1mM
$MgCl_2$	25mM
T7 Polymerase	7mg
H_2O dd	ad 10ml

Reaction was incubated for 3-4h at 37ºC

Reaction stop was carried out by adding 2x RNA loading buffer. RNA was either immediately purified by denaturing urea-PAGE or size-exclusion chromatography or stored at -20ºC.

RNA PURIFICATION (LARGE SCALE)

20ml of RNA sample were loaded on 8-15% pre-heated denaturing Urea gels and was allowed to separate at a rating of 20 Watts for 6h. After visualization by UV shadowing, the corresponding band was excised and transferred into a 50ml plastic tube (Falcon). A sterile spatula was used to crush the gel to a smooth mass and 0.3M Na-Acetate pH5.3 was added up to 50ml. RNA was allowed to elute by gentle agitation at 4°C, O/N.

Eluate was passed through a 0.22µm filter unit (Millipore) and the gel was carefully scratched out with a sterile spatula for another elution-round with 50ml fresh Na-acetate buffer (4°C, O/N). The filtration step was repeated.

The obtained eluate was passed on a 1ml HiTrap-DEAE column (GE Healthcare), pre-equilibrated with 0.3M Na-acetate pH 5.3. Column was washed with 10 CV of the mentioned buffer and RNA was eluted with 3M Na-acetate pH5.3. Isopropanol precipitation was carried out by adding 1 vol. of chilled Isopropanol and sample incubation at -80°C for 30min.

After spinning the samples for 10min at 14000rpm, supernatant was decanted and pellets were washed with 70% ethanol. The resulting pellet was allowed to dry for 1h at RT. RNA pellets were dissolved in 2.5ml (final volume) nuclease-free H_2O. A PD10

column (GE Healthcare) was used to desalt the RNA according to the protocol provided by GE Healthcare.

RNA was finally concentrated to desired concentration by lyophilisation.

2.2.4 POLYCRYLAMIDE GELELECTROPHORESIS (PAGE)

Analysis of proteins and RNA was done by PAGE:

Denaturing SDS-PAGE was performed according to (Schägger & von Jagow, 1987; Ploegh, 1995) at 140V for Tris-Tricine PAGE and according to (Laemmli, 1970; Sambrook *et al.*, 1989) for Tris-Glycine PAGE at 180V. Native PAGE for acidic proteins was performed at 100-120V with a modified recipe from Tris-Glycine PAGE, without SDS and a stacking gel. Denaturing Urea-PAGE for RNA analysis was performed according to (Price *et al.*, 1995).

2.2.5 SIZE-EXCLUSION CHROMATOGRAPHY MULTI-ANGLE LASERLIGHT SCATTERING (SEC-MALLS)

SEC-MALLS is a relatively new and reliable technique for determining molar mass and molar mass distributions of macromolecules. Molecules are separated according to size by a size exclusion column and the light scattering signal from the eluting molecules is collected simultaneously at numerous angles (Wyatt, 1993; Jumel *et al.*, 1996). The corresponding concentration trace is obtained downstream by a refractive index detector (Figure 23). For each point on the HPLC chromatogram, the amount of light scattered is directly proportional to the product of protein concentration and molar mass, according to Zimm's formula for a diluted polymer solution (Wyatt, 1998; Gerard *et al.*, 2007). The simplified formula for calculation of the molar mass is:

$$M = \frac{R_\theta}{CK^*}$$

Whereas M is the molar mass (g/mol), R_θ is the measured excess Raleigh's ratio, K* an equation-defined optical constant and C is the protein concentration.

Size exclusion chromatography was performed with a Shodex Protein KW-804 HPLC column (300 mm x 8.0 mm). Briefly, the column was equilibrated in buffer 1 and proteins were separated at 25 °C with a flow rate of 0.8 ml/min. On-line detection was performed by multi-angle laser light scattering (MALLS) using a DAWN-EOS detector (Wyatt Technology Corp., Santa Barbara, CA) equipped with a laser emitting at 690 nm and by refractive index measurement using a RI2000 detector (Schambeck SFD). Light scattering intensities were measured at different angles relative to the incident beam, and analysis of the data was performed with the ASTRA software (Wyatt Technology Corp., Santa Barbara, CA).

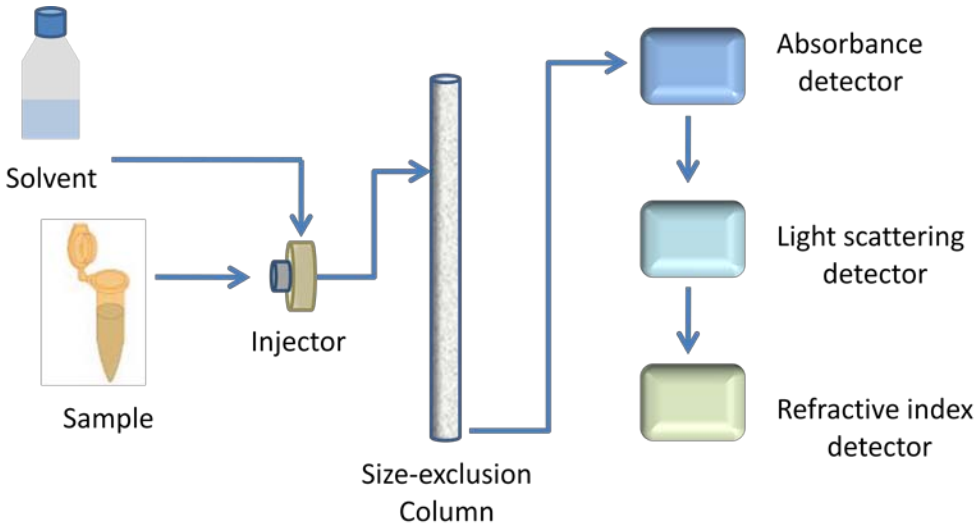

Figure 23: Experimental setup for SEC-MALLS
The sample is injected over a size-exclusion column and passes after separation and elution the indicated detectors.

Weight-averaged (Mw) molecular weights were obtained from the molecular weight distribution across the elution peak. For both P' and N-P' complexes the molecular mass was constant across the elution peak. The polydispersity factor (*M*W/*M*N) equaled 1.00 ± 0.02 for P' and 1.00 ±0.026 for N-P' indicating monodisperse species in both cases. For regular size exclusion chromatography (SEC), stokes radii were determined by calibrating the column with globular proteins of known stokes radii.

2.2.6 CHEMICAL CROSS-LINKING

N-P' and StrepTagII-P' (both in buffer 1) -samples of 20 µg were cross-linked with 0, 0.1,0.2, 0.5, 1, 2 and 5mM Sulpho-ethyleneglycol bis(-succinimidylsuccinate) (Sulpho-EGS, Pierce) or Glutaraldehyde (Sigma). The reactions were incubated for 20 minutes at room temperature and quenched by adding 4x SDS-PAGE sample buffer. Cross-linked material was analysed by discontinuous gradient Tris-Tricine-PAGE of 8 on 15% and bands were visualized by Coomassie Brilliant Blue.

2.2.7 SURFACE PLASMON RESONANCE (SPR) MEASUREMENTS

SPR allows the user to study the interaction between immobilized ligands and analytes in solution, in real time and without labeling of the analyte. Observed binding rates and binding levels can be interpreted in different ways to provide information on the specificity, kinetics and affinity of the interaction, or on the concentration of the analyte. It detects changes in the refractive index in the immediate vicinity of the surface layer of a sensor chip. SPR is observed as a sharp shadow in the reflected light from the surface at an angle that is dependent on the mass of material at the surface. The SPR angle shifts (from I to II in the lower left-hand diagram) when biomolecules bind to the surface and change the mass of the surface layer (Figure 24). This change in resonant angle can be monitored non-invasively in real time as a plot of resonance signal (proportional to mass change) versus time.

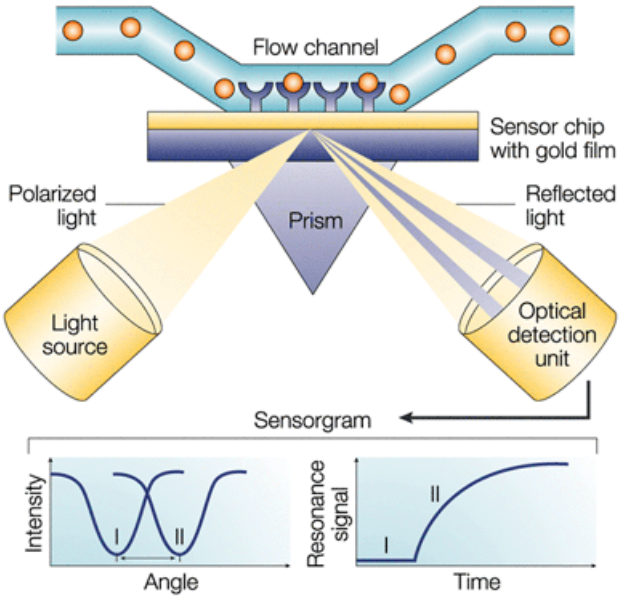

Figure 24: Setup for Surface Plasmon Resonance Biosensor
The image was taken from (Cooper, 2002)

To study the direct interaction between BDV-N and BDV-P' the (SPR) technique on a Biacore 2000 instrument and reagents from Biacore AB (Germany) were used. Immobilization of the ligand (BDV-N) was performed *via* amino coupling on a CM5 sensor chip. BDV-N (treated with 10mM acetate buffer, pH 4.5) was injected over a flow cell (activated with EDC/NHS) and immobilized to 8,800 response units (RU). The flow cell was then deactivated with ethanol amine (EA). Another flow cell, activated with EDC/NHS and deactivated with EA was used as a reference cell.

Immobilization and interaction analysis were performed at 25°C, using HBS as running buffer. Aliquots of 60 µl of analyte (BDV-P') (0.8-16 µM) were injected at a flow rate of 20µl/min over sensor chip surfaces. The signal in the reference cell was subtracted online during all measurements. Alternative, aliquots of 25µl BDV-P' (6.4 µM) incubated with a DEWDIIP-peptide (0-280µM) were injected over sensor

chip. Furthermore 6.4 µM of each BDV-P mutant were injected over sensor chip. Evaluation of binding specificity and kinetics of interaction were performed using the BIAevaluation 3.2RC1 software (Biacore).

2.2.8 LYSINE METHYLATION

Treatment of proteins with ABC (dimethylamine-borane complex), leads to the reductive methylation of lysines, thereby reducing surface entropy, which can have a favourable effect on crystallisation and may thus lead to improved diffraction (Rayment *et al.*, 1993). Since this modification is performed on purified mature proteins, there is no misfolding induced and only those residues on the exposed protein surface are modified while others remain protected within the core.

Lysine-methylation of proteins was adopted and slightly modified from the protocol of (Walter *et al.*, 2006). The methylation reaction was performed overnight in 50mM HEPES (pH 7.5), 250mM NaCl at protein concentrations of 0.1mg/ml or 5mg/ml. 20µl of freshly prepared 1M dimethylamine- borane complex (ABC; Fluka) and 40µl 1M formaldehyde (made from 37% stock; Fluka) were added per ml protein solution, and the reactions were gently mixed and incubated at 4°C for 2h. The procedure was repeated once, followed by a final addition of 10µl ABC and overnight incubation at 4°C.

To remove precipitated protein, the sample was spinned for 5min at 14000rpm and filtered carefully and consecutively through filters with 0.4 and 0.2µm pore size. The reaction was quenched and reaction components were removed by buffer exchange into 20mM Tris, pH 7.5, 200mM NaCl via a PD10 column (GE Healthcare). The sample was again buffer-exchanged into Buffer 1 and concentrated prior to crystallization experiments.

2.2.9 CRYSTALLIZATION OF BDV MACROMOLECULAR COMPLEXES

All protein-protein-, protein-RNA-complexes and RNA were purified to homogeneity and sent, at different concentrations (Table 5) to the High-throughput crystallization facility (EMBL Grenoble, https://htxlab.embl.fr). Except BDV 5'-RNA (sent in 2mM $MgCl_2$) all proteins were sent in buffer 1. N-5'-RNA complexes were purified as described in (see 2.2.3)

After screening for initial hits, N-P' crystals were grown in hanging drops. Crystals grew (amongst similar conditions) at room temperature using reservoir buffer containing 0.1M Hepes, pH 7.0; 2M Ammoniumphosphate by pipetting 1-2µl of protein solution

into 1-2µl of reservoir solution. Several attempts were made to improve the crystal morphology from plates to singular 3-dimensional crystals, including the addition of 1-20% Glycerol, raising and lowering the concentration of the precipitant, pH screen, buffer exchange and adding the Hampton additive screen. A better crystal was obtained by addition of 30mM $CaCl_2$. All N-P constructs led to crystals of identical morphologies which grew in similar conditions. They contained either high molarities (0.8-2M) of Ammoniumphosphate or –sulphate and a pH between 7 and 8.5. Further screening around the initial conditions was performed, but crystal improvement was not successful.

Construct	Concentration
BDV N-P’	10, 6 and 3mg/ml
BDV N-P_{67-201}	6 and 3mg/ml
BDV N-$P_{169-201}$	7 and 3.5mg/ml
N+ $P_{195-201}$ (DEWDIIP)	7mg/ml + peptide 1:1, 1:2 and 1:3 molar excess respectively
P’	15, 10 and 5mg/ml
N-P’-X	6 and 3mg/ml
N +BDV 5’-RNA (25nt)	18, 5 and 4mg/ml
BDV 5’-RNA (25nt)	2, 1 and 0.5mg/ml

Table 5: Concentration of constructs sent to the crystallization platform

BDV N and putative BDV N-$P_{169-201}$ (Figure 13) crystals grew at room temperature in 0.1M Bicine pH9 or MES pH 6/6.5 and 5-20% PEG 6000. No further screening was necessary in this case.

N crystals were soaked with the P derived C-terminal peptide $P_{195-201}$ (DEWDIIP), applying the following strategies:

1. 0.5µl of peptide (in 20mM Hepes, pH 7.8) was directly added to a 2µl drop, containing crystals, thus that the molar N to peptide ratio was 1:3.
2. The peptide was taken up in the respective condition and Hepes pH7.8 and NaCl were added thus that conditions corresponded to those, the nucleoprotein crystals grew in. 1µl of the mixture was added directly to the crystal-containing drops, at the ratio corresponding to 1.
3. The peptide was treated as in 2. 2µl of the mixture were pipetted onto a cover slip and nucleoprotein crystals were fished out of their initial drop and transferred to the new drop which was containing the peptide.

All other crystallization attempts from table produced no initial hits.

N-P' crystals were cryo-protected in reservoir solution containing 20-30% glycerol, whereas the best diffracting crystal was frozen with 25% glycerol. N (-$P_{169-201}$) and N crystals soaked with $P_{195-201}$ were frozen with reservoir solution, containing 20% glycerol. Crystals were harvested in nylon loops and plunged into liquid nitrogen (for storage until data collection) or directly frozen in the beam line cryo-stream. Complete data sets were collected at ESRF beam lines ID23-2 and ID14-2.

2.2.10 N-RNA and N-P'-RNA interaction

SEC purified N and N-P' were incubated overnight at 4°C with a 2M excess of BDV-3'-Leader-, 5'-Trailer- and total *E. coli* RNA in buffer 3 (20mM Hepes, 20 mM NaCl, pH 7,8) and in absence and presence of Urea (1, 2, 3 and 4 M). The effect of Urea on N and N-P' alone was tested by incubation with 4 M Urea. Samples were analyzed by 6.5% native PAGE and stained with Coomassie Brilliant Blue after verifying RNA presence by Methylene Blue staining. Furthermore, N, N-P' and P' were incubated overnight at 4°C with a 2M excess of BDV-5'-Trailer RNA (125 nucleotides) to verify that P' does not interact with RNA. Samples were analyzed by discontinuous gradient 6.5 on 16% native PAGE and stained with Coomassie Brilliant Blue after verifying RNA presence by Methylene Blue stain. The same experiments were performed with N carrying specific point mutations.

2.2.11 ELECTRON MICROSCOPY.

BDV-N was purified by SEC and analyzed by electron microscopy (Electron microscopy platform, Grenoble) using negative staining with sodium silicotungstate (pH 7.0). The grids were observed using a JEOL 2010 FEG electron microscope working at 100kV with a nominal magnification of 40.000 (Schoehn *et al.*, 2001). Gel filtration purified N was incubated with BDV-5'-Trailer- RNA (125 nucleotides) in buffer 3 and purified by glycerol gradient centrifugation. The gradient was continuous from 45% glycerol at the bottom to 25% at the top. Glycerol was buffered with buffer 3. Samples were spun for 16h at 4°C and 40000 rpm in an ultracentrifuge (Beckman). Samples present in the bottom fractions were collected and analyzed by electron microscopy.

2.2.12 RNASE PROTECTION ASSAY

N-RNA and N-P'-RNA were purified as described above for electron microscopy analyses. Complexes were incubated for 15 min at 37° with 0.05, 0.1, 0.2 and 0.5µg/ml RNase A (Roche). Controls were performed with buffer 3 instead of RNase A.

After incubation samples were treated with RNAGuard RNase inhibitor (GE Healthcare) and stored on ice prior to further treatment. One half was boiled with 8M Urea before subjection to a 16% denaturing polyacrylamide-urea gel. The gel was stained with ethidiumbromide. The other half was mixed with a 4x native PAGE sample buffer and samples were separated by 6.5% native PAGE. The bands were visualized with Coomassie Brilliant Blue staining.

2.2.13 RNASE PROTECTION ASSAY WITH DIG-LABELED RNA.

DIG-labeled BDV-5'-RNA (125 nucleotides) was incubated with N and N-P' or buffer 3 as a control. N-RNA and N-P'-RNA were incubated for 15min at 37°C with 0.05, 0.1 and 0.2µg/ml RNase A. After incubation samples were treated with RNAGuard RNase inhibitor (GE Healthcare) and subjected to 18% denaturing Urea PAGE. Samples were electro-blotted to a nylon membrane (Sigma) according to (Günzl *et al.*, 2002). Band detection was performed with alkaline phosphatase-conjugated anti-DIG-Fab-fragments

(DIG northern starter kit, Roche), following the manufacturers protocol for direct detection.

3 RESULTS

3.1 EXPRESSION AND PURIFICATION OF BORNA DISEASE VIRUS PROTEINS

Previous studies (like *in silico* secondary structure and disorder predictions, Figure 13) indicated that the full-length BDV phosphoprotein was not suitable for crystallization. Furthermore, its high susceptibility to degradation and tendency to precipitate at higher concentrations, lead to the decision to express and purify the N-terminal truncated isoform of P termed P' (aminoacids 56-201). Thus, P' has been used for most of the experiments, since it exhibits better solubility at higher concentrations and higher stability upon storage.

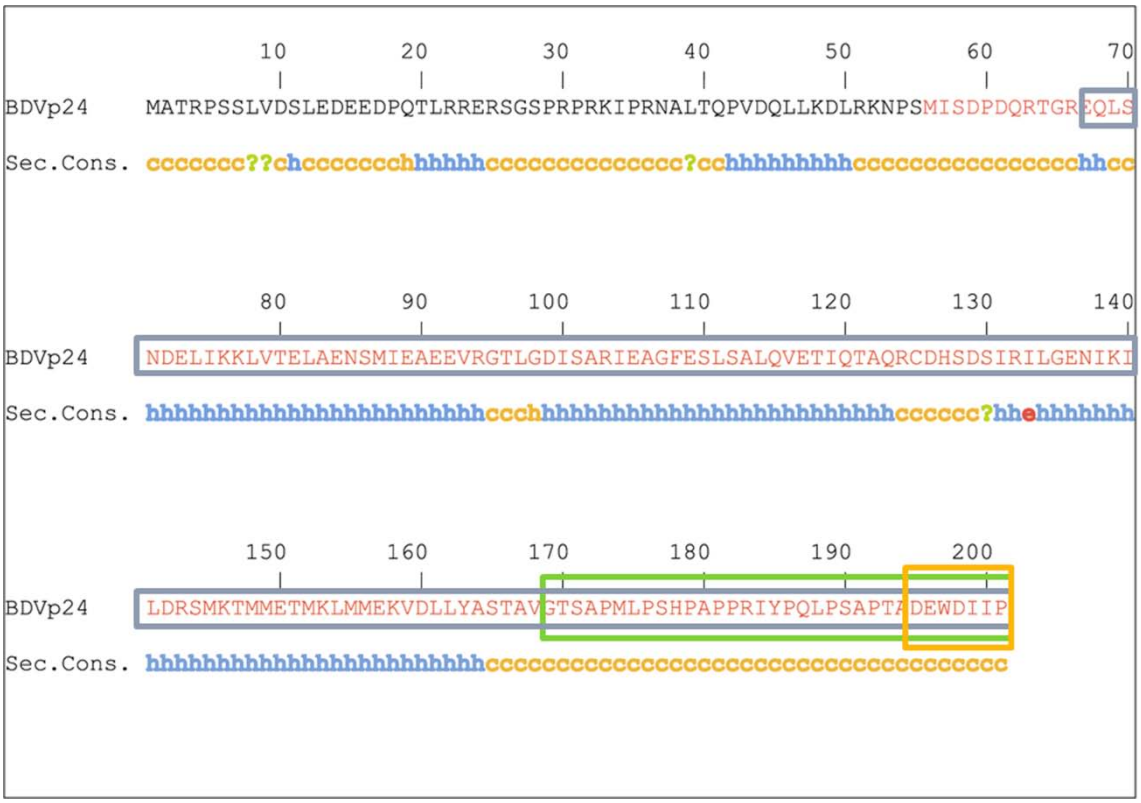

Figure 13: Secondary structure consensus prediction for BDV P.
The Sequence of P' is depicted in red, the boxes indicate the other P constructs used for crystallization: P_{67-201} (blue), $P_{169-201}$ (green), $P_{195-201}$ (yellow). The prediction is displayed below the sequence as follows: Alpha helix(Hh), Extended strand (Ee), Random coil (Cc), Ambiguous states (?). Prediction was performed on the NPS@ platform (http://npsa-pbil.ibcp.fr).

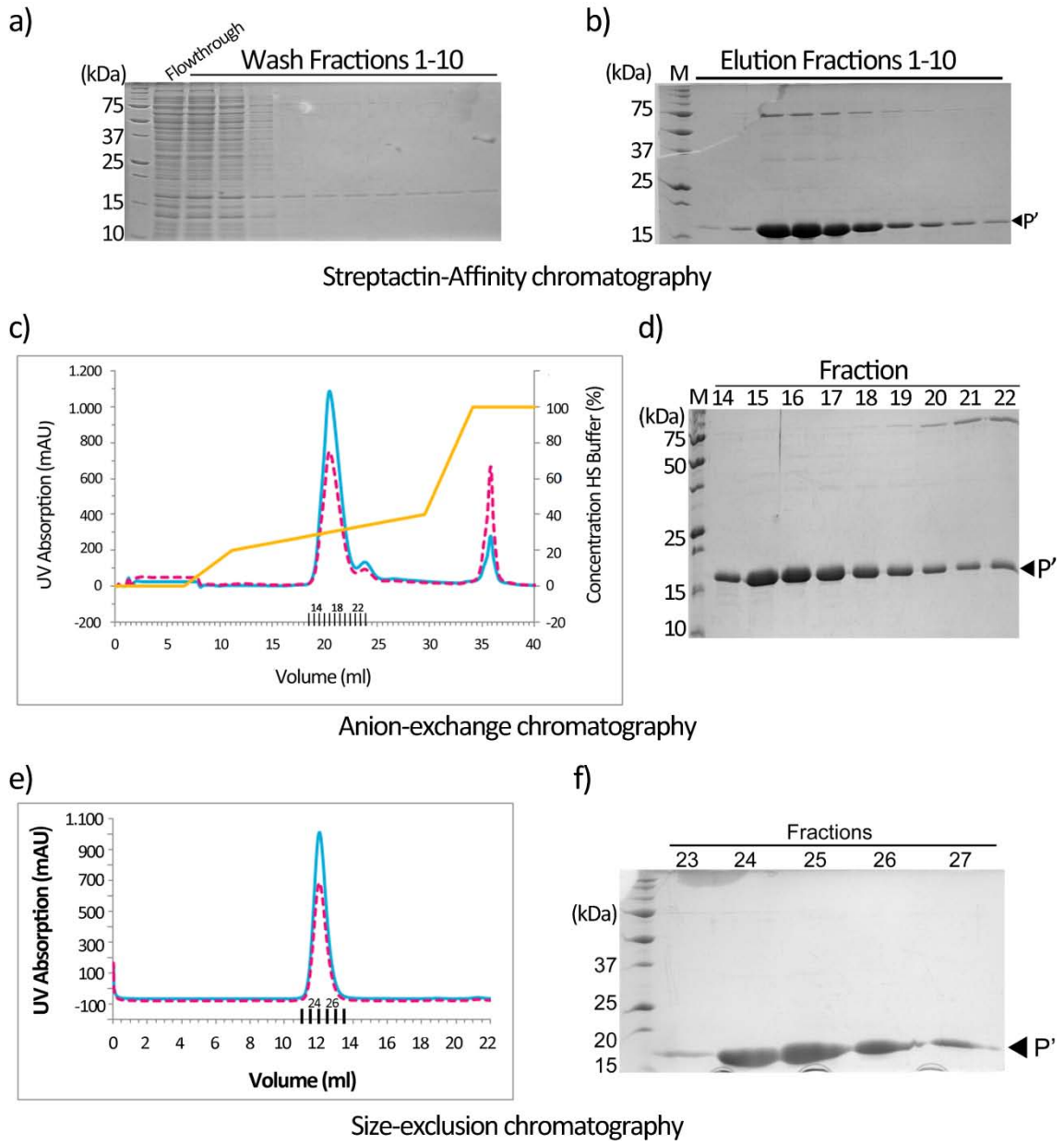

Figure 14: Purification of BDV P'
Denaturing SDS-PAGE analysis of affinity purification of BDV P', containing a non-cleavable N-terminal StrepTagII, with **a)** showing the flowthrough and the different washing steps and **b)** the elutions with Desthiobiotin from a Streptactin sepharose column. **c)** Anion exchange chromatography elution profile of BDV P'. The blue line shows the UV absorption (left ordinate axis in mAU) at 280, the dashed red line at 260nm. The concentration of the high salt (HS) buffer (right ordinate axis, in %) is depicted by a yellow line. The peak fractions are indicated by bold black bars on the X-axis, together with the elution volume. **d)** Analysis of anion exchange peak fractions from c) by 16% denaturing SDS-PAGE. P' bands are indicated by an arrow. Fractions 14-18 were pooled and subjected to gelfiltration. **e)** Gelfiltration elution profile and **f)** analysis of the indicated fractions by 16% denaturing PAGE. All bands were visualized by Coomassie brilliant blue. The molecular weights in (kDa) of marker proteins (M) are indicated on all gels.

As all other BDV proteins, P' was expressed as a recombinant protein with a cleavable or non-cleavable (as in Figure 14) StrepTagII in *E. coli,* allowing affinity purification via a

Streptactin matrix (IBA, Göttingen), (Figure 14 a). The protein was finally purified to homogeneity by anion exchange and size exclusion chromatography (Figure 14 c-f).

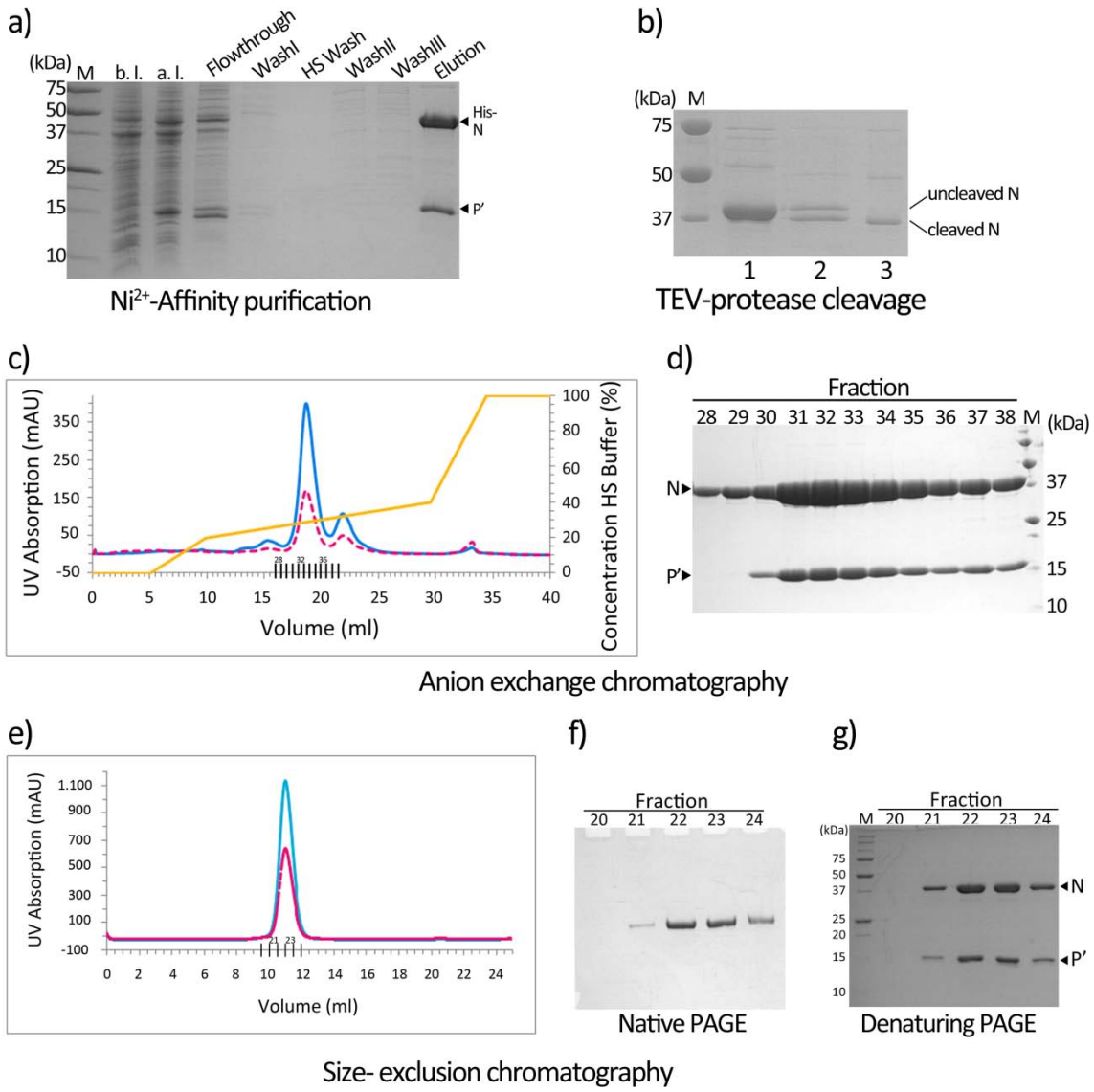

Figure 14: Purification of BDV N-P'

a) Denaturing PAGE analysis of N-P' expression in *E. coli* before (b.I.) and after induction (a.I) and purification of the protein complex by a Ni^{2+}-charged chelating Sepharose column with the different washing steps, including a high-salt (HS) wash. The proteins are indicated by arrows. **b)** His-tag removal from N by TEV protease cleavage. Lane 1 shows uncleaved N, lanes 2 and 3 show N after cleavage, before and after purification via a second Ni^{2+}-charged chelating Sepharose column, respectively. **c)** Anion exchange chromatography elution profile of N-P'. The blue line shows the UV absorption (left ordinate axis in mAU) at 280, the dashed red line at 260nm. The concentration of the high salt (HS) buffer (right ordinate axis, in %) is depicted by a yellow line. The peak fractions are indicated by bold black bars on the X-axis, together with the elution volume. **d)** Analysis of anion exchange peak fractions from c) by 16% denaturing SDS-PAGE. N and P' bands are indicated by arrows. Fractions 32-35 were pooled and subjected to gelfiltration. **e)** Size-exclusion chromatography elution profile and **f)** analysis of the indicated (bold bars on X-axis) fractions by 16% denaturing PAGE and **g)** 7% native PAGE. All bands were visualized by Coomassie brilliant blue. The molecular weights in (kDa) of marker proteins (M) are indicated on all gels.

The protein eluted at 11.31ml from a Superdex 200 (GE Healthcare) gelfiltration column (Figure 14e). Similarly BDV N and P' were co-expressed in *E. coli* (Figure 15), whereas the untagged P' was co-purified with a His-tagged nucleoprotein by a Ni^{2+}-charged affinity resin (Figure 15).

After cleavage of the His-tag by TEV-protease, the N-P' complex was purified to homogeneity by anion exchange and gelfiltration (elution peak at 10.77ml) (Figure 15c-g). Both purified recombinant P' and N-P' complexes eluted from a size exclusion chromatography column as single peaks (Figure 14e and 15e).

3.2 PROPERTIES OF P' AND N-P' OLIGOMERS

The molecular weight determined by multi-angle laser light scattering (MALLs) revealed a molecular weight of 75.57± 0.35 kDa for P' corresponding to a tetramer (the theoretical MW of a tetramer is 75.397 kDa) (Figure 15a) and of 235.3± 9 kDa for the N-P' complex consistent with a P' tetramer interacting with the N tetramer (calculated MW of the heterooctamer is 233.99 kDa) (Figure 15b).

These results were further confirmed by chemical cross-linking of N-P' complexes or P' alone (see 2.2.6). Therefore, 0.5 mg of N-P' and P' were incubated with different concentrations of Glutaraldehyde and ethylene glycol bis[succinimidylsuccinate] (EGS). The cross-linked proteins were analyzed by SDS-PAGE as shown in Figure 16. Since BDV-P' carried an N-terminal Strep-Tag and a TEV-protease cleavage site, the P' control migrates at ~23kDa instead of 16kDa. Cross-linking revealed intermediate states of P' (migrating at ~ 50 and ~70 kDa) and the fully cross linked P' migrating at ~90 kDa (Figure 16a). BDV N-P' cross-linking is shown in figure 16b. Multiple bands are visible between ~50 and 200 kDa at lower cross-linker concentrations. The highest bands migrate at ~250 kDa, which is roughly consistent with a hetero-octameric N-P'-complex.

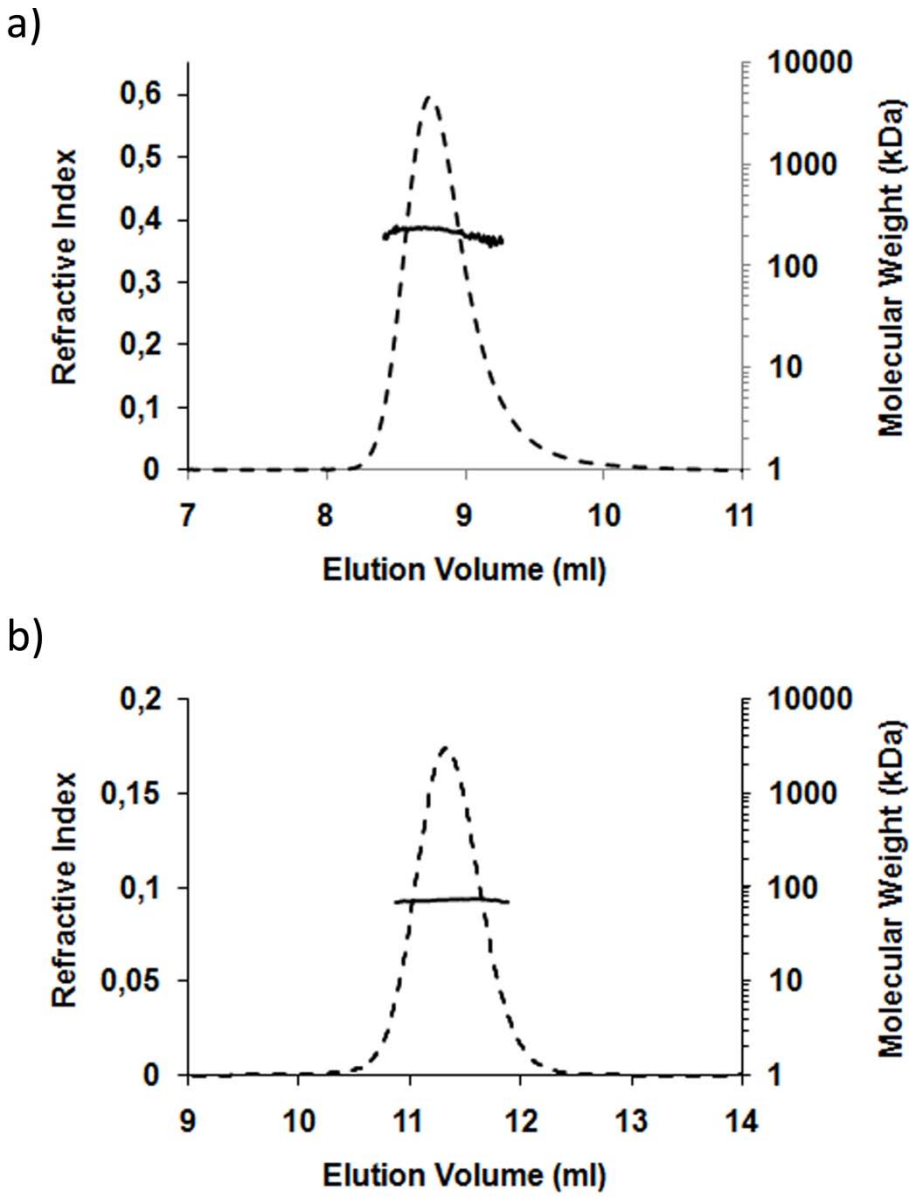

Figure 15: Molecular weight of BDV-P' and BDV-N-P' determined by multiangle laser light scattering and refractometry combined with size-exclusion chromatography (MALLS).
a) BDV-P' and **b)** BDV-N-P' SEC elution profiles revealing molecular weights of ~75 kDa for P' and ~235 kDa for N-P'. The dashed line shows the elution profile 24 monitored by excess refractive index (left ordinate axis). The black line shows the molecular mass distribution (right ordinate axis) determined by MALLS and refractometry data.

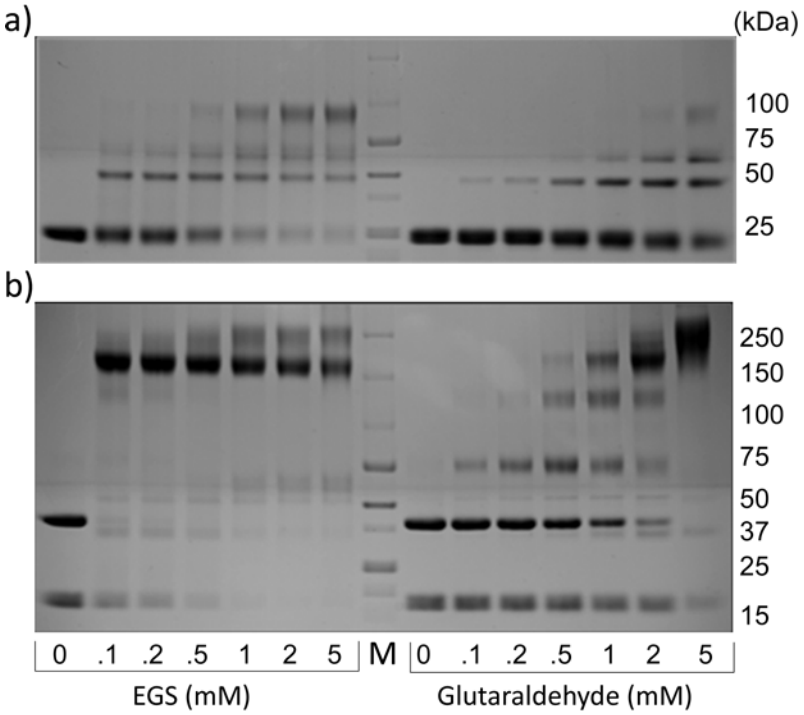

Figure 16: Chemical crosslinking of BDV P' and N-P'
a) Analysis of BDV P', cross-linked with different concentrations of EGS and Glutaraldehyde, by Tris-Tricine discontinuous-gradient (10 over 16%) PAGE. **b)** The same as a) but with the BDV N-P' complex. The used cross-linking reagents EGS and Glutaraldehyde and their concentrations are indicated at the bottom in milli Molar (mM), M indicates the lane with the marker proteins. Bands were visualized with Coomassie brilliant blue.

3.3 AFFINITY OF THE N-P' INTERACTION

The affinity of the N-P' interaction was determined by surface plasmon resonance (SPR) measurements (see 2.2.7).

Binding of BDV-P' to immobilized BDV-N was performed with different analyte (P') concentrations. The experiments showed rapid protein-protein association and fast dissociation (Figure 17a). Binding association curves enabled the calculation of the KD by plotting SPR values for each injection as a function of the concentration of BDV-P' (08-16µM) added. A bimolecular binding model was determined based on the interaction data and used to compute the binding constant (KD) of ~ 1.66µM, fitting the experimental data with a closeness of fit χ^2 of 1.6. Individual rate constants were determined for k_{on}, k_a to be $1.8x10^3$ (1/ms) and for the k_{off}, k_d to be 3x10-3(1/s). Since deletion of the C-terminal four residues of P' abrogates N interaction (Schwemmle *et al.*, 1998) a peptide composed of the C-terminal 7 amino acids (sequence: DEWDIIP, $P_{195-201}$)

was used as analyte. Although no response signal was detected with this peptide alone (data not shown), it showed an effect in a competition assay. Incubation of the peptide with full-length BDV-P' as analyte prior to injection over immobilized BDV-N decreased the SPR-signals proportional to the increase of peptide concentration (Figure 17b). This confirmed that the C-terminal seven P' residues are important for N interaction, which was further corroborated by pull-down assays. Deletion mutants of P' lacking either 1 (P-CΔ1) or 5 C-terminal amino acids (P-CΔ5) (see Figure 17c) were used to pull down N upon co-expression. P' was labeled with a Strep-TagII and N carried a His-Tag. Full-length P' co-eluted with N (Figure 17c, lanes 1 and 4) as well as P-CΔ1 (Figure 17cc, lanes 2 and 5) but not with P-CΔ5 using pull down via the Strep- or the His- Tags (Figure 17c, lanes 3 and 6).

Together these results suggest that a short C-terminal linear peptide region of P is required for a low affinity interaction with N.

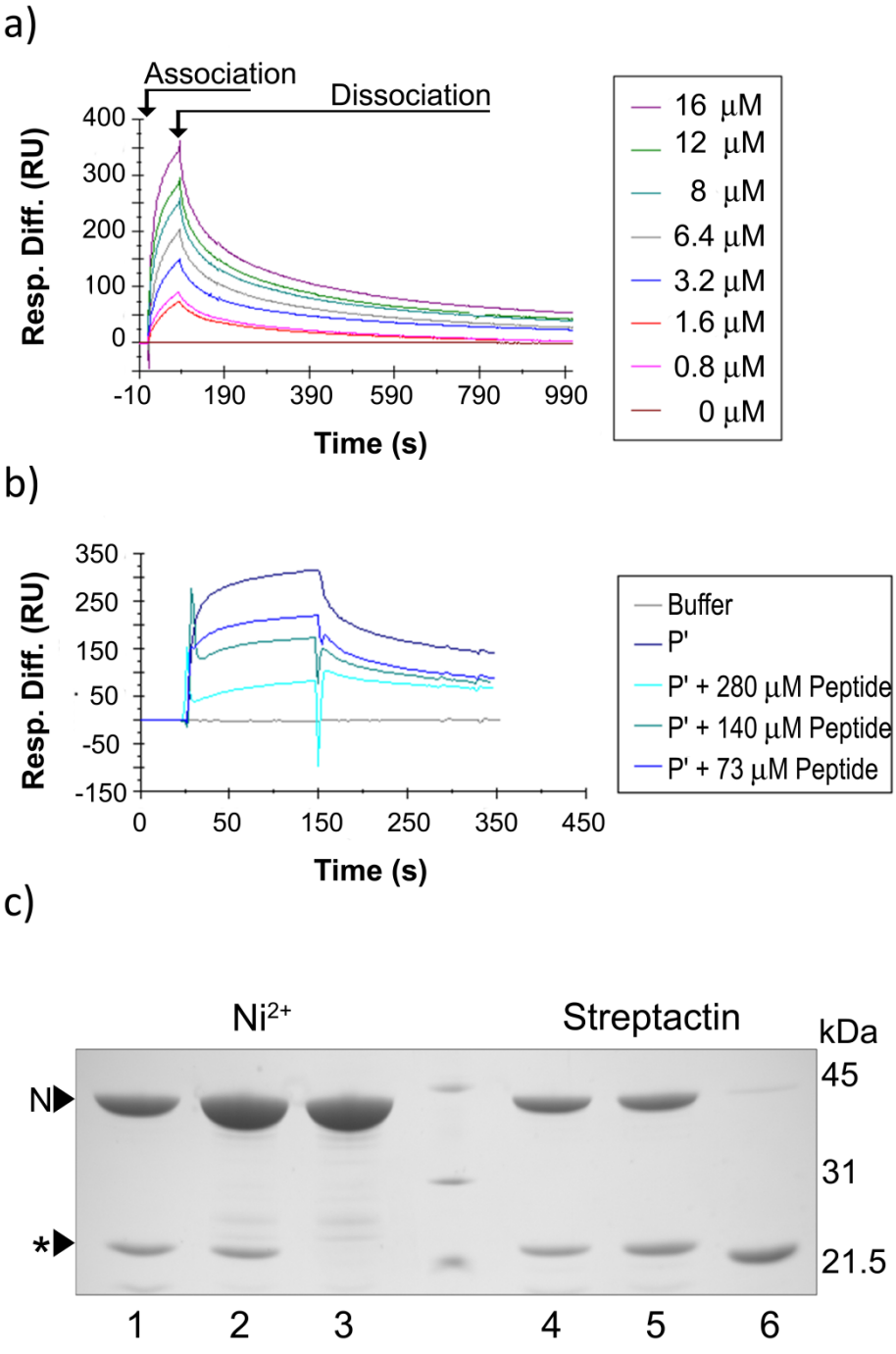

Figure 17: Characterization of the N-P' interaction.
a) Specificity of BDV-P' binding to BDV-N Plot of sensorgrams associated to injection of BDV-P (c=0-16µM) to immobilized BDV-N. The arrows indicate the association and dissociation phase respectively. The dissociation constant was evaluated according to a 1:1 binding model with drifting base line as 1.66µM. **b)** Decrease of interaction between BDV-P' and BDV-N due to the blocking of binding sites on BDV-P' by a C-terminal peptide of the BDV phosphoprotein with a length of 7 amino acids (see Figure 13, yellow box). BDV-P' (6.4µM) was injected over the sensor chip surface coupled with BDV-N after prior incubation at 4°C of 30 min with the peptide (c=0-280µM). **c)** Pull down assay of N with C-terminal P' mutants. All pull downs were performed with Ni2+-agarose beads and streptactin resin simultaneously. Proteins were separated by 16% SDS-PAGE and visualized by Coomassie brilliant blue stain. The asterisk indicates the bands of the different P proteins StrepTagII-P' (lanes 1 and 4), -P-CΔ1 (lanes 2 and 5) and –P-CΔ5 (lanes 3 and 6). Lanes 1-3 indicate Ni^{2+}-, lanes 4-6 indicate streptactin-purified protein.

3.4 CRYSTALLIZATION AND PRELIMINARY X-RAY ANALYSIS OF THE BDV NUCLEOPROTEIN-P' COMPLEX

After concentration of the purified complex (see Figure 15) to ~5mg/ml it was exposed to 576 crystallization conditions at 20°C in sitting nano-drops (*High-Throughput crystallisation platform*, EMBL Grenoble). Crystals were obtained after two weeks in numerous conditions (see 2.2.9). Reproduction of the initial hits using the same protein sample has been successful in larger drops of 2µl. Those crystals were not yet subjected to an X-ray beam, but washed with mother liquor prior to pooling and analysis by SDS-PAGE. Neither Coomassie nor subsequent silver staining of the gel revealed interpretable bands. Since neither protein nor crystals were left, fresh N-P' samples were purified. However, crystals could not be reproduced in these conditions. The failure may be explained by the age of the samples and resulting protein degradation. While the age of the new batches did not exceed 4 days; the age of the initial sample however, surpassed two weeks which probably lead to protein degradation that may have facilitated crystallization. Reproducible crystals were finally obtained in conditions containing high concentrations of Ammoniumphosphate or –sulphate (Figure 18).
The crystals were made up of thin plates which were stuck within and overlaying each other (Figure 18a). Subjection to an X-ray beam gave rather poor diffraction (~ 6Å) and crystals had to be improved with an additive screen (Hampton).

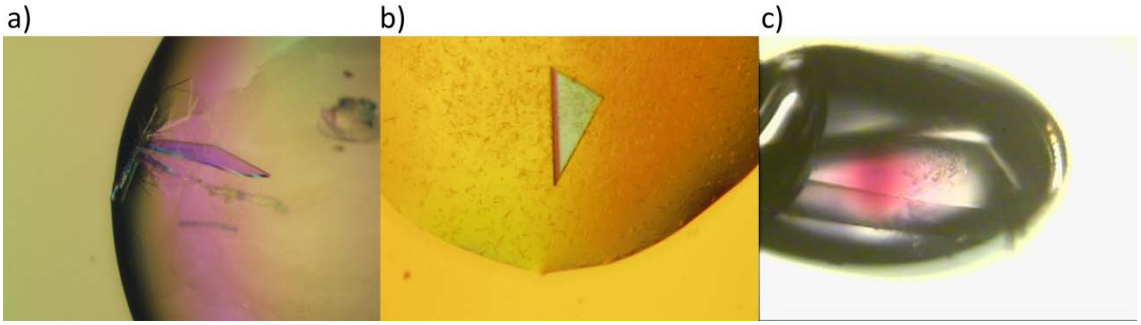

Figure 18: Crystals of N-P'
a) Crystals obtained with BDV N-P' in 0.1M Hepes, pH 7.0; 2M Ammoniumphosphate. **b)** Crystal grown at the same conditions as in a) with 30mM $CaCl_2$ as an additive. **c)** Same crystal as in b) in a nylon loop after exposure to an X-ray beam.

A single triangular crystal (within vast numbers of microcrystals) grew after of 30mM $CaCl_2$ were added to the initial condition. Observed through a light microscope with polarizing optics, the crystal showed high birefringency and sharp edges.

A complete data set was collected at ESRF beam line ID14-2 (Grenoble, France). The crystal diffracted to 4Å (Figure 19) and belongs to space group C2 with unit cell parameters of a= 276Å, b= 81Å and c= 81.5Å. Data were indexed and integrated with the *MOSFLM* (Leslie, 1992) and *XDS* (Kabsch, 1993) packages and scaled using *SCALA* (Collaborative Computational Project, 1994). Data-collection statistics are listed in Table 6. Structure determination was attempted by molecular replacement using *MOLREP* (Collaborative Computational Project, 1994) and a search model corresponding to BDV N (Protein Data Bank code 1PP1) (Rudolph *et al.*, 2003). Unfortunately, no extra density indicated the presence of P' or a P'-derived peptide.

DATA COLLECTION[a]	**BDV N-P'**
Resolution (Å)	4.04- 29.92
Rmerge (%)	14
Space group	C2
Unit Cell parameters a, b, c (Å)	276x81x81.5
α β γ	90° 98° 90º
Number. of Molecules/ Asymmetric Unit[b]	1
Number of Reflections	13840
Wilson B factor (Å^2)	122.474

Table 6: Crystal Data of BDV N-P'
[a]Data were collected from single crystals at the beamline ID14-2 at the European Synchrotron Radiation Facility (ESRF), Grenoble, France.
[b]Estimated using Matthews coefficient probabilities (corresponding solvent content of 60.88 %).

One explanation is that P' degraded and remained undetected due to the rather poor resolution; or N crystallized alone because of the dissociation of N-P' in the respective condition. Further crystal improvement by modulation of the initial hit conditions (see 2.2.9) led to the formation of large, birefringent crystal plates with mostly irregular edges. All of them were tested on beamline ID 23 (ESRF Grenoble) but turned out to be of inorganic origin. The high abundance of salt crystals and the unsuccessful reproduction of protein crystals indicate that the latter is probably dependent on a highly sensitive equilibrium within the crystallisation drop.

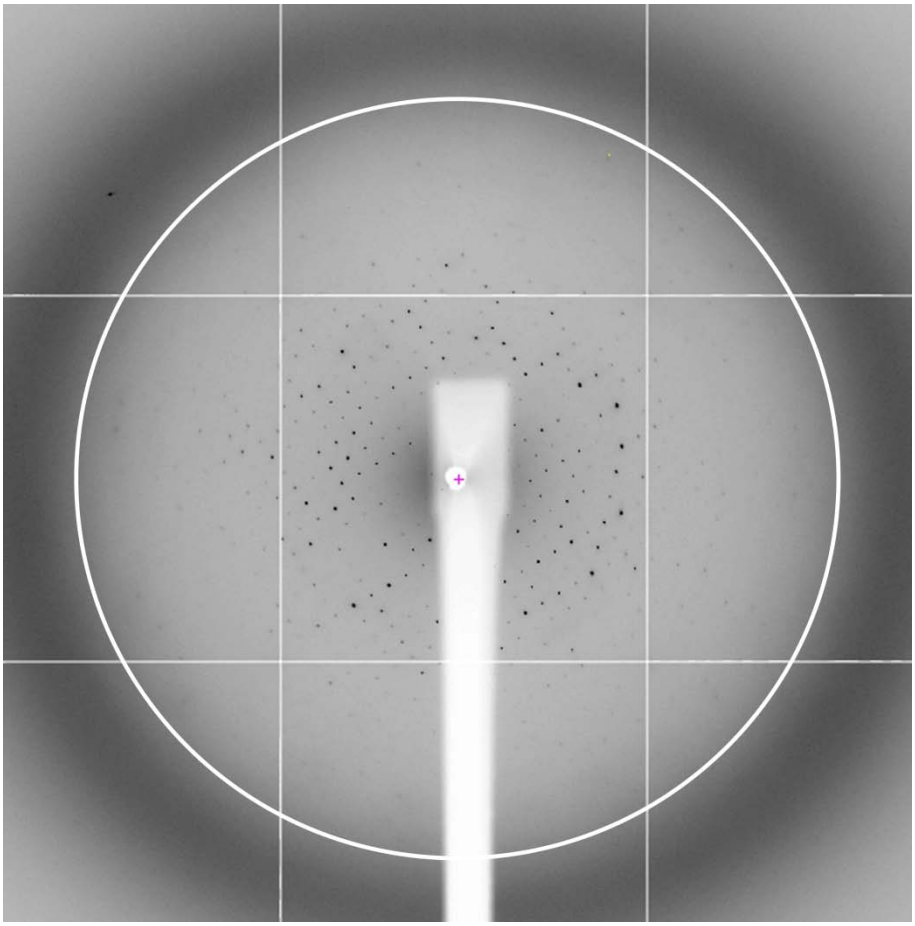

Figure 19: X-ray diffraction pattern of BDV N-P'
The white circle marks 4Å.

3.4.1 CHANGE OF STRATEGY: CRYSTALLIZATION OF BDV N-P_{67-201} AND N-$P_{169-201}$

Compact globular proteins are rather suitable for crystallization than those exhibiting high degrees of flexibility. Thus, limited proteolysis is used as a tool to identify compact protein segments, since they are generally not accessible for proteolytic enzymes, such as e. g. trypsin. Purified N crystallizes easily and exhibits a compact structure, thus I assumed that P' was responsible for the unsuccessful crystallization trials (see 3.3 and 2.9), as it was predicted to contain large disordered regions (Figure 13). In consequence, P' was subjected to limited proteolysis with trypsin (Figure 20) to identify a stable core, rather suitable for co-crystallisation with the nucleoprotein.

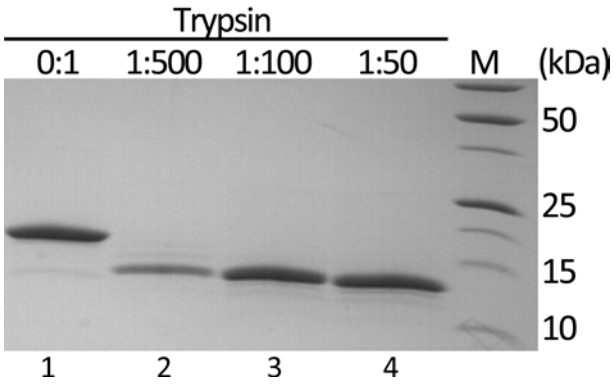

Figure 20: Limited Proteolysis of BDV P' with Trypsin
50 µg of purified P' was incubated for 10 min at 37°C with protein:trypsin ratios of 1:500 1:100 and 1:50 (lanes 2-4). A reaction without trypsin was carried out as a control (lane 1). Reactions were stopped by boiling the sample in SDS sample buffer, and the digested products were analyzed by 16% denaturing SDS-PAGE. Marker (M) bands are visible at the very right. Stain: Coomassie brilliant blue.

A band migrating at ~14 kDa was identified and sent for N-terminal sequencing. The identified sequence started at Glu67 and a respective construct (P_{67-201}) was generated for co-crystallisation trials with the BDV nucleoprotein. Figure 21 shows the last purification step of the N-P_{67-201} complex. Crystals appeared, but did not differ in morphology or growth-conditions from those shown in Figure 18a. This led to the assumption that further N-terminal truncation of P_{67-201} was necessary.

The consensus disorder prediction (Figure 13) of BDV P showed a disordered stretch of ~30 amino acids, comprising the interaction domain with N at the very C-terminus. Folding is sometimes induced on regions of intrinsic disorder upon association with an interaction partner (Wright & Dyson, 1999; Uversky, 2002; Uversky, 2002). Assuming this was probably the case for the c-terminal region of BDV-P upon interaction with N, a new construct was generated. It comprised the C-terminal 33 amino acids of P and was expressed as a His-GST-fusion peptide ($P_{169-201}$, Figure 13, green box).

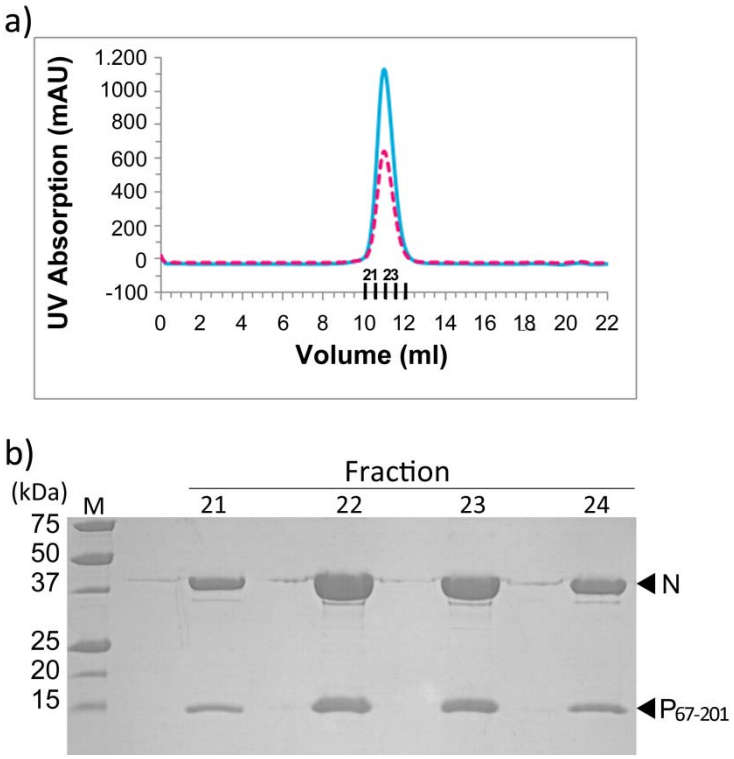

Figure 21: Purification of N-P_{67-201}
a) Size-exclusion chromatography profile of BDV N-P_{67-201} after affinity chromatography, TEV- cleavage and anion-exchange. UV absorption peak is depicted in red at 260nm and in blue at 280nm. Fractions, taken for analysis and crystallisation are marked by bold black bars on the X-axis. Every second fraction number is depicted **b)** Denaturing SDS-PAGE analysis of size exclusion chromatography fractions on 16% gel. M indicates the marker proteins. Bands were visualized with Coomassie brilliant blue.

$P_{169-201}$ was co-purified to homogeneity in complex with N (Figure 22) and sent to the *High-Throughput crystallization facility* (EMBL Grenoble) for crystallization. Again, crystals similar to those in figure 18a appeared under the same respective conditions after two days. Hence, upscaling and improvement was not directly performed, but the complex was further treated with the dimethylamine-borane complex (ABC, Fluka). Treatment with ABC leads to the methylation of lysines, exposed on the protein surface, which reduces protein flexibility and may thus facilitate crystallization (see 2.2.8)

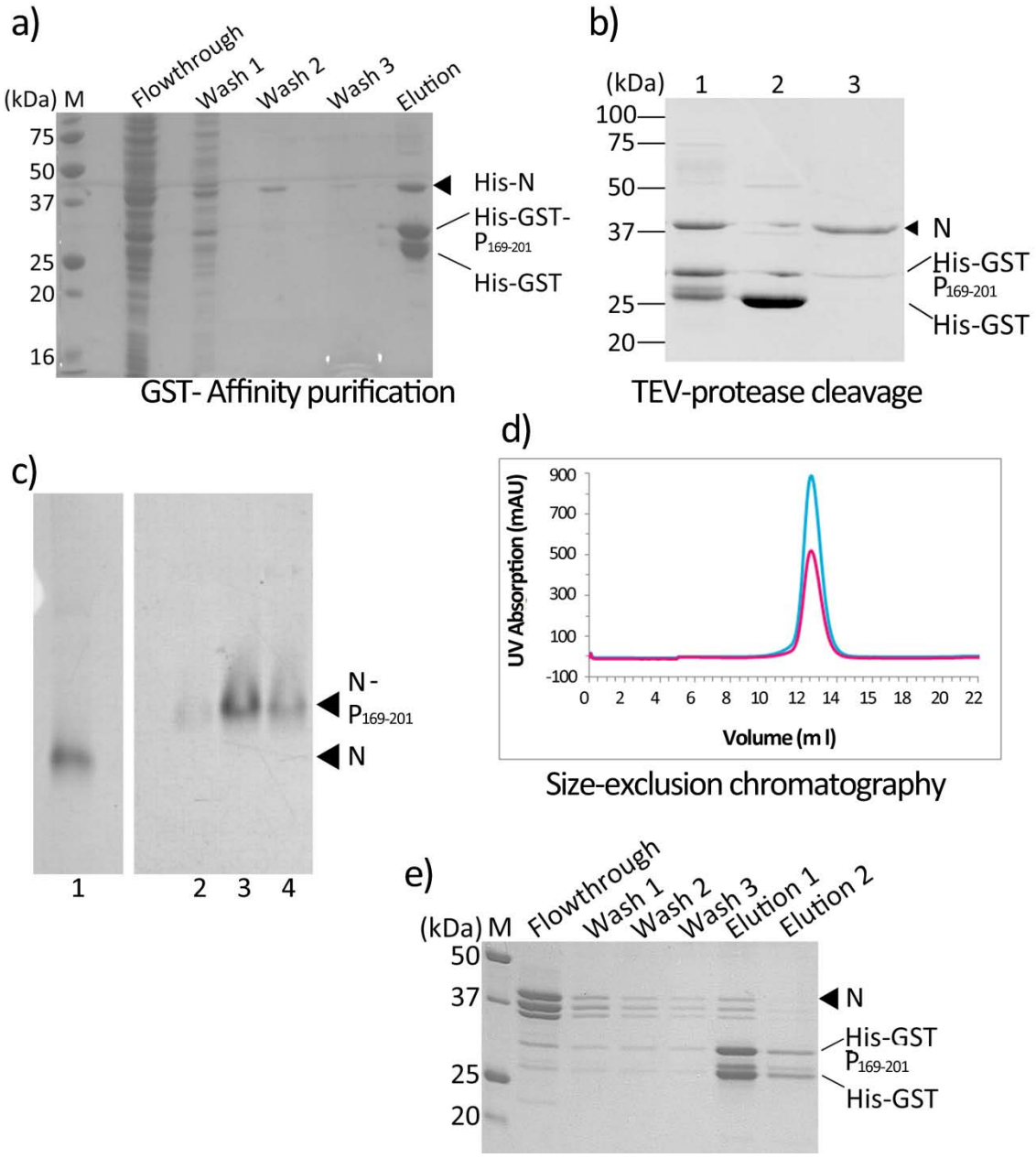

Figure 22: Purification of N-$P_{169-201}$

a) Denaturing SDS-PAGE analysis of glutathion-S-transferase (GST) affinity-purification of His-N with His-GST-P-NΔ168 from a glutathion-sepharose column. Flowthrough and washing steps are indicated. Proteins were eluted with 10mM reduced glutathion. **b)** Affinity tags were cleaved off with TEV-protease and proteins were subjected to a Ni^{2+}-charged chelating sepharose column for separation from the affinity tags. Samples were analysed by 16% SDS-PAGE. Lane 1 shows an uncleaved protein complex, lane 2 the elution sample containing His-GST and lane 3 shows N in the flowthrough. Since $P_{169-201}$ could not be deteced, the sample was subjected to **c)** 7% native PAGE together with purified and cleaved N as a control (lane 1) in order to verify complex assembly (lanes 2-4). Note that both N-control and complex were on the same gel. **d)** Size-Exclusion chromatography profile of N-$P_{169-201}$ of the pooled samples from c) lanes 2-4. The blue line depicts the UV absorption per ml at 280nm, the red line at 260nm. Stain: Coomassie brilliant blue. All proteins are indicated (arrows and bars). **e) SDS-PAGE analysis of a pulldown experiment after mixing ABC-treated N with His-GST-$P_{169-201}$.** Sample was subjected to a glutathion-sepharose column. After washing (flowthrough and washing steps are indicated) proteins were eluted with 10mM reduced glutathion. Note that 3 bands migrate around 37 kDa, mostprobably due to partial degradation of BDV N.

Proteins were again subjected to the crystallization robot and simultaneously sent for mass spectrometry (MALDI-TOF) (PSB platform, IBS, Grenoble) to verify that the N-$P_{169-201}$ complex sustained ABC treatment. Crystals appeared 3 days after in 5-15% PEG 6000 and 100mM of the buffers Bicine pH 9 or MES pH 6.5. The crystal morphology corresponded to those in figure 23a, generally obtained with the nucleoprotein alone. Larger crystals were produced, which diffracted to ~1.7 Å. However, the structure obtained by molecular replacement revealed only the nucleoprotein. The data were identical to those reported by Rudolph et al., (Rudolph *et al.*, 2003).

Regarding the crystal lattice, the N-tetramers were tightly packed within the crystal, which hardly left any space for another compound to bind. Additionally, the putative interaction domain with BDV-P (amino acids 51-100), (Berg *et al.*, 1998)) is involved in crystal contacts with the C-terminal domain of a neighbouring molecule.

The results from mass spectrometry (MALDI-TOF) of an N-$P_{169-201}$ sample confirmed that $P_{169-201}$ was not present in the sample anymore after treatment with ABC. The sample used for crystallisation had a mass of 41505 Da, which is approximately consistent with the theoretic mass of a nucleoprotein tetramer with 20 methylated lysines (the mass increases by 28 Da per methylated lysine; the total number of lysines in the nucleoprotein is 21). The mass was identical to the ABC –treated N-control, indicating that ABC treatment of N-$P_{169-201}$ probably led to disruption of the complex and precipitation of $P_{169-201}$.

Thus, I tried to assemble the complex after independent purification and ABC treatment of one or the other protein. Both His-N and His-GST- $P_{169-201}$ were purified independently and subjected to ABC treatment at two different concentrations (0.1mg/ml and 5mg/ml). After filtration, the His-GST-$P_{169-201}$ sample did not absorb UV light (at 280, 260 and 230nm) anymore, indicating that it precipitated upon lysine methylation. ABC treated N however, partially degraded and did not co-elute with non-treated His-GST-$P_{169-201}$ from a glutathion-sepharose column (Figure 22e). This suggests either that lysines may be strongly involved in P-association or that the induced stability of N interfered with the interaction of the two proteins. Due to this outcome, a different strategy was applied.

3.4.2 CO-CRYSTALLIZATION OF THE BDV NUCLEOPROTEIN WITH THE PHOSPHOPROTEIN-DERIVED PEPTIDE $P_{195-201}$

A short peptide (Figure 13, yellow box) of 7 amino acids from the very C-terminus of P ($_{195}$DEWDIIP$_{201}$, $P_{195-201}$) has been shown to be sufficient for interaction with the nucleoprotein (see 3.3, Figure 17b). Assuming that such a short peptide may not interfere with crystal formation, this peptide was added to purified N 12h prior to subjection to the crystallisation robot (see 2.2.9). No crystals appeared except those shown in figure 18a under the same respective conditions, which were of poor diffraction earlier. Thus, we decided to crystallise N alone with 10% PEG 6000 and 0.1M MES, pH 6 and soak the thus generated crystals with the peptide.

3.4.3 SOAKING OF BDV NUCLEOPROTEIN CRYSTALS WITH $P_{195-201}$

Two crystal morphologies were obtained for N, exhibiting different stabilities in respect of dehydration of the drop: Figure 23a shows highly birefringent rhombic bipyramids, which are characterized by high stability upon air exposure and touch. Figures 23b and c show hexagonal prisms of low birefringence, which were stable upon touching, but lost their hexagonal outline and turned into drop-like entities after ~1min of air-exposure. Despite the difficulties with the latter crystals, both forms were used for soaking with $P_{195-201}$.

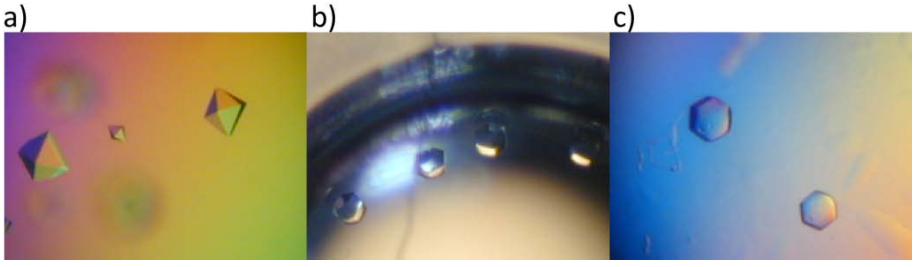

Figure 23: BDV Nucleoprotein crystals
a) Bipyramid BDV N crystals. **b**) and **c)** hexagonal BDV N crystals from different perspectives. Crystals grew in 0.1M MES, 10% PEG 6000.

Independent of the applied soaking method and crystal form, some of the crystals cracked and broke down upon peptide-dispersion in the drop. Others slowly (~1min)

dissolved. Nevertheless, a few of them (both forms) sustained the treatment and were analyzed on beamline ID 14-2 (ESRF, Grenoble) 3-7d after soaking. None of those crystals diffracted at all. Considering these results, it is most likely that the peptide bound to N within the crystal and thus disrupted the crystal lattice. This left so-called non-diffracting "phantom-crystals". Such a phenomenon may happen without destroying the crystal outline. It should be noted that the rhombic bipyramid crystals without the peptide, usually diffracted to ~1.7 Å and displayed a very tight crystal packing. Furthermore their morphology was identical to those used to solve the initial structure of N (Rudolph *et al.*, 2003). The peptide may have bound at the putative P-interaction domain (amino acids 51-100) (Berg *et al.*, 1998), involved in close crystal contacts with a neighbouring molecule and thus disrupted the crystal lattice.

The hexagon prism crystals did not diffract independently of the presence of the peptide.

A last attempt was made, trying to crystallize N-P' in a triple complex with BDV X. It has been shown earlier that BDV P interacts with X via amino acids 72-86 (Schwemmle *et al.*, 1998; Kobayashi *et al.*, 2000; Schneider *et al.*, 2004) (Figure 10). Furthermore, N, P and X were shown to form triple complexes, whereas P is the connector between N and X (Schwemmle *et al.*, 1998). X may have had an additional stabilizing influence on P'. Figure 24 shows the last purification step of the triple complex via size-exclusion chromatography and the analysis by SDS-PAGE. The elution peak is at 12.98ml and shows a shoulder on the left, therefore fractions 10-12 were pooled and subjected to the crystallization robot at concentrations of 3 and 6mg/ml. No crystals appeared in any of the conditions and thus, no further crystallization attempts were made.

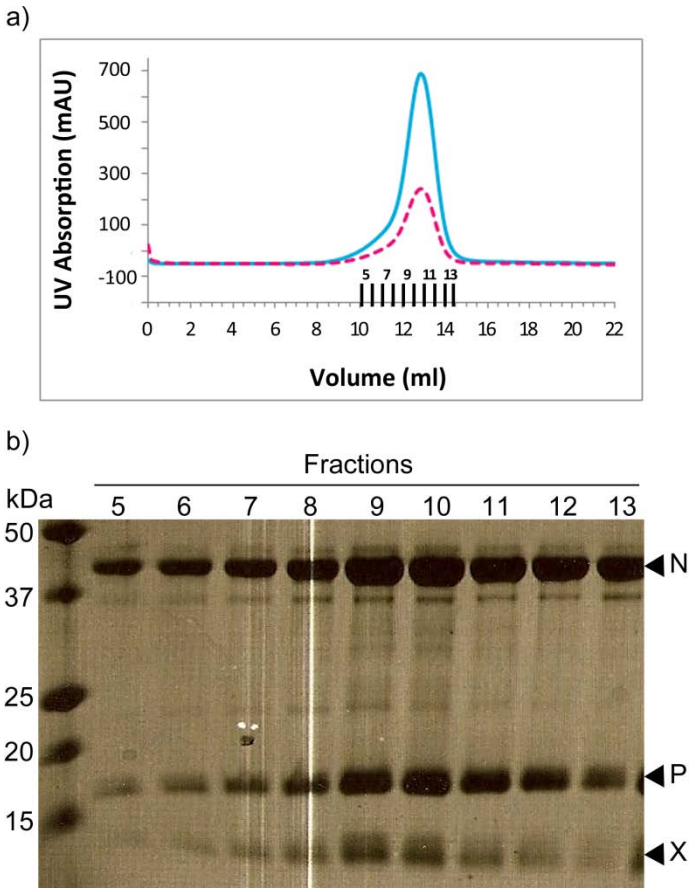

Figure 24: Purification of the BDV N-P-X triple complex
a) Size-exclusion chromatography profile of N-P-X, displaying a shoulder left of the major peak. Fractions taken for analysis are depicted by black bars on the horizontal axis and green numbers. The blue line depicts the UV absorption per ml at 280nm, the red dashed line at 260nm. **b)** Analysis by 16% Tris-Tricine PAGE. Fractions 10-12 were taken for crystallisation.

3.5 N-RNA AND N-P'-RNA INTERACTION

Although RABV and VSV nucleoprotein expression in *E. coli* or insect cells induces the spontaneous uptake of cellular RNA, which results in the formation of N-RNA polymers (Spehner *et al.*, 1991; Iseni *et al.*, 1998; Schoehn *et al.*, 2001; Mavrakis *et al.*, 2002; Schoehn *et al.*, 2004), such a phenomenon is not observed upon recombinant BDV N expression (Rudolph *et al.*, 2003). I thus prepared BDV-genomic RNA fragments which derived from the 5' and the 3' termini (NCBI Nucleotide ID: AJ311522 Borna disease virus, strain He/80/FR, complete genome) (Figure 25) and incubated N and N-P' complexes with a two molar excess of RNA alone or in combination with increasing concentrations of urea to aid in tetramer destabilization (Figure 26).

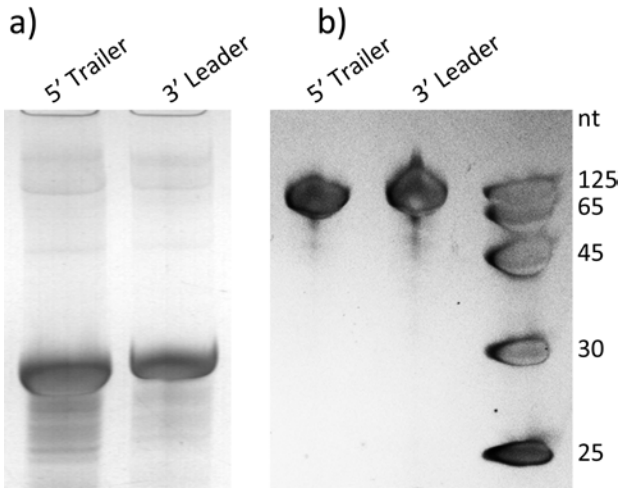

Figure 25: BDV 5' Trailer and 3'Leader RNA
a) BDV 5' Trailer and 3' Leader RNA after *in vitro* transcription and **b)** after purification, analyzed by 8% urea PAGE. Stain: Methylene blue

Both N and N-P' bands shift to a new position in a native gel when incubated with BDV-genomic 5'-trailer RNA (125 nucleotides) in the absence of urea (Figure 26a, upper panel). In contrast, no gel shifts were observed when N and N-P' were incubated with BDV genomic 3'-leader RNA (125 nucleotides) and total *E.coli* RNA (Figure 26a, lanes 1 and 2).

The efficiency of N-RNA and N-P'-RNA complex formation with 5' genomic RNA improved with increasing urea concentrations, leading to the appearance of prominent new bands in both cases (Figure 26a, lanes 4, 5 and 6). Notably N and N-P' incubation with 4 M urea did not change their mobility on a native gel indicating that the urea treatment did not affect the oligomerization or conformation of N and N-P complexes (Fig.26a, lane 7). Some complex formation was observed when N and N-P' were incubated with 3' genomic RNA or even *E. coli* RNA (of variable length) under 4M urea conditions, leading to the appearance of a ladder of new bands (Fig.25a lanes 6). To verify the presence of P' in the N-P'-RNA complex, the bands corresponding to N-P' and N-P'-RNA were excised from a native gel, the proteins eluted from the gel and separated on SDS-PAGE. This indicated that the N-P' complex contained P' as expected as well as the N-P'-RNA complex (Fig.26c). I then compared complex formation of 5'trailer RNA and 5' antigenomic RNA with N using DIG labeled RNA. This indicated N interaction with the 5'antigenomic RNA in the presence and absence of urea (Figure 26b, lanes 2 and 3);

however the band shift produced by 5’ antigenomic RNA N-interaction are less compact than those produced by N interaction with 5’ trailer RNA (Figure 26b, lanes 5 and 6).

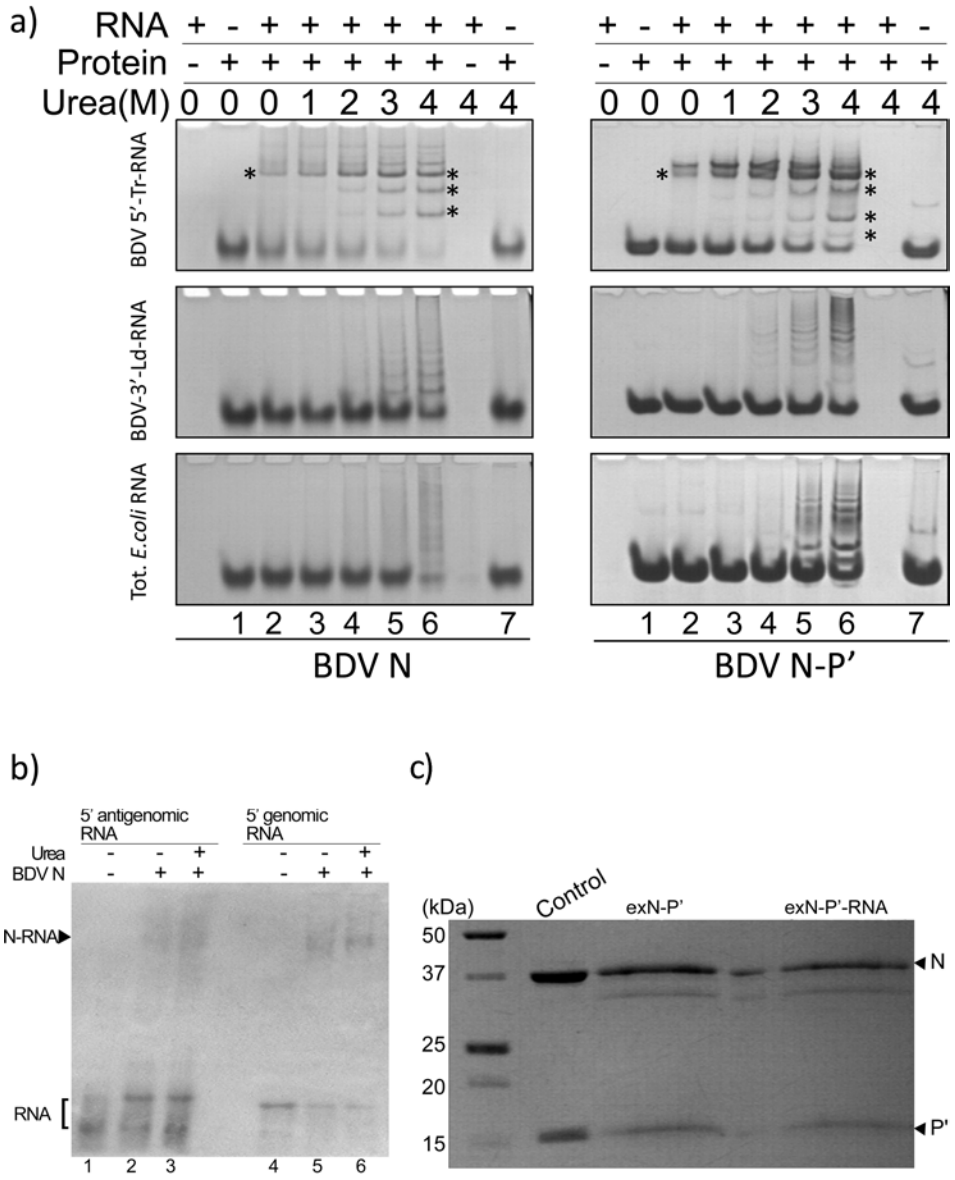

Figure 26: N-RNA and N-P’-RNA gel shift experiments.
a) BDV-N and BDV-N-P’ (left and right panel, respectively) incubated with a 2M excess of BDV-5’-Trailer-BDV-3’-Leader and total *E. coli* RNA (indicated as BDV-5’-Tr, BDV-3’-Ld- and tot. *E. coli* RNA, respectively) in presence of 0-4M Urea, subjected to 6.5% native PAGE. Asterisks mark prominent shift bands. **b)** Gel shift analysis of DIG-labeled 5’trailer RNA and 5’antigenomic RNA. The positions of free RNA and N-RNA complexes are indicated. **c)** Presence of P’ in RNA-shift bands. Bands corresponding to N-P’ (exN-P’) and N-P’-RNA (exN-P’-RNA) were excised from a native gel and extracted from gel slices prior to separation on a 16% SDS-PAGE together with a control of purified N-P’ complex. Faint bands at ~30 kDa may be a degradative product of N or contamination, resulting from band excision. Bands were visualized with Coomassie Brilliant Blue. Protein standards are indicated.

These results indicate that encapsidation of RNA by N is more efficient in the presence of 5’ genomic RNA. Since viral nucleoproteins need to recognize RNA in a non-sequence-specific manner, the preference for 5’ genomic RNA might be explained by the formation of a hairpin structure adopted by the 5’ RNA segment that might specifically interact with N. Secondly, we show that N-RNA complexes are still able to bind to P as required for a functional N-RNA polymer present in a nucleocapsid. These results indicate that encapsidation of RNA by N is more efficient in the presence of 5’ genomic RNA. Since viral nucleoproteins need to recognize RNA in a sequence non-specific manner, the preference for 5’ genomic RNA could be explained by the formation of a hairpin structure adopted by the 5’ RNA segment that could specifically interact with N. Secondly, I could show that N-RNA complexes are still able to bind to P as required for a functional N-RNA polymer present in a nucleocapsid.

3.6 ELECTRON MICROSCOPY OF N-RNA AND N-P’-RNA POLYMERS

N and N-P’ were incubated with BDV genomic 5’-RNA and protein-RNA complexes were separated from RNA-free protein by glycerol gradient centrifugation producing a single band on native gel electrophoresis (Figure 27a Fractions 11 and 12 and 27b, Fractions 10 and 11). Negatively stained electron microscopy images revealed open circular and rod-like structures for N-RNA and N-P’-RNA complexes which were not distinguishable from the former (Figure 28a and c).

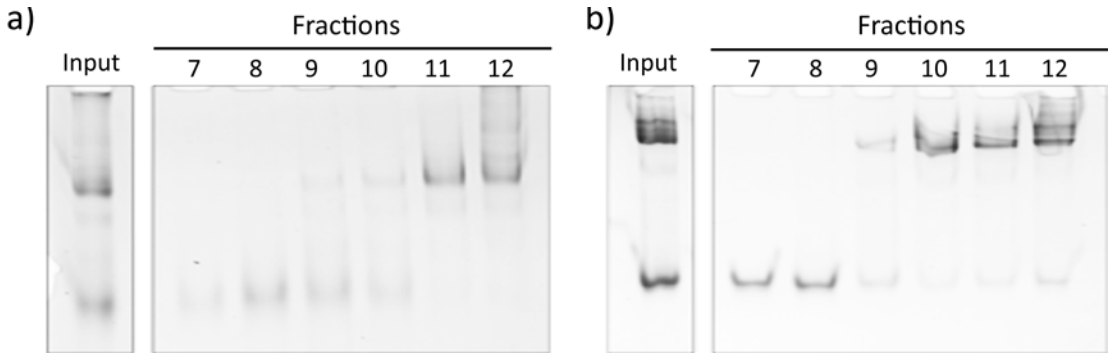

Figure 27: Glycerol Gradient Purification of N-RNA and N-P’-RNA complexes
a) Native PAGE analysis (6.5%) of BDV N-RNA and **b)** N-P’-RNA after glycerol gradient centrifugation. Input indicates the samples before purification. Fractions 11 and 12 from a) and 10 and 11 from b) were pooled, dialyzed into 20mM Hepes, pH 7.8, 20mM NaCl prior to EM analysis.

The circular polymers have an outer diameter of ~10-11 nm and the rods show a length of ~12-14 nm. The absence of the typical shape of N tetramers (Figure 28b) in the N-RNA complex images and the width of the N-RNA rods (35 ±4 Å) indicated that the tetramer (~59x59x87 Å), (Rudolph *et al.*, 2003) disassembled; this led most likely to N protomers lining up along the RNA chain, as demonstrated for VSV and RABV N-RNA (Albertini *et al.*, 2006; Green *et al.*, 2006) (Figure 28c).

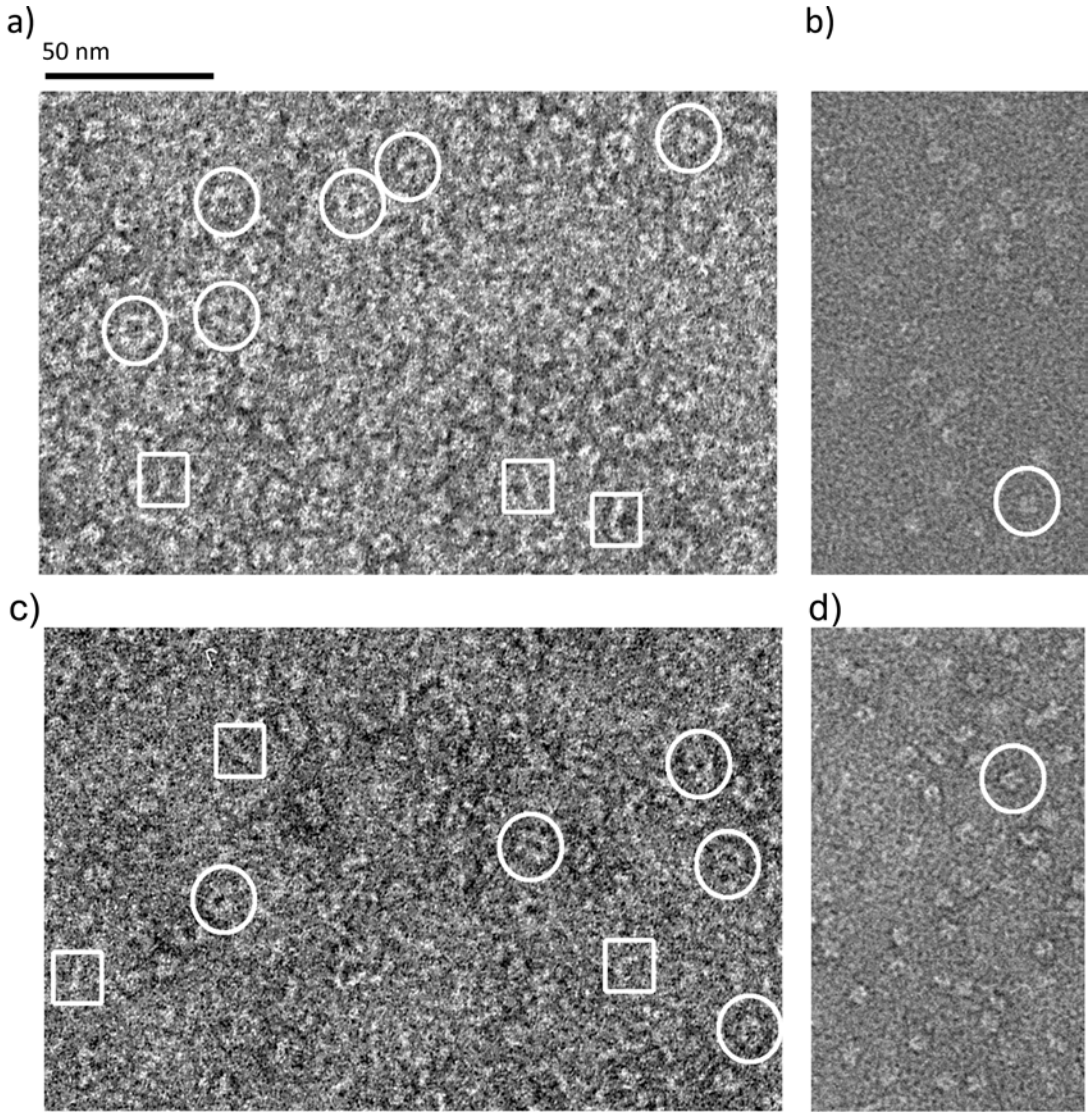

Figure 28: Electron microscopy of N-RNA and N-P'-RNA polymers
a) Negative staining electron microscopy of N in complex with RNA; open ring and rod-like structures can be observed for the protein-RNA complexes, which are highlighted by white rings and squares, respectively. **b)** Negative staining EM images of N-tetramers revealed smaller complexes (top view highlighted by white ring). **c)** and **d)** correspond to a) and b), showing N-P'-RNA and N-P', respectively. The scale bar corresponds to all images.

3.7 BDV N SEQUESTERS RNA IN A CLEFT BETWEEN THE N-AND C-TERMINAL DOMAINS

The global structural similarity of BDV N and rhabdoviridae N (Albertini *et al.*, 2006; Green *et al.*, 2006) suggested that the cleft between the N- and C-terminal domains of N harbors the RNA interaction sites. In order to test this hypothesis, N mutants were generated and analyzed for their ability to form polymers in the presence of 5' genomic RNA. All purified N mutants elute in monodisperse peaks from a gel filtration chromatography column and migrate as single bands on a native gel indicating that the mutations did not unfold N. These mutations of K164D, R165D, K242A and R297D were identified as critical contact points for the RNA, since single mutations and double mutations abrogated N-RNA complex formation as evidenced by native gel analysis (Figure 29a; lanes 1-6). A Glu161Ser mutation and the deletion of 24 C-terminal residues had no significant effect and produced band shifts on a native gel, indicating polymer formation (Figure 29a; lanes 7-10). Wild type N produces a band shift under the same conditions (Figure 29a; lanes 11, 12). Thus, residues K164, R165, K242 and R297 from both the N-terminal and the C-terminal domains are implicated in RNA coordination, indicating that a stretch of RNA could bind within the cleft made up by the N- and C-terminal domains (Figure 29b).

To test whether the RNA in complex with N or N-P' is sequestered by N or partly exposed, the degradation of the RNA was analyzed. Glycerol gradient centrifugation purified N-RNA and N-P'-RNA complexes were incubated with increasing concentrations of RNase A, divided into equal volumes and subjected to denaturing and native PAGE. This revealed that the RNA was not protected in both BDV N- and N-P'-RNA complexes, indicated by the rapid degradation of RNA at low RNase A concentrations (Figure 30a). However, the positions of the protein bands did not change on the native gel (Figure 30b); indicating that N can form stable polymers in the absence of RNA once the polymers have been formed. RNA degradation was further confirmed by analyzing N-RNA and N-P'-RNA complexes formed with DIG-labeled BDV-5'-RNA (see 2.2.13) incubated with 0.05 µg/ml RNase A.

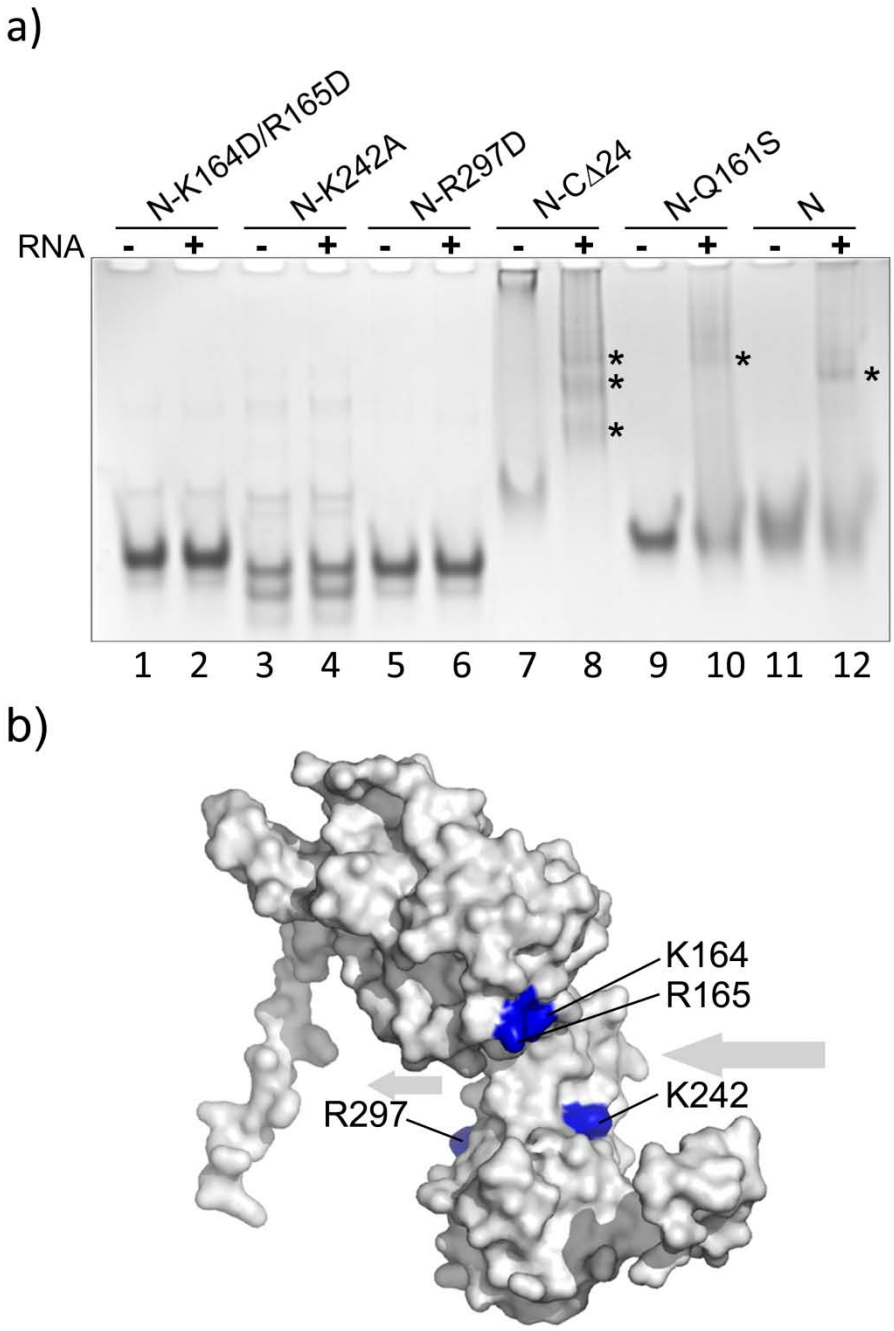

Figure 29: Mapping of the N-RNA interaction site.
a) Gel mobility shift assay of BDV genomic 5'-RNA interaction with mutants of N (indicated at the top) on a 6.5 % native acrylamide gel visualized by Coomassie brilliant blue**.** The asterisks indicate the shift bands obtained after incubation of the different N mutants with the BDV genomic 5' RNA. **b)** Surface representation of BDV-N monomer structure. The surfaces of amino acids found to be essential for RNA-interaction are colored in blue. The direction of the RNA interaction is marked by arrows. The surface representation was generated with Pymol 0.99.

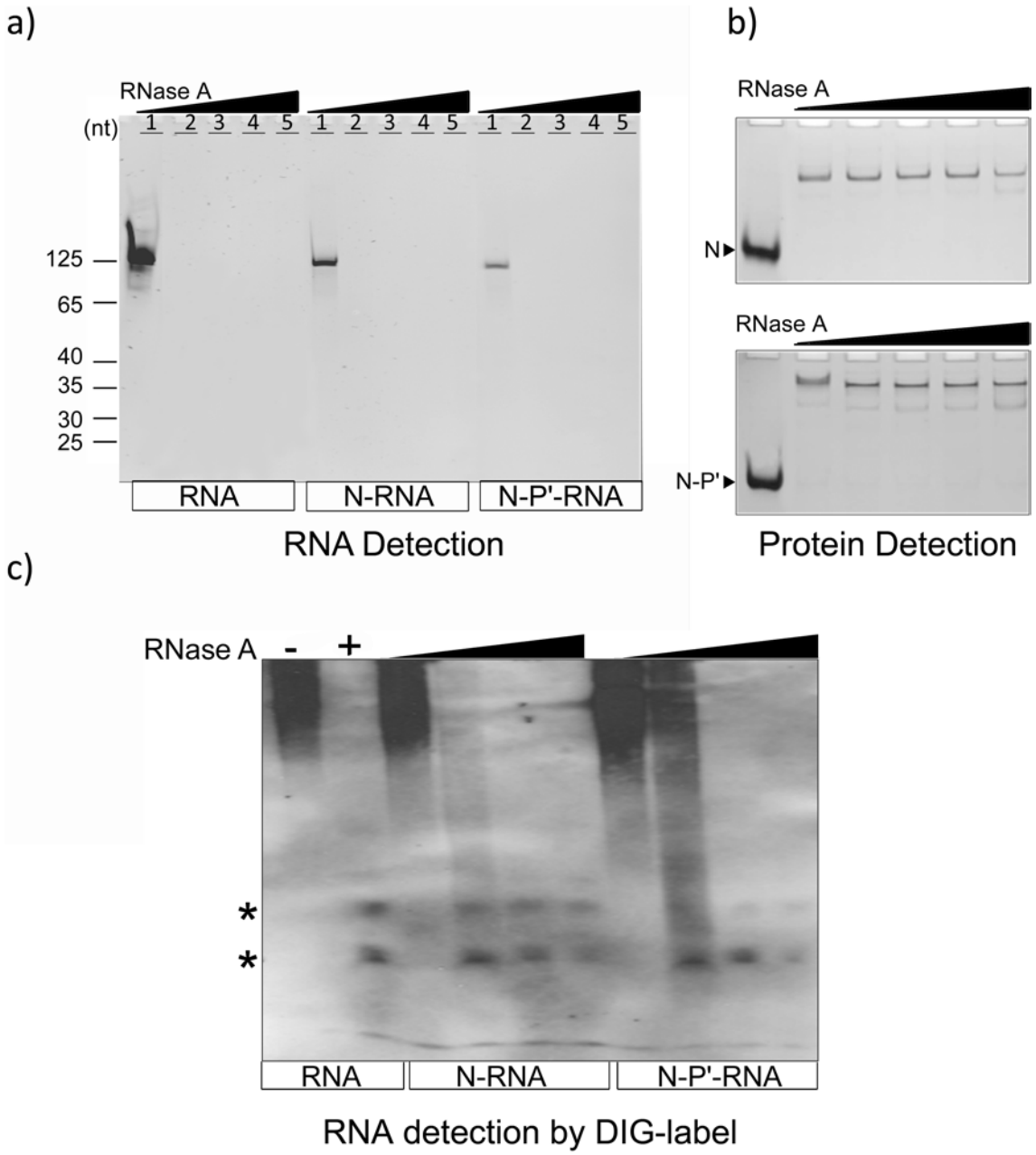

Figure 30: RNA in the N-RNA complex is accessible for degradation.
a) Glycerol gradient purified N-RNA and N-P'-RNA complexes were incubated with 0, 0.05, 0.1, 0.2 and 0.5µg/ml RNase A for 15 min at 37°C (lanes 1-5 of each panel, respectively). Reactions were stopped with RNA Guard RNase inhibitor (GE Healthcare) prior to separation on a 16% denaturing Urea acrylamide gel stained with ethidium bromide; the RNA marker is indicated on the left. Separation of the RNase A treated complexes **b)** N-RNA (upper gel) and N-P'-RNA (Lower gel) on a 6.5% native PAGE stained with Coomassie Brilliant Blue s. The positions of N and N-P' complexes are shown as controls in lane 1, respectively. **c)** RNase protection assay with DIG labeled BDV-5'-Trailer-RNA. RNA mixed with N and N-P' was incubated with 0, 0.05, 0.1 and 0.2 µg/ml RNase A. (-) corresponds to untreated RNA, (+) to RNA treated with RNase A at a concentration of 0.05 µg/ml. Samples were separated by 15% denaturing Urea PAGE and electro-blotted on a Nylon membrane. RNA was detected by AP-coupled anti-DIG-Fab fragments (Roche). Black bars indicate increasing RNAse A concentrations per lane. Asterisks mark the two bands of protected RNA fragments.

The higher sensitivity of this assay revealed the appearance of two small RNA bands upon RNase A treatment of RNA alone, N-RNA and N-P'-RNA complexes (Figure 30c). Although we could not determine the size of the small RNAs, the bands could represent the 5' RNA region that is thought to adopt a hairpin structure; it is thus most likely that this region is not directly incorporated into the nucleoprotein RNA interaction cleft. The presence of a specific tertiary RNA structure within the 5' genomic RNA is further supported by the fact that the same small RNA fragments are produced upon RNase A treatment of the RNA alone (Figure 30c).

4 Discussion

4.1 N-P' Crystallization attempts

They may act in nuclear trafficking and maintenance of a favourable N-to-P ratio in the nucleus, required for efficient replication and transcription (Schneider *et al.*, 2003; Schneider *et al.*, 2004; Schneider, 2005).

A crystal structure would have provided exact structural information about N-P interaction properties, such as amino acids involved in interaction; the P binding site on N and interaction-induced conformational changes on N.

However, none of the attempts to obtain a structure of BDV N with any P-derived peptide has been successful. Nevertheless, the crystal morphologies and the crystallization conditions differed, dependent if BDV N alone or in complex with a P-peptide were present in the setup (Figure 18a and 23a). This indicates that the P-peptides dissociated from N and induced faster nucleation, thus generating low-quality N-crystals. Another explanation is that the P-peptides did not dissociate, but degraded and hence could not be detected by molecular replacement due to the poor crystal quality. Crystals growing in drops containing N only (Figure 23a), belonged to the tetragonal space group I4, with unit cell dimensions of a=100Å and c=103.2Å, identical with those used to solve the initial structure by (Rudolph *et al.*, 2003); the N- and C-terminal domains of the nucleoprotein tetramers were facing away from each other in the crystal lattice and the putative P-binding site (aa 56-100) (Berg *et al.*, 1998) was involved in crystal contacts with a neighbouring tetramer. Crystals growing in drops containing N-P' however (Figure 18b and c), belonged to the monoclinic space group C2, with unit cell dimensions of a=274Å, b=81Å and c=81,5Å (Table 6). Each N tetramer was positioned face-to-face with another one and the putative P binding region was not involved in crystal contacts, theoretically leaving space for a bound P-peptide. These data indicate that a P-peptide may have co-crystallised with N in the respective conditions. Presence of such a peptide in the crystal remains to be proved though, because crystal analysis by SDS-PAGE was never conclusive. In addition, the N structure obtained from the C2 crystals is not complete, especially around the putative P-binding region, which does not allow precise conclusions.

Thus, better methods need to be employed to verify P-peptide presence within those crystals and further crystal improvement should be considered in case of proof.

4.2 N-RNA AND N-P'-RNA INTERACTION

Nucleoproteins from negative strand RNA viruses such as VSV and RABV encapsidate their RNA genome and protect it from the hostile environment in the host cell. The interaction of N with RNA induces polymerization of N along the RNA genome and each protomer interacts with a short stretch of RNA in a non-sequence specific manner. This has been demonstrated by the crystal structures of N-RNA rings from recombinantly expressed nucleoproteins, bound to cellular RNA (Albertini *et al.*, 2006; Green *et al.*, 2006) (Figure 31b and c). Polymerization is achieved by short N- and C-terminal extensions, involved in domain exchange (Figure 31b and c). A similar mode has been proposed for influenza N, although only one flexible tail loop accounts for trimerization or polymerization respectively (Figure 31a and b) (Ye *et al.*, 2006; Coloma *et al.*, 2009).

The RNA in the RABV and VSV rings is entirely occluded within a predominantly basic cleft, formed by helical N- and C-terminal domains of each N protomer (Figure 31 b and c). Likewise, the influenza virus nucleoprotein, exhibits such a basically charged cleft proposed to constitute the RNA binding site.(Ye *et al.*, 2006; Albertini *et al.*, 2008; Coloma *et al.*, 2009) (Figure 31b).

The overall structural similarity of BDV N and VSV or RABV N suggested that BDV N might coordinate RNA in a similar manner (Figure 31a) (Albertini *et al.*, 2006; Green *et al.*, 2006; Albertini *et al.*, 2008).

I thus employed an assay that permitted destabilization of the N tetramers, which led to the formation of N-RNA polymers *in vitro*.

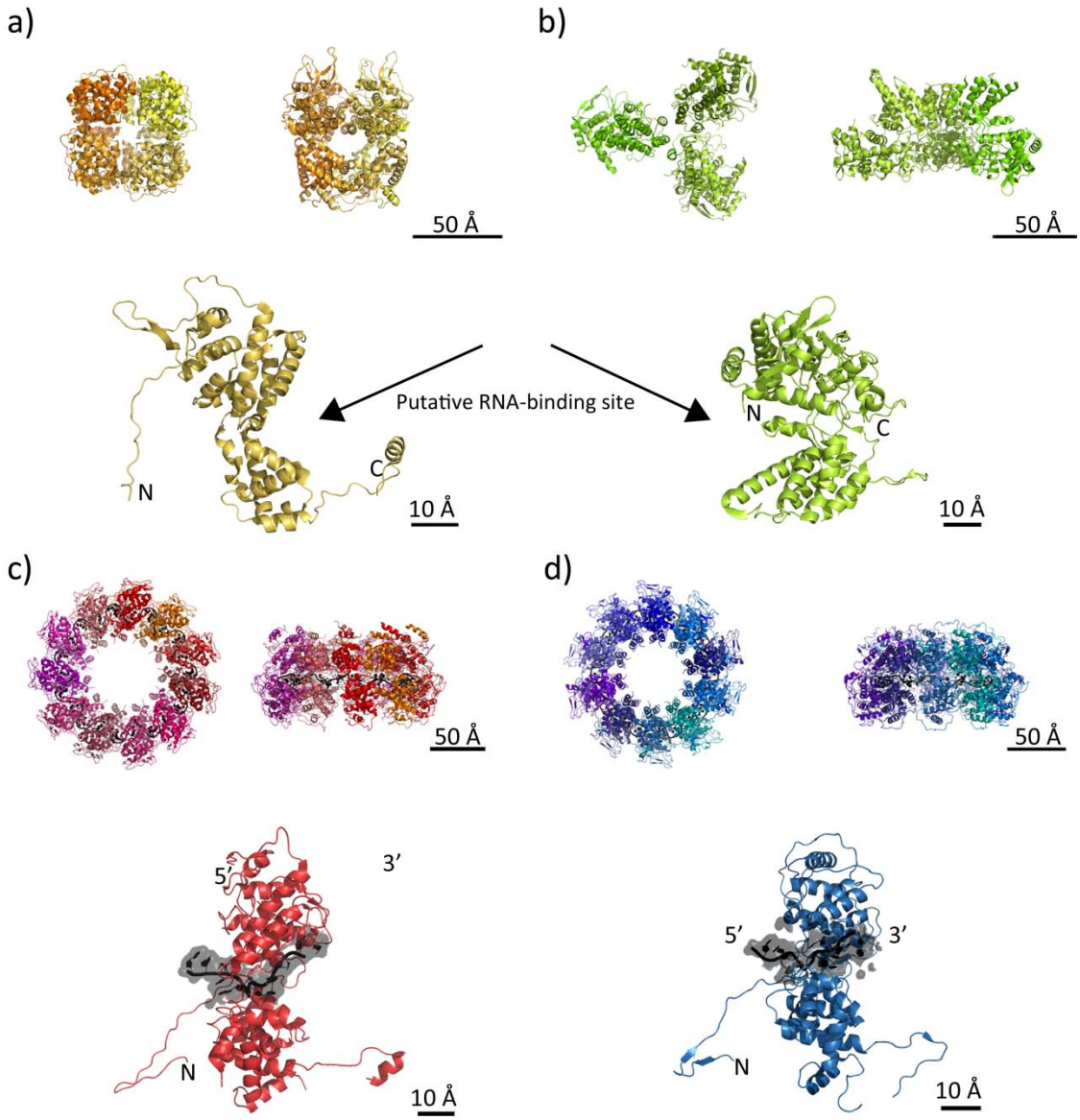

Figure 31: Comparison of known viral nucleoprotein structures in polymeric and monomeric states.
a) Ribbon diagram of the BDV nucleoprotein in its unliganded form. The upper panel shows the tetrameric form found in solution and in the crystal; lower panel shows the monomer composed of two main domains and two small extra domains emanating from the N- and C-terminal domains and involved in domain exchange in the tetramer structure. The putative RNA binding site in the monomer is indicated by an arrow. **b)** Ribbon diagram of the influenza virus nucleoprotein in its RNA-free conformation. The upper panel shows the trimer found in solution and in the crystal. The lower panel shows the monomer composed of two helical domains whose arrangement generates a cleft, which was proposed to constitute the RNA binding site (arrow). A flexible tail loop extends from the C-terminal domain is implicated in trimerisation and polymerization. **c)** Ribbon diagram of the rabies virus N-RNA complex; upper panel shows the two 11-mer NRNA ring complexes contained in the crystal asymmetric unit; lower panel shows the monomer in complex with RNA. **d)** Ribbon diagram of the VSV N-RNA complex; upper panel shows the recombinant 10 mer N-RNA ring complex; lower panel shows the monomer in complex with RNA.
Figure was adopted and modified from (Albertini *et al.*, 2008). Ribbon diagrams were generated with Pymol 0.99. PDB IDs: BDV-N, 1PPT; Influenza virus N, 2IQH; Rabies virus N-RNA, 2GTT; VSV N-RNA, 2GIC.

One dimension of the polymers, their width, resemble that of nucleocapsids present in BDV (Figure 1c, see 1.2.1 and 3.5) (Kohno *et al.*, 1999). Mutagenesis of basic residues within the cleft made up by the N- and C-terminal domains confirmed this region as major RNA binding site. This is in contrast to previous assumptions that the RNA might run through the basically charged channel (Figure 32a and b) in the middle of the tetramer or a basic cleft, running diagonally across the tetramer (Figure 32c) (Rudolph *et al.*, 2003).

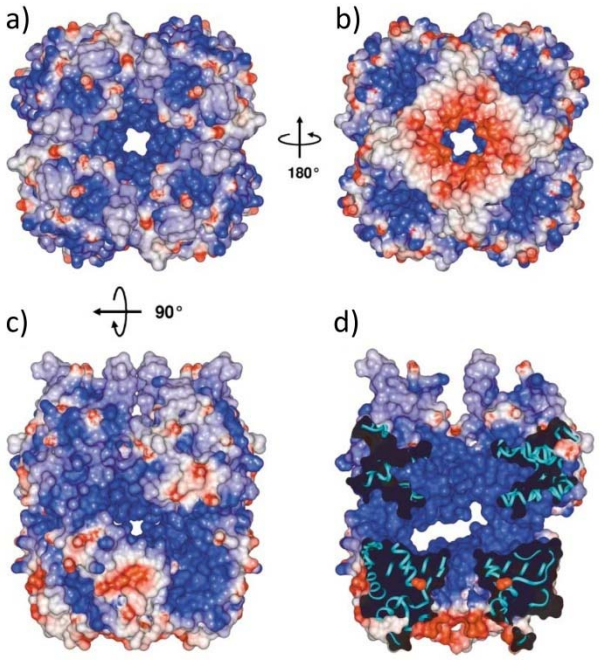

Figure 32: Surface Potential Representation of the BDV-N Tetramer
a) Electrostatic potential distribution of N. The view is on the N-terminal domains, showing the entrance to the positively charged channel. Areas coloured in white, red, and blue denote neutral, negative, and positive potential, respectively. **b)** Bottom view of a) rotated 180° around the y-axis. The channel is negatively charged at this end. **c)** Side-view of a) rotated by 90° around the horizontal axis. A deep groove of positive surface potential runs diagonally across the side of the tetramer and marks the other assumed RNA binding site. **d)** Slab through the central channel showing the large cavity and the positively charged side channels normal to the central channel that lead to the surface of the tetramer. The backbone trace of the BDV-N is shown as a cyan ribbon. Figures were taken from (Rudolph *et al.*, 2003).

The bound RNA was sensitive to enzymatic RNA degradation suggesting that it is exposed in the N-RNA complex. This is in contrast to previous reports that showed that isolated BDV virus particles and RNPs are resistant against RNA degradation (Richt *et al.*, 1993; Cubitt & de la Torre, 1994). In the first case, BDV-infected cells were treated with Freon-113, liberating BDV which was still infectious. This means that RNase A treatment was applied on intact BDV virions. The *in-vitro* conditions applied here for N-RNA

assembly are thus not comparable to those conditions of ancient work. The difference might be due to the presence of other viral proteins such as G and probably the lipid envelope. Furthermore this may be because of the fact that the strings of N-RNA complexes might be packaged tighter in the nucleocapsid due to M that interacts with RNA and potentially with N (Mayer *et al.*, 2005; Chase *et al.*, 2007; Neumann *et al.*, 2009) or due to the presence of full length P in the wild type RNPs. However, it cannot be excluded that the usage of different RNases might have affected the outcome. BDV RNPs were protected from degradation by Micrococcus nuclease, but had not been tested for RNase A degradation before (Cubitt & de la Torre, 1994). This is consistent with RNA protection observed in case of N-RNA complexes from RABV, whereas RNA present in nucleocapsids was entirely protected from micrococcal nuclease degradation, albeit RNase A treatment produced small RNA fragments of 4-9 nucleotides (Iseni *et al.*, 1998; Albertini *et al.*, 2006). Sensitivity to RNase degradation was further reported for RNA within influenza virus RNPs (Duesberg, 1969; Kingsbury & Webster, 1969; Baudin *et al.*, 1994) similar to my results. Another explanation is that the RNA is not fully coated along its entire length by N, thus leaving portions of the phosphate backbone exposed to nuclease attack. There may also be regions of RNA that are looped out within and between adjacent nucleoprotein.

A requirement for RNA protection might depend on the replication site within the cell. Both influenza and Borna disease viruses replicate in the nucleus, protected from the RNA degradation machinery. Other factors such as viral matrix proteins interacting with RNA themselves (Gomis-Rüth *et al.*, 2003; Money *et al.*, 2009; Neumann *et al.*, 2009) or the formation of a compact structure of the RNPs might protect them during the transport in the cytosol to the sites of virus assembly. In contrast viruses such as RABV and VSV might have to protect their genomes better since they replicate in the cytosol.

BDV N alone or in complex with P' formed preferentially complexes with 5' genomic RNA, indicating that N has the capacity to discriminate between RNA sequences, which is important for the specific encapsidation of genomic RNA during the replication cycle. This is consistent with previous studies on RABV, suggesting that the 5' leader RNA plays an important role in conferring specific RNA encapsidation (Blumberg *et al.*, 1983; Kouznetzoff *et al.*, 1998). This process can be further modulated by P (Yang *et al.*, 1998) and by phosphorylation of N (Toriumi & Kawai, 2004). The *in vitro* degradation of a 5'

genomic RNA fragment revealed that two small regions are protected from complete degradation by RNase A, independent of the presence of N or N-P'. This suggests that part of the 5' genomic RNA used in the study adopts a secondary or tertiary structure that is insensitive to RNase A degradation. This may be most likely due to the extreme 5' end. Such a defined RNA structure could be recognized by N and thus serve as a starting signal to encapsidate RNA in a sequence unspecific manner as observed for RABV and VSV N-RNA interactions. Furthermore, RNA recognition by the N tetramer might help to destabilize the tetramer thus exposing the RNA binding sites. This hypothesis is supported by the fact that N tetramers do not interact with 3' genomic RNA or *E. coli* RNA in the absence of urea as a destabilizing agent. Even in the presence of urea, neither N nor N-P tetramers are efficiently destabilized by 3' genomic RNA or by *E. coli* RNA when compared to the effect of 5' genomic RNA and to some extend of the 5'anti-genomic RNA. Since the 3' end of the genome is complementary to the 5' region, it would be expected that the 5' antigenome might adopt a similar conformation that permits N interaction, as we observe in the current study.

The EM images of N-RNA and N-P'-RNA complexes do not reveal closed ring-like structures as observed for other negative strand RNA viruses (Iseni *et al.*, 1998; Schoehn *et al.*, 2001; Maclellan *et al.*, 2007; Cox *et al.*, 2009). This is most likely due to the presence of the 5' end of the RNA genome that might adopt a defined structure that itself is not incorporated into the RNA binding cleft or may interact with native M protein. My data also suggest that the N tetramers have to disassemble upon RNA interaction. Firstly, the appearances of the EM images suggest the absence of N tetramers as building blocks of the polymers. Secondly, important basic residues required for RNA binding were mapped to the cleft that itself is sequestered in the interior of the N tetramer (Rudolph *et al.*, 2003).

Depletion of the RNA from the N-RNA and N-P'-RNA polymers indicate that polymerization is mainly stabilized via N-N protein interactions as shown for empty VSV ring-like nucleocapsids (Zhang *et al.*, 2008). This suggests that polymerization is also most likely supported by domain exchange between protomers within the polymer similar to RABV and VSV N-RNA polymerization (Albertini *et al.*, 2006; Green *et al.*, 2006).

The N-RNA complex constitutes the target for the polymerase complex composed of L and the phosphoprotein P. P regulates transcription and replication by linking the N-RNA complex to L (Schneider *et al.*, 2004). Although it has been speculated that P forms dimers, trimers or tetramers based on gel filtration results (Schneider *et al.*, 2004; Schneider, 2005) my analysis clearly shows that P forms tetramers in solution similar to P from Sendai virus (Tarbouriech *et al.*, 2000). A similar oligomerization motif was predicted for BDV P (Schneider *et al.*, 2004; Schneider, 2005). Although Cys 125 of BDV-P was implicated previously in disulfide cross-linked dimerization (Kliche *et al.*, 1996) MALLs analysis of N-P complexes produced the same results in a reducing buffer (data not shown), indicating that Cys crosslinking is not required for oligomerization. My results suggest further that tetramer formation of P does not depend on phosphorylation as shown for Ps from Rhabdoviruses (Gigant *et al.*, 2000; Gerard *et al.*, 2007).

I could further show that P interaction with N requires a short C-terminal region of P including the last seven amino acids. This region binds N with a micromolar affinity similar to other N-P interactions; the C-terminal nucleocapsid-binding domain of measles virus P binds the nucleoprotein N_{TAIL} peptide with an affinity constant of 13µM (Kingston *et al.*, 2004) and the Sendai virus N_{TAIL}-PX interaction has an affinity of ~57 µM (Houben *et al.*, 2007). A low binding affinity is consistent with a model proposed for Sendai virus, whereas P is “cart wheeling” along the N-RNA during RNA-synthesis, by employing on-and-off interactions (Kolakofsky *et al.*, 2004).

Therefore a weak binding affinity between P and N proteins is energetically beneficial for movement of the L protein along the nucleocapsid. Since P proteins from negative strand RNA viruses adopt a modular structure (Karlin *et al.*, 2003; Gerard *et al.*, 2009) whereas the single domains are flexibly linked, BVD P might be similarly organized by utilizing a C-terminal domain for interaction with N tetramers as well as N-RNA polymers. The short N interaction site might further ensure that multiple Ps can simultaneously interact with at least four Ns while being linked to the polymerase L during replication and transcription. In summary our study provides a first model of the RNA interaction mode of BDV N and suggests that such N-RNA polymers could be targets

for low affinity interaction with tetrameric P and thus provide a link to the polymerase L during replication and transcription.

.

5 CONCLUSIONS

- P’ oligomerizes into tetramers in solution.
- N and P’ assemble into hetero-octamers with four P’ bound to the N-tetramer.
- N-P’ interaction requires the last five C-terminal P residues to form a stable complex with a KD of 1.66 µM, consistent with an on-and-off interaction mode, which would theoretically allow the phosphoprotein to move along the nucleocapsid during replication and transcription.
- The BDV N tetramer is destabilized upon formation of N-RNA complexes and polymerizes along the RNA chain as shown for N proteins of other MNVs. N-RNA assembles into open circular and rod-like structures, with the RNA exposed and accessible for degradation
- BDV N interacts specifically with BDV specific genomic and antigenomic 5’ RNA, but not with genomic 3’ RNA or total *E. coli* RNA.
- N-RNA polymers are formed in the presence of P’ leading to P’-N-RNA polymers.

6 BIBLIOGRAPHY

Albertini A A V, Clapier C R, Wernimont A K, Schoehn G, Weissenhorn W and Ruigrok R W H. **2007.** Isolation and crystallization of a unique size category of recombinant Rabies virus Nucleoprotein-RNA rings. *Journal of Structural Biology*, **158**:129-133.

Albertini A A V, Schoehn G, Weissenhorn W and Ruigrok R W H. **2008.** Structural aspects of rabies virus replication. *Cellular and Molecular Life Sciences: CMLS*, **65**:282-294.

Albertini A A V, Wernimont A K, Muziol T, Ravelli R B G, Clapier C R, Schoehn G, Weissenhorn W and Ruigrok R W H. **2006.** Crystal structure of the rabies virus nucleoprotein-RNA complex. *Science (New York, N.Y.)*, **313**:360-363.

Baudin F, Bach C, Cusack S and Ruigrok R W. **1994.** Structure of influenza virus RNP. I. Influenza virus nucleoprotein melts secondary structure in panhandle RNA and exposes the bases to the solvent. *The EMBO Journal*, **13**:3158-3165.

Becht H and Richt J. **1996.** *Borna Disease. Pages MC Horzinek, Ed. Virus Infection of Vertebrates*: Elsevier, Amsterdam.

Berg M, Ehrenborg C, Blomberg J, Pipkorn R and Berg A L. **1998.** Two domains of the Borna disease virus p40 protein are required for interaction with the p23 protein. *The Journal of General Virology*, **79 (Pt 12)**:2957-2963.

Blumberg B M, Giorgi C and Kolakofsky D. **1983.** N protein of vesicular stomatitis virus selectively encapsidates leader RNA in vitro. *Cell*, **32**:559-567.

Briese T, de la Torre J C, Lewis A, Ludwig H and Lipkin W I. **1992.** Borna disease virus, a negative-strand RNA virus, transcribes in the nucleus of infected cells. *Proceedings of the National Academy of Sciences of the United States of America*, **89**:11486-11489.

Briese T, Lipkin W I and de la Torre J C. **1995.** Molecular biology of Borna disease virus. *Current Topics in Microbiology and Immunology*, **190**:1-16.

Briese T, Schneemann A, Lewis A J, Park Y S, Kim S, Ludwig H and Lipkin W I. **1994.** Genomic organization of Borna disease virus. *Proceedings of the National Academy of Sciences of the United States of America*, **91**:4362-4366.

Chase G, Mayer D, Hildebrand A, Frank R, Hayashi Y, Tomonaga K and Schwemmle M. **2007.** Borna disease virus matrix protein is an integral component of the viral ribonucleoprotein complex that does not interfere with polymerase activity. *Journal of Virology*, **81**:743-749.

Chenik M, Schnell M, Conzelmann K K and Blondel D. **1998.** Mapping the interacting domains between the rabies virus polymerase and phosphoprotein. *Journal of Virology*, **72**:1925-1930.

Choudhary S K, Malur A G, Huo Y, De B P and Banerjee A K. **2002.** Characterization of the oligomerization domain of the phosphoprotein of human parainfluenza virus type 3. *Virology*, **302**:373-382.

Collaborative Computational Project N. **1994.** The CCP4 suite: Programs for protein crystallography. *Acta Crystallogr. D Biol. Crystallogr.*, **50**:760-763.

Coloma R, Valpuesta J M, Arranz R, Carrascosa J L, Ortín J and Martín-Benito J. **2009.** The structure of a biologically active influenza virus ribonucleoprotein complex. *PLoS Pathogens*, **5**:e1000491.

Cooper M A. **2002.** Optical biosensors in drug discovery. *Nature Reviews. Drug Discovery*, **1**:515-528.

Cox R, Green T J, Qiu S, Kang J, Tsao J, Prevelige P E, He B and Luo M. **2009.** Characterization of a Mumps Virus Nucleocapsid-like Particle. *Journal of Virology*.

Cubitt B and de la Torre J C. **1994.** Borna disease virus (BDV), a nonsegmented RNA virus, replicates in the nuclei of infected cells where infectious BDV ribonucleoproteins are present. *Journal of Virology*, **68**:1371-1381.

Cubitt B, Oldstone C and de la Torre J C. **1994.** Sequence and genome organization of Borna disease virus. *Journal of Virology*, **68**:1382-1396.

Cubitt B, Oldstone C, Valcarcel J and Carlos de la Torre J. **1994.** RNA splicing contributes to the generation of mature mRNAs of Borna disease virus, a non-segmented negative strand RNA virus. *Virus Research*, **34**:69-79.

Curran J. **1998.** A role for the Sendai virus P protein trimer in RNA synthesis. *Journal of Virology*, **72**:4274-4280.

Danner K and Mayr A. **1979.** In vitro studies on Borna virus. II. Properties of the virus. *Archives of Virology*, **61**:261-271.

de la Torre J C. **1994.** Molecular biology of borna disease virus: prototype of a new group of animal viruses. *Journal of Virology*, **68**:7669-7675.

de la Torre J C. **2002.** Molecular biology of Borna disease virus and persistence. *Frontiers in Bioscience: A Journal and Virtual Library*, **7**:d569-579.

de la Torre J C. **2006.** Reverse-genetic approaches to the study of Borna disease virus. *Nature Reviews. Microbiology*, **4**:777-783.

DeLano W L. *The PyMOL Molecular Graphics System, DeLano Scientific, San Carlos, CA, USA, 2002*: OpenURL.

Deléage G, Blanchet C and Geourjon C. **1997.** Protein structure prediction. Implications for the biologist. *Biochimie*, **79**:681-686.

Dürrwald R, Kolodziejek J, Herzog S and Nowotny N. **2007.** Meta-analysis of putative human bornavirus sequences fails to provide evidence implicating Borna disease virus in mental illness. *Reviews in Medical Virology*, **17**:181-203.

Duesberg P H. **1969.** Distinct subunits of the ribonucleoprotein of influenza virus. *Journal of Molecular Biology*, **42**:485-499.

Eickmann M, Kiermayer S, Kraus I, Gössl M, Richt J A and Garten W. **2005.** Maturation of Borna disease virus glycoprotein. *FEBS Letters*, **579**:4751-4756.

Emerson S U and Schubert M. **1987.** Location of the binding domains for the RNA polymerase L and the ribonucleocapsid template within different halves of the NS phosphoprotein of vesicular stomatitis virus. *Proceedings of the National Academy of Sciences of the United States of America*, **84**:5655-5659.

Emerson S U and Wagner R R. **1972.** Dissociation and reconstitution of the transcriptase and template activities of vesicular stomatitis B and T virions. *Journal of Virology*, **10**:297-309.

Emerson S U and Yu Y. **1975.** Both NS and L proteins are required for in vitro RNA synthesis by vesicular stomatitis virus. *Journal of Virology*, **15**:1348-1356.

Fooks A R, Stephenson J R, Warnes A, Dowsett A B, Rima B K and Wilkinson G W. **1993.** Measles virus nucleocapsid protein expressed in insect cells assembles into nucleocapsid-like structures. *The Journal of General Virology*, **74 (Pt 7)**:1439-1444.

Furrer E, Bilzer T, Stitz L and Planz O. **2001.** High-dose Borna disease virus infection induces a nucleoprotein-specific cytotoxic T-lymphocyte response and prevention of immunopathology. *Journal of Virology*, **75**:11700-11708.

Gerard F C A, Ribeiro E d A, Albertini A A V, Gutsche I, Zaccai G, Ruigrok R W H and Jamin M. **2007.** Unphosphorylated rhabdoviridae phosphoproteins form elongated dimers in solution. *Biochemistry*, **46**:10328-10338.

Gerard F C A, Ribeiro E d A, Leyrat C, Ivanov I, Blondel D, Longhi S, Ruigrok R W H and Jamin M. **2009.** Modular organization of rabies virus phosphoprotein. *Journal of Molecular Biology*, **388**:978-996.

Gertz E M. *BLAST scoring parameters. 2005*.

Gigant B, Iseni F, Gaudin Y, Knossow M and Blondel D. **2000.** Neither phosphorylation nor the amino-terminal part of rabies virus phosphoprotein is required for its oligomerization. *The Journal of General Virology*, **81**:1757-1761.

Gomis-Rüth F X, Dessen A, Timmins J, Bracher A, Kolesnikowa L, Becker S, Klenk H D and Weissenhorn W. **2003.** The matrix protein VP40 from Ebola virus octamerizes into pore-like structures with specific RNA binding properties. *Structure (London, England: 1993)*, **11**:423-433.

Gonzalez-Dunia D, Cubitt B and de la Torre J C. **1998.** Mechanism of Borna disease virus entry into cells. *Journal of Virology*, **72**:783-788.

Gonzalez-Dunia D, Cubitt B, Grasser F A and de la Torre J C. **1997.** Characterization of Borna disease virus p56 protein, a surface glycoprotein involved in virus entry. *Journal of Virology*, **71**:3208-3218.

Green T J and Luo M. **2006.** Resolution improvement of X-ray diffraction data of crystals of a vesicular stomatitis virus nucleocapsid protein oligomer complexed with RNA. *Acta Crystallographica. Section D, Biological Crystallography*, **62**:498-504.

Green T J, Zhang X, Wertz G W and Luo M. **2006.** Structure of the vesicular stomatitis virus nucleoprotein-RNA complex. *Science (New York, N.Y.)*, **313**:357-360.

Günzl A, Palfi Z and Bindereif A. **2002.** Analysis of RNA-protein complexes by oligonucleotide-targeted RNase H digestion. *Methods (San Diego, Calif.)*, **26**:162-169.

Hilbe M, Herrsche R, Kolodziejek J, Nowotny N, Zlinszky K and Ehrensperger F. **2006.** Shrews as reservoir hosts of borna disease virus. *Emerging Infectious Diseases*, **12**:675-677.

Holmes D E and Moyer S A. **2002.** The phosphoprotein (P) binding site resides in the N terminus of the L polymerase subunit of sendai virus. *Journal of Virology*, **76**:3078-3083.

Honkavuori K S, Shivaprasad H L, Williams B L, Quan P L, Hornig M, Street C, Palacios G, Hutchison S K, Franca M, Egholm M, Briese T and Lipkin W I. **2008.** Novel borna virus in psittacine birds with proventricular dilatation disease. *Emerging Infectious Diseases*, **14**:1883-1886.

Horikami S M, Curran J, Kolakofsky D and Moyer S A. **1992.** Complexes of Sendai virus NP-P and P-L proteins are required for defective interfering particle genome replication in vitro. *Journal of Virology*, **66**:4901-4908.

Horikami S M and Moyer S A. **1995.** Alternative amino acids at a single site in the Sendai virus L protein produce multiple defects in RNA synthesis in vitro. *Virology*, **211**:577-582.

Houben K, Marion D, Tarbouriech N, Ruigrok R W H and Blanchard L. **2007.** Interaction of the C-terminal domains of sendai virus N and P proteins: comparison of polymerase-nucleocapsid interactions within the paramyxovirus family. *Journal of Virology*, **81**:6807-6816.

Imai Y, Matsushima Y, Sugimura T and Terada M. **1991.** A simple and rapid method for generating a deletion by PCR. *Nucleic Acids Research*, **19**:2785.

Iseni F, Barge A, Baudin F, Blondel D and Ruigrok R W. **1998.** Characterization of rabies virus nucleocapsids and recombinant nucleocapsid-like structures. *The Journal of General Virology*, **79 (Pt 12)**:2909-2919.

Jehle C, Lipkin W I, Staeheli P, Marion R M and Schwemmle M. **2000.** Authentic Borna disease virus transcripts are spliced less efficiently than cDNA-derived viral RNAs. *The Journal of General Virology*, **81**:1947-1954.

Joest E. **1911.** Untersuchungen über die pathologische Histologie, Pathogenese und postmortale Diagnose der seuchenhaften Gehirn-Rückenmarksentzündung (Bornaschen Krankheit) des Pferdes. Ein Beitrag zur vergleichenden Pathologie des Zentralnervensystems. *Journal of Neurology*, **42**:293-324.

Joest E and Degen K. **1909.** Über eigentümliche Kerneinschlüsse der Ganglienzellen bei der enzootischen Gehirn-Rückenmarksentzündung der Pferde. *Zschr. Inf. krkh. Haustiere*, **6**:348.

Jumel K, Fiebrig I and Harding S E. **1996.** Rapid size distribution and purity analysis of gastric mucus glycoproteins by size exclusion chromatography/multi angle laser light scattering. *International Journal of Biological Macromolecules*, **18**:133-139.

Kabsch W. **1993.** Automatic processing of rotation diffraction data from crystals of initially unknown symmetry and cell constants. *Journal of applied crystallography*, **26**:795-800.

Karlin D, Ferron F, Canard B and Longhi S. **2003.** Structural disorder and modular organization in Paramyxovirinae N and P. *The Journal of General Virology*, **84**:3239-3252.

Kiermayer S, Kraus I, Richt J A, Garten W and Eickmann M. **2002.** Identification of the amino terminal subunit of the glycoprotein of Borna disease virus. *FEBS Letters*, **531**:255-258.

Kingsbury D W and Webster R G. **1969.** Some Properties of Influenza Virus Nucleocapsids. *Journal of Virology*, **4**:219-225.

Kingston R L, Baase W A and Gay L S. **2004.** Characterization of nucleocapsid binding by the measles virus and mumps virus phosphoproteins. *Journal of Virology*, **78**:8630-8640.

Kishi M, Tomonaga K, Lai P K and de la Torre J C. **2002.** Borna disease virus molecular virology. *Borna disease virus and its role in neurobehavioral disease. ASM Press, Washington DC*:23-44.

Kliche S, Stitz L, Mangalam H, Shi L, Binz T, Niemann H, Briese T and Lipkin W I. **1996.** Characterization of the Borna disease virus phosphoprotein, p23. *Journal of Virology*, **70**:8133-8137.

Kobayashi T, Kamitani W, Zhang G, Watanabe M, Tomonaga K and Ikuta K. **2001.** Borna disease virus nucleoprotein requires both nuclear localization and export activities for viral nucleocytoplasmic shuttling. *Journal of Virology*, **75**:3404-3412.

Kobayashi T, Shoya Y, Koda T, Takashima I, Lai P K, Ikuta K, Kakinuma M and Kishi M. **1998.** Nuclear targeting activity associated with the amino terminal region of the Borna disease virus nucleoprotein. *Virology*, **243**:188-197.

Kobayashi T, Watanabe M, Kamitani W, Tomonaga K and Ikuta K. **2000.** Translation initiation of a bicistronic mRNA of Borna disease virus: a 16-kDa phosphoprotein is initiated at an internal start codon. *Virology*, **277**:296-305.

Kohno T, Goto T, Takasaki T, Morita C, Nakaya T, Ikuta K, Kurane I, Sano K and Nakai M. **1999.** Fine structure and morphogenesis of Borna disease virus. *Journal of Virology*, **73**:760-766.

Kolakofsky D, Le Mercier P, Iseni F and Garcin D. **2004.** Viral DNA polymerase scanning and the gymnastics of Sendai virus RNA synthesis. *Virology*, **318**:463-473.

Kouznetzoff A, Buckle M and Tordo N. **1998.** Identification of a region of the rabies virus N protein involved in direct binding to the viral RNA. *The Journal of General Virology*, **79 (Pt 5)**:1005-1013.

Kraus I, Bogner E, Lilie H, Eickmann M and Garten W. **2005.** Oligomerization and assembly of the matrix protein of Borna disease virus. *FEBS Letters*, **579**:2686-2692.

Laemmli U K. **1970.** Cleavage of structural proteins during the assembly of the head of bacteriophage T4. *Nature*, **227**:680-685.

Leslie A G W. **1992.** Jnt CCP4/EACBM Newsl. *Protein Crystallogr*, **26**.

Lipkin W and Briese T. **2007.** *Bornaviridae*: Philadelphia: Lippincott, Williams and Wilkins.

Ludwig H and Bode L. **2000.** Borna disease virus: new aspects on infection, disease, diagnosis and epidemiology. *Revue Scientifique Et Technique (International Office of Epizootics)*, **19**:259-288.

Maclellan K, Loney C, Yeo R P and Bhella D. **2007.** The 24-angstrom structure of respiratory syncytial virus nucleocapsid protein-RNA decameric rings. *Journal of Virology*, **81**:9519-9524.

Malik T H, Kishi M and Lai P K. **2000.** Characterization of the P protein-binding domain on the 10-kilodalton protein of Borna disease virus. *Journal of Virology*, **74**:3413-3417.

Mavrakis M, Kolesnikova L, Schoehn G, Becker S and Ruigrok R W H. **2002.** Morphology of Marburg virus NP-RNA. *Virology*, **296**:300-307.

Mayer D, Baginsky S and Schwemmle M. **2005.** Isolation of viral ribonucleoprotein complexes from infected cells by tandem affinity purification. *Proteomics*, **5**:4483-4487.

Mellon M G and Emerson S U. **1978.** Rebinding of transcriptase components (L and NS proteins) to the nucleocapsid template of vesicular stomatitis virus. *Journal of Virology*, **27**:560-567.

Möller P, Pariente N, Klenk H-D and Becker S. **2005.** Homo-oligomerization of Marburgvirus VP35 is essential for its function in replication and transcription. *Journal of Virology*, **79**:14876-14886.

Money V A, McPhee H K, Mosely J A, Sanderson J M and Yeo R P. **2009.** Surface features of a Mononegavirales matrix protein indicate sites of membrane interaction. *Proceedings of the National Academy of Sciences of the United States of America*, **106**:4441-4446.

Murphy M F and Lazzarini R A. **1974.** Synthesis of viral mRNA and polyadenylate by a ribonucleoprotein complex from extracts of VSV-infected cells. *Cell*, **3**:77-84.

Narayan O, Herzog S, Frese K, Scheefers H and Rott R. **1983.** Behavioral disease in rats caused by immunopathological responses to persistent borna virus in the brain. *Science (New York, N.Y.)*, **220**:1401-1403.

Neumann P, Lieber D, Meyer S, Dautel P, Kerth A, Kraus I, Garten W and Stubbs M T. **2009.** Crystal structure of the Borna disease virus matrix protein (BDV-M) reveals ssRNA binding properties. *Proceedings of the National Academy of Sciences of the United States of America*, **106**:3710-3715.

Newcomb W W and Brown J C. **1981.** Role of the vesicular stomatitis virus matrix protein in maintaining the viral nucleocapsid in the condensed form found in native virions. *Journal of Virology*, **39**:295-299.

Pattnaik A K, Ball L A, LeGrone A W and Wertz G W. **1992.** Infectious defective interfering particles of VSV from transcripts of a cDNA clone. *Cell*, **69**:1011-1020.

Pauli G and Ludwig H. **1985.** Increase of virus yields and releases of Borna disease virus from persistently infected cells. *Virus Research*, **2**:29-33.

Perez M and de la Torre J C. **2005.** Identification of the Borna disease virus (BDV) proteins required for the formation of BDV-like particles. *The Journal of General Virology*, **86**:1891-1895.

Perez M, Sanchez A, Cubitt B, Rosario D and de la Torre J C. **2003.** A reverse genetics system for Borna disease virus. *The Journal of General Virology*, **84**:3099-3104.

Perez M, Watanabe M, Whitt M A and de la Torre J C. **2001.** N-terminal domain of Borna disease virus G (p56) protein is sufficient for virus receptor recognition and cell entry. *Journal of Virology*, **75**:7078-7085.

Pleschka S, Staeheli P, Kolodziejek J, Richt J A, Nowotny N and Schwemmle M. **2001.** Conservation of coding potential and terminal sequences in four different isolates of Borna disease virus. *The Journal of General Virology*, **82**:2681-2690.

Ploegh H L. **1995.** Current protocols in protein science. *Wiley, New York*, **10**:10.12.

Poch O, Blumberg B M, Bougueleret L and Tordo N. **1990.** Sequence comparison of five polymerases (L proteins) of unsegmented negative-strand RNA viruses: theoretical assignment of functional domains. *The Journal of General Virology*, **71 (Pt 5)**:1153-1162.

Poenisch M, Staeheli P and Schneider U. **2008.** Viral accessory protein X stimulates the assembly of functional Borna disease virus polymerase complexes. *The Journal of General Virology*, **89**:1442-1445.

Poenisch M, Unterstab G, Wolff T, Staeheli P and Schneider U. **2004.** The X protein of Borna disease virus regulates viral polymerase activity through interaction with the P protein. *The Journal of General Virology*, **85**:1895-1898.

Poenisch M, Wille S, Ackermann A, Staeheli P and Schneider U. **2007.** The X protein of borna disease virus serves essential functions in the viral multiplication cycle. *Journal of Virology*, **81**:7297-7299.

Poenisch M, Wille S, Schneider U and Staeheli P. **2009.** Second-site mutations in Borna disease virus overexpressing viral accessory protein X. *The Journal of General Virology*.

Poenisch M, Wille S, Staeheli P and Schneider U. **2008.** Polymerase read-through at the first transcription termination site contributes to regulation of borna disease virus gene expression. *Journal of Virology*, **82**:9537-9545.

Portner A and Murti K G. **1986.** Localization of P, NP, and M proteins on Sendai virus nucleocapsid using immunogold labeling. *Virology*, **150**:469-478.

Price S R, Ito N, Oubridge C, Avis J M and Nagai K. **1995.** Crystallization of RNA-protein complexes. I. Methods for the large-scale preparation of RNA suitable for crystallographic studies. *Journal of Molecular Biology*, **249**:398-408.

Rayment I, Rypniewski W R, Schmidt-Bäse K, Smith R, Tomchick D R, Benning M M, Winkelmann D A, Wesenberg G and Holden H M. **1993.** Three-dimensional structure of myosin subfragment-1: a molecular motor. *Science (New York, N.Y.)*, **261**:50-58.

Richt J A, Clements J E, Herzog S, Pyper J, Wahn K and Becht H. **1993.** Analysis of virus-specific RNA species and proteins in Freon-113 preparations of the Borna disease virus. *Medical Microbiology and Immunology*, **182**:271-280.

Richt J A, Fürbringer T, Koch A, Pfeuffer I, Herden C, Bause-Niedrig I and Garten W. **1998.** Processing of the Borna disease virus glycoprotein gp94 by the subtilisin-like endoprotease furin. *Journal of Virology*, **72**:4528-4533.

Richt J A, Grabner A, Herzog S, Garten W and Herden C. **2006.** Borna disease. *Equine Infectious Diseases*:207.

Richt J A and Rott R. **2001.** Borna disease virus: a mystery as an emerging zoonotic pathogen. *Veterinary Journal (London, England: 1997)*, **161**:24-40.

Richt J A, VandeWoude S, Zink M C, Clements J E, Herzog S, Stitz L, Rott R and Narayan O. **1992.** Infection with Borna disease virus: molecular and immunobiological characterization of the agent. *Clinical Infectious Diseases: An Official Publication of the Infectious Diseases Society of America*, **14**:1240-1250.

Rodríguez L, Cuesta I, Asenjo A and Villanueva N. **2004.** Human respiratory syncytial virus matrix protein is an RNA-binding protein: binding properties, location and identity of the RNA contact residues. *The Journal of General Virology*, **85**:709-719.

Rosario D, Perez M and de la Torre J C. **2005.** Functional characterization of the genomic promoter of borna disease virus (BDV): implications of 3'-terminal sequence heterogeneity for BDV persistence. *Journal of Virology*, **79**:6544-6550.

Rott R and Becht H. **1995.** Natural and experimental Borna disease in animals. *Current Topics in Microbiology and Immunology*, **190**:17-30.

Rudolph M G, Kraus I, Dickmanns A, Eickmann M, Garten W and Ficner R. **2003.** Crystal structure of the borna disease virus nucleoprotein. *Structure (London, England: 1993)*, **11**:1219-1226.

Sambrook J, Fritsch E F and Maniatis T. **1989.** Molecular cloning: a laboratory manual 2nd edn. *New York: Cold Spring Harbor Laboratory*:362-271.

Schägger H and von Jagow G. **1987.** Tricine-sodium dodecyl sulfate-polyacrylamide gel electrophoresis for the separation of proteins in the range from 1 to 100 kDa. *Analytical Biochemistry*, **166**:368-379.

Schmid S, Mayer D, Schneider U and Schwemmle M. **2007.** Functional characterization of the major and minor phosphorylation sites of the P protein of Borna disease virus. *Journal of Virology*, **81**:5497-5507.

Schmid S, Mayer D, Schneider U and Schwemmle M. **2007.** Functional characterization of the major and minor phosphorylation sites of the P protein of Borna disease virus. *Journal of Virology*, **81**:5497-5507.

Schneemann A, Schneider P A, Kim S and Lipkin W I. **1994.** Identification of signal sequences that control transcription of borna disease virus, a nonsegmented, negative-strand RNA virus. *Journal of Virology*, **68**:6514-6522.

Schneemann A, Schneider P A, Lamb R A and Lipkin W I. **1995.** The remarkable coding strategy of borna disease virus: a new member of the nonsegmented negative strand RNA viruses. *Virology*, **210**:1-8.

Schneider P A, Hatalski C G, Lewis A J and Lipkin W I. **1997.** Biochemical and functional analysis of the Borna disease virus G protein. *Journal of Virology*, **71**:331-336.

Schneider P A, Schneemann A and Lipkin W I. **1994.** RNA splicing in Borna disease virus, a nonsegmented, negative-strand RNA virus. *Journal of Virology*, **68**:5007-5012.

Schneider U. **2005.** Novel insights into the regulation of the viral polymerase complex of neurotropic Borna disease virus. *Virus Research*, **111**:148-160.

Schneider U, Blechschmidt K, Schwemmle M and Staeheli P. **2004.** Overlap of interaction domains indicates a central role of the P protein in assembly and regulation of the Borna disease virus polymerase complex. *The Journal of Biological Chemistry*, **279**:55290-55296.

Schneider U, Naegele M and Staeheli P. **2004.** Regulation of the Borna disease virus polymerase complex by the viral nucleoprotein p38 isoform. Brief Report. *Archives of Virology*, **149**:1409-1414.

Schneider U, Naegele M, Staeheli P and Schwemmle M. **2003.** Active borna disease virus polymerase complex requires a distinct nucleoprotein-to-phosphoprotein ratio but no viral X protein. *Journal of Virology*, **77**:11781-11789.

Schneider U, Schwemmle M and Staeheli P. **2005.** Genome trimming: a unique strategy for replication control employed by Borna disease virus. *Proceedings of the National Academy of Sciences of the United States of America*, **102**:3441-3446.

Schoehn G, Iseni F, Mavrakis M, Blondel D and Ruigrok R W. **2001.** Structure of recombinant rabies virus nucleoprotein-RNA complex and identification of the phosphoprotein binding site. *Journal of Virology*, **75**:490-498.

Schoehn G, Mavrakis M, Albertini A, Wade R, Hoenger A and Ruigrok R W H. **2004.** The 12 A structure of trypsin-treated measles virus N-RNA. *Journal of Molecular Biology*, **339**:301-312.

Schwardt M, Mayer D, Frank R, Schneider U, Eickmann M, Planz O, Wolff T and Schwemmle M. **2005.** The negative regulator of Borna disease virus polymerase is a non-structural protein. *The Journal of General Virology*, **86**:3163-3169.

Schwemmle M, De B, Shi L, Banerjee A and Lipkin W I. **1997.** Borna disease virus P-protein is phosphorylated by protein kinase Cepsilon and casein kinase II. *The Journal of Biological Chemistry*, **272**:21818-21823.

Schwemmle M, De B, Shi L, Banerjee A and Lipkin W I. **1997.** Borna disease virus P-protein is phosphorylated by protein kinase Cepsilon and casein kinase II. *The Journal of Biological Chemistry*, **272**:21818-21823.

Schwemmle M, Jehle C, Shoemaker T and Lipkin W I. **1999.** Characterization of the major nuclear localization signal of the Borna disease virus phosphoprotein. *The Journal of General Virology*, **80 (Pt 1)**:97-100.

Schwemmle M, Salvatore M, Shi L, Richt J, Lee C H and Lipkin W I. **1998.** Interactions of the borna disease virus P, N, and X proteins and their functional implications. *The Journal of Biological Chemistry*, **273**:9007-9012.

Shoya Y, Kobayashi T, Koda T, Ikuta K, Kakinuma M and Kishi M. **1998.** Two proline-rich nuclear localization signals in the amino- and carboxyl-terminal regions of the Borna disease virus phosphoprotein. *Journal of Virology*, **72**:9755-9762.

Spehner D, Kirn A and Drillien R. **1991.** Assembly of nucleocapsidlike structures in animal cells infected with a vaccinia virus recombinant encoding the measles virus nucleoprotein. *Journal of Virology*, **65**:6296-6300.

Staeheli P, Sauder C, Hausmann J, Ehrensperger F and Schwemmle M. **2000.** Epidemiology of Borna disease virus. *The Journal of General Virology*, **81**:2123-2135.

Stitz L, Bilzer T and Planz O. **2002.** The immunopathogenesis of Borna disease virus infection. *Frontiers in Bioscience: A Journal and Virtual Library*, **7**:d541-555.

Stitz L, Bilzer T, Richt J A and Rott R. **1993.** Pathogenesis of Borna disease. *Archives of Virology. Supplementum*, **7**:135-151.

Stoyloff R, Strecker A, Bode L, Franke P, Ludwig H and Hucho F. **1997.** The glycosylated matrix protein of Borna disease virus is a tetrameric membrane-bound viral component essential for infection. *European Journal of Biochemistry / FEBS*, **246**:252-257.

Szilágyi J F and Uryvayev L. **1973.** Isolation of an infectious ribonucleoprotein from vesicular stomatitis virus containing an active RNA transcriptase. *Journal of Virology*, **11**:279-286.

Tarbouriech N, Curran J, Ruigrok R W and Burmeister W P. **2000.** Tetrameric coiled coil domain of Sendai virus phosphoprotein. *Nature Structural Biology*, **7**:777-781.

Tomonaga K, Kobayashi T, Lee B-J, Watanabe M, Kamitani W and Ikuta K. **2000.** Identification of alternative splicing and negative splicing activity of a nonsegmented negative-strand RNA virus, Borna disease virus. *Proceedings of the National Academy of Sciences of the United States of America*, **97**:12788-12793.

Tordo N, De Haan P, Goldbach R and Poch O. 1992. Evolution of negative-stranded RNA genomes. In *Seminars in Virology*.

Toriumi H and Kawai A. **2004.** Association of rabies virus nominal phosphoprotein (P) with viral nucleocapsid (NC) is enhanced by phosphorylation of the viral nucleoprotein (N). *Microbiology and Immunology*, **48**:399-409.

Uversky V N. **2002.** Cracking the folding code. Why do some proteins adopt partially folded conformations, whereas other don't? *FEBS Letters*, **514**:181-183.

Uversky V N. **2002.** Natively unfolded proteins: a point where biology waits for physics. *Protein Science: A Publication of the Protein Society*, **11**:739-756.

Walker M P, Jordan I, Briese T, Fischer N and Lipkin W I. **2000.** Expression and characterization of the Borna disease virus polymerase. *Journal of Virology*, **74**:4425-4428.

Walker M P and Lipkin W I. **2002.** Characterization of the nuclear localization signal of the borna disease virus polymerase. *Journal of Virology*, **76**:8460-8467.

Walter A E, Turner D H, Kim J, Lyttle M H, Müller P, Mathews D H and Zuker M. **1994.** Coaxial stacking of helixes enhances binding of oligoribonucleotides and improves predictions of RNA folding. *Proceedings of the National Academy of Sciences of the United States of America*, **91**:9218-9222.

Walter T S, Meier C, Assenberg R, Au K-F, Ren J, Verma A, Nettleship J E, Owens R J, Stuart D I and Grimes J M. **2006.** Lysine methylation as a routine rescue strategy for protein crystallization. *Structure (London, England: 1993)*, **14**:1617-1622.

Wehner T, Ruppert A, Herden C, Frese K, Becht H and Richt J A. **1997.** Detection of a novel Borna disease virus-encoded 10 kDa protein in infected cells and tissues. *The Journal of General Virology*, **78 (Pt 10)**:2459-2466.

Wolff T, Pfleger R, Wehner T, Reinhardt J and Richt J A. **2000.** A short leucine-rich sequence in the Borna disease virus p10 protein mediates association with the viral phospho- and nucleoproteins. *The Journal of General Virology*, **81**:939-947.

Wolff T, Unterstab G, Heins G, Richt J A and Kann M. **2002.** Characterization of an unusual importin alpha binding motif in the borna disease virus p10 protein that directs nuclear import. *The Journal of Biological Chemistry*, **277**:12151-12157.

Wright P E and Dyson H J. **1999.** Intrinsically unstructured proteins: re-assessing the protein structure-function paradigm. *Journal of Molecular Biology*, **293**:321-331.

Wyatt. **1998.** Submicrometer Particle Sizing by Multiangle Light Scattering following Fractionation. *Journal of Colloid and Interface Science*, **197**:9-20.

Wyatt P J. **1993.** Light scattering and the absolute characterization of macromolecules. *Analytica Chimica Acta*, **272**:1-40.

Yanai H, Kobayashi T, Hayashi Y, Watanabe Y, Ohtaki N, Zhang G, de la Torre J C, Ikuta K and Tomonaga K. **2006.** A methionine-rich domain mediates CRM1-dependent nuclear export activity of Borna disease virus phosphoprotein. *Journal of Virology*, **80**:1121-1129.

Yang J, Hooper D C, Wunner W H, Koprowski H, Dietzschold B and Fu Z F. **1998.** The specificity of rabies virus RNA encapsidation by nucleoprotein. *Virology*, **242**:107-117.

Ye Q, Krug R M and Tao Y J. **2006.** The mechanism by which influenza A virus nucleoprotein forms oligomers and binds RNA. *Nature*, **444**:1078-1082.

Zhang X, Green T J, Tsao J, Qiu S and Luo M. **2008.** Role of intermolecular interactions of vesicular stomatitis virus nucleoprotein in RNA encapsidation. *Journal of Virology*, **82**:674-682.

Zimmermann W, Breter H, Rudolph M and Ludwig H. **1994.** Borna disease virus: immunoelectron microscopic characterization of cell-free virus and further information about the genome. *Journal of Virology*, **68**:6755-6758.

Zuker M. **2003.** Mfold web server for nucleic acid folding and hybridization prediction. *Nucleic Acids Research*, **31**:3406-3415.

Zwick W and Seifried O. **1925.** Uebertragbarkeit der seuchenhaften Gehirn-und Rückenmarksentzündung des Pferdes (Borna'schen Krankheit) auf kleine Versuchstiere (Kaninchen). *Berl Tierärztl Wochenschr*, **41**:129-132.

Zwick W, Seifried O and Witte J. **1926.** Experimentelle Untersuchungen über die seuchenhafte Gehirn-und Rückenmarksentzündung der Pferde (Bornasche Krankheit). *Zeitschrift für Infektionskrankheiten, Parasitäre Krankheiten und Hygiene der Haustiere*, **30**:142-136.

7 Abbreviations

Aminoacids

A	Ala	Alanin
C	Cys	Cystein
D	Asp	Aspartat
E	Glu	Glutamat
F	Phe	Phenylalanin
G	Gly	Glycin
H	His	Histidin
I	Ile	Isoleucin
K	Lys	Lysin
L	Leu	Leucin
M	Met	Methionin
N	Asn	Asparagin
P	Pro	Prolin
Q	Gln	Glutamin
R	Arg	Arginin
S	Ser	Serin
T	Thr	Threonin
V	Val	Valin
W	Trp	Tryptophan
Y	Tyr	Tyrosin

Viral Proteins

G	Glycoprotein
L	Viral polymerase
M	Matrixprotein
N	Nucleoprotein
P	Phosphoprotein
P’	N-terminal truncated isoform of BDV P
X	BDV X protein

General

aa	Aminoacid
ATP	Adenosine triphosphate
bp	Base pairs
BDV	Borna Disease virus
CNS	Central nervous system
C-terminal	Carboxy-terminal
CTP	Cytosine triphosphate
Da	Dalton
DNA	Deoxyribonucleic acid
dNTP	Deoxynucleosid triphosphate
E. coli	*Escherichia coli*
et al.	*et aliter* (and others)

GTP	Guanosin triphosphate
His-Tag	Affinity tag, consisting of 6 Histidines
MCS	Multiple cloning site
MNV	*Mononegavirales*
NNS RNA virus	non-segmented negative-sense single-strand RNA virus
N-terminal	Amino-terminal
OD	Optical density
ORF	Open reading frame
PAGE	Polyacrylamide gelelectrophoresis
Pi	Isoelectric point
RABV	Rhabies virus
RNA	Ribonucleic acid
UTP	Uridin triphosphate
VSV	Vesicular stomatitis virus

8. Appendix

Danksagungen

Mein ganz besonderer Dank gilt Prof. Dr. Winfried Weissenhorn, für die hervorragende wissenschaftliche Betreuung und dafür, dass ich meine Arbeiten all die Jahre in seiner Arbeitsgruppe durchführen durfte und er nie die Geduld mit mir verloren hat. Außerdem möchte ich ihm für sein reges Interesse an meiner Arbeit, seine stete Diskussionsbereitschaft und seine wissenschaftlichen Anregungen danken.

Prof. Dr. Wolfgang Garten möchte ich für die Überlassung dieses interessanten Themas, sowie für die Freiheiten die er mir gelassen hat danken.

Weiterhin möchte ich mich bei Herrn Prof. Dr. Klaus Lingelbach für die Betreuung meiner Dissertation am Fachbereich Biologie bedanken.

Herrn Prof. Dr. Erhard Bremer und Herrn Prof. Dr. Wolfgang Buckel danke ich für die Bereitschaft als Kommissionsmitglieder im vorliegenden Promotionsverfahren zur Verfügung zu stehen.

Dr. Thomas Strecker möchte ich dafür danken, dass er mich über die Jahre hinweg mit schwer erhältlicher Literatur versorgt hat.

Den folgenden Menschen danke ich dafür, dass sie zu meiner Arbeit beigetragen haben:

Dr. Guy Schoehn für die EM Studien, Dr. Cornelia Andrei-Selmer für die Biacore Analysen, Dr. Marc Jamin und Dr. Euripedes Ribeiro für die Hilfe bei der Durchführung von MALLS, Charles Sabin und Tadeusz Muziol für die Unterstützung bei der Auswertung und Bearbeitung kristallographischer Daten und Dr. Thibaut Crepin für die Starthilfe bei der RNA -Aufreinigung.

Danke an alle jetzigen und ehemaligen Mitarbeiter am EMBL und UVHCI für das ausgesprochen angenehme und inspirierende Arbeitsklima am Institut. Für die stete Diskussionsbereitschaft und Hilfe gilt mein besonderer Dank Dr. Estela Pineda-Molina, die es immer wieder geschafft hat mich zu motivieren und Dr. Andreas Hinz.

Bei Dr. Ricardo Pires, Julianna Solomons, Anja Drees, Dr. Victor Buzon-Redorta, Carlos Fernandez-Tornero, Jordi Xiol, Manuela Delvecchio, Eva Kowalinski und ganz besonders Dr. Estela Pineda-Molina bedanke ich mich dafür, dass sie mit mir gelacht, geweint, gejubelt und genörgelt haben.

Mein herzlichster Dank gilt meinen Eltern, Chrisi und Michael, die mich während meines gesamten Ausbildungsweges bedingungslos unterstützt haben. Danke, dass Ihr immer für mich da seid!

Curriculum Vitae

Persönliche Daten

Geboren am: 20.05.1980
in: Gernsbach
Familienstatus: Ledig

Berufserfahrung

11/2005-12/2006	Studentische Hilfskraft, Philipps-Universität Marburg, Institut für Virologie
04/2007-04/2009	Wissenschaftliche Mitarbeiterin, Philipps-Universität Marburg, Institut für Virologie
2002-2004	Studentische Hilfskraft, Philipps-Universität Marburg Fachbereich Biologie, Abteilung Tierphysiologie, Neurobiologie
1998-2005	Flexible Aushilfskraft bei Daimler-Benz Gaggenau

Ausbildung

11/2005- heute:	Doktorarbeit in Strukturbiologie Philipps- Universität Marburg und *l'unité mixte internationale 3265* (*Europäisches Molekularbiologielabor,* Grenoble und *Unit of Virus Host Cell Interactions*, Grenoble) Betreuer: Prof. Dr. Winfried Weissenhorn und Prof. Dr. Wolfgang Garten Titel des Projekts: *Structural Analyses of Borna Disease Virus Nucleoprotein- Phosphoprotein and Nucleoprotein- RNA Interactions*
07/09/2005	Diplom in Biologie Philipps-Universität Marburg, Institut für Virologie
11/2004-08/2005	Diplomarbeit in Biologie in der Arbeitsgruppe von Prof. Dr. Wolfgang Garten, Philipps-Universität Marburg, Institut für Virologie

	Studiengang Biologie
10/1999- 08/2005	Philipps-Universität Marburg und
09/2001- 03/2002	Ruprecht-Karls- Universität Heidelberg
21/06/1999	Abitur
	Gymnasium Gernsbach

Ehrenwörtliche Erklärung

Ich versichere, dass ich meine Dissertation:

“Structural Analyses of Borna Disease Virus Nucleoprotein- Phosphoprotein and Nucleoprotein- RNA Interactions“

selbstständig, ohne unerlaubte Hilfe angefertigt und mich dabei keiner anderen als der von mir ausdrücklich bezeichneten Quellen und Hilfen bedient habe.

Die Dissertation wurde in der jetzigen oder einer ähnlichen Form noch bei keiner anderen Hochschule eingereicht und hat noch keinen sonstigen Prüfungszwecken gedient.

_____ Marburg, den _____

Miriam Hock